

Implication of Cytokines Released from Gingival  
Fibroblasts Exposed by Areca Nut Extract in  
Carcinogenesis

Rasika Pawithtra Illeperuma

The Graduate School  
Yonsei University  
Department of Dental Science

# Implication of Cytokines Released from Gingival Fibroblasts Exposed by Areca Nut Extract in Carcinogenesis

Directed by Professor Jin Kim

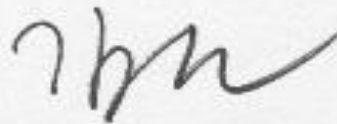
A Dissertation

Submitted to the Department of Dental Science  
and the Graduate School of Yonsei University  
in partial fulfillment of the  
requirements for the degree of  
Doctor of Philosophy

Rasika Pawiththra Illeperuma

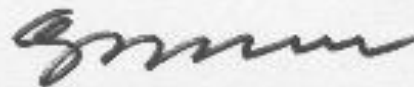
December 2011

This certifies that the doctoral dissertation of  
Rasika Pawiththra Illeperuma is approved.



---

Thesis Supervisor: Jin Kim



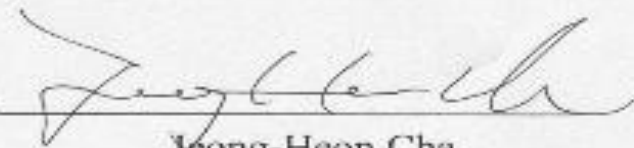
---

Jong In Yook



---

Kwang-Kyun Park



---

Jeong-Heon Cha



---

Da-Woon Jung

The Graduate School  
Yonsei University  
December 2011

## **ACKNOWLEDGEMENTS**

In year 2007 my beloved teacher Prof. W.M Tilakaratne, professor of oral pathology of the Faculty of Dental Sciences, University of Peradeniya, Sri Lanka, sent me a message asking to contact him. I called him. He asked me "Rasika, would you like to read for your PhD under the supervision of my good friend, Jin at Yonsei, South Korea". This was how it was initiated and now as a proud Yonseian I am completing my PhD, thanks to great teachers, Prof. Jin Kim and Prof. W.M Tilakaratne.

There were so many who were behind me encouraging and pushing me forward to complete this endeavor. I should acknowledge my dear parents who brought me up to become a doctor giving me their fullest possible support in my education. I remember all my beloved teachers with much respect at this moment. Foremost among these, is my beloved supervisor who trained me to be a scientist as well as to face the challenges of the life, Prof. Jin Kim. She strictly trained me as a teacher but tenderly looked after me as a mother. Without her advice, guidance and support this endeavor wouldn't have been a success. I am indebted to her for all my achievements and would like express my heartfelt love and gratitude as well.

I also would like to extend my appreciation and thanks to the Professors, Jong In Yook, Kwang-Kyun Park, Jeong-Heon Cha and Da-Woon Jung for sparing their valuable time to advice, guide and encourage me during my PhD programme and also for their comments, suggestions and corrections which supported the completion of this thesis. Special thanks due to Prof. Ryu Mi Heon who taught me the first lessons of lab techniques and Prof Ki Yeol Kim who always helped me with statistical data analysis. With much love I acknowledge all the teachers of the Yonsei Dental College, those who kept me happy with kind words and smiles always.

The first and best friend I met in Korea, Young Jin Park who was my senior, mentor and almost my guardian, who continuously helped me to cope with the new life in Korea, is gratefully acknowledged, with out whose help my life would have been much miserable. I regret for the burden which I caused her during her busy schedules. I am so grateful to my seniors as well as tutors Dr. Zong Min Che, Dr Jin Mi Kim, and Hwa Kyung Son who taught and helped me to gain skills necessary for research and corrected me when ever I did mistakes. All the members of the department of Oral Pathology, Yonsei University College of Dentistry and Mrs. Cha Eun Young our department secretary, together, who made a lovely family like environment, are warmly acknowledged.

Last but not least I would like to express deepest gratitude with love to my beloved wife Dr. Surangi, who took all the burden and worries of my family and kids enabling me to fulfill my task with easy mind. If I don't mention my two lovely daughters who gave me moral support to be a proud father, is a miss. They influenced me to work harder to be with them again as soon as possible.

## TABLE OF CONTENTS

List of figures and table.....	iv
Abbreviation.....	vii
ABSTRACT.....	viii
I. INTRODUCTION.....	1
II. MATERIALS AND METHODS.....	5
1. Cell culture.....	5
2. Preparation of AN extract (ANE).....	6
3. Cytotoxicity assessment of fibroblasts by ANE exposure	6
4. Cytokine antibody array.....	7
5. Stimulation of hNOF and hTERT-hNOF with ANE.....	7
6. Senescence assay with $\beta$ -galactosidase staining.....	8
7. Collection of conditioned media and cytokine secretion assessment by ELISA.....	9
8. Reverse transcription PCR (RT-PCR).....	10
9. Immunocytochemistry.....	11
10. Immunohistochemistry.....	13
11. Effect of cytokines on IHOK proliferation.....	14
12. Measurement of oxidative stress (ROS detection).....	14

13. Detection of DNA Damage by Histone H2A.X .....	15
14. Detection of Oxidative DNA Damage.....	16
15. Detection of cell ploidy change by flowcytometry (FACS).....	17
16. Wound healing assay.....	18
17. Statistical Analysis.....	19
III. RESULTS.....	20
1. Cytotoxicity assessment of ANE.....	20
2. Screening of cytokines secreted from ANE-stimulated fibroblasts.....	23
3. Assessment of cytokine secretion by ELISA.....	25
4. Detection of mRNA expression of cytokines in fibroblasts by RT-PCR.....	30
5. Immunofluorescence staining to detect cytokine secretion.....	32
6. Immunohistochemistry to detect cytokine expressions in human tissue.....	35
7. Senescence of long-term ANE-treated hTERT-hNOF.....	38
8. Cytokine secretion in long-term ANE-treated hTERT-hNOF Assessed by ELISA.....	40
9. Cytokine secretion in long-term ANE-treated hTERT-hNOF Assessed by immunofluorescence .....	42
10. IHOK growth by cytokine treatment .....	44

11.ROS production in IHOK by cytokine treatment.....	46
12.Detection of DNA damage in IHOK treated by cytokines .....	49
13.ROS produced by cytokines causing DNA damage in IHOK...	52
14.DNA damage in OSF tissue .....	54
15.Oxidative DNA damage in IHOK by cytokine treatment .....	56
16.Oxidative DNA damage in OSF tissues.....	59
17.Aneuploid cell population in IHOK by cytokine treatment.....	61
18.Cytokines effect on cell migration.....	63
19.Effect of cytokines and conditioned medium on IHOK inducing EMT.....	66
 IV. DISCUSSION.....	 70
 REFEENCE.....	 83
 ABSTRACT in KOREAN.....	 91

## LIST OF FIGURES and TABLE

Figure 1. Schematic diagram explaining main hypotheses postulated to explain carcinogenesis in OSF.....	4
Figure 2. Cytotoxicity assessment of ANE on fibroblasts .....	21
Figure 3. Cytokine antibody array to screen cytokine secretion by ANE-stimulated fibroblasts.....	24
Figure 4. Assessment of cytokine secretion by ANE-stimulated fibroblasts by ELISA.....	26
Figure 5. Relative mRNA expressions of the cytokines in ANE-stimulated hNOF and hTERT hNOF .....	31
Figure 6. Short-term ANE-stimulated hNOF and hTERT-hNOF stained for immunofluorescence .....	33
Figure 7. H & E staining and immunoperoxidase staining of NOM and OSF tissues.....	36
Figure 8. Senescence-associated $\beta$ -galactosidase staining of long-term ANE-stimulated hTERT-hNOF .....	39
Figure 9. Cytokine secretion in long-term ANE-treated hTERT-hNOF - ELISA .....	41
Figure 10. Long-term ANE-stimulated hTERT-hNOF stained for immunofluorescence .....	43
Figure 11. Cytokine-treated IHOK were tested for proliferation by MTT assay.....	45

Figure 12. Cytokines caused ROS generation in IHOK was detected using H <sub>2</sub> DCFDA dye .....	47
Figure 13. Detection of DNA Damage by Phospho-Histone H2A.X in cytokine-treated IHOK...	50
Figure 14. Effect of Anti-Oxidant (Glutathione) in cytokine-induced DNA damage, measured with Phospho-Histone H2A.X dye .....	53
Figure 15. Detection of DNA damage in OSF tissue by Phospho-Histone H2A.X staining .....	55
Figure 16. Detection of oxidative DNA damage in IHOK treated with cytokines using OxyDNA assay.....	57
Figure 17. Detection of oxidative DNA damage in OSF and NOM by OxyDNA assay.....	60
Figure 18. FACS analysis of cytokine-treated IHOK for cell cycle status.....	62
Figure 19. Cytokines causing increased cell motility in IHOK detected by wound healing assay .....	65
Figure 20. IHOK exposed to cytokines for 2 wks, showed fibroblast-like change in the morphology .....	67
Figure 21. Immunofluorescence staining of CM-treated IHOK to detect EMT changes .....	68
Figure 22. Immunofluorescence staining of GRO- $\alpha$ -treated IHOK to detect EMT changes .....	69

Figure 23. Proposed mechanism that ANE-exposed gingival fibroblasts caused DNA damage in oral mucosal epithelium..... 82

Table 1. Primer sequences used for RT-PCR..... 11

## ABBREVIATIONS

AN	Areca Nut
ANE	Areca Nut extract
CM	Conditioned medium
EMT	Epithelial-mesenchymal transition
GRO- $\alpha$ / CXCL1	Growth-regulated oncogene alpha
hNOF	Human normal oral / gingival fibroblasts
hTERT-hNOF	hTERT transfected immortalized human oral / gingival fibroblasts
hTERT	Human telomerase reverse transcriptase
IHOK	Immortalized human oral keratinocytes
IL-6	Interleukin 6
IL-8 / CXCL8	Interleukin 8
IFN - $\gamma$	Interferon gamma
NOM	Normal oral mucosa
OSF	Oral submucous fibrosis
OSCC	Oral Squamous cell carcinoma
ROS	Reactive oxygen species
SCC	Squamous cell carcinoma
SASP	Senescence associated secretory phenotype
TNF- $\alpha$	Tumor necrosis factor alpha

## ABSTRACT

# Implication of Cytokines Released from Gingival Fibroblasts Exposed by Areca Nut Extract in Carcinogenesis

Rasika Pawithtra Illeperuma  
Department of Dental Science  
The Graduate School  
Yonsei University  
(Directed by Professor Jin Kim)

The mechanism that cancers develop in Oral Submucous Fibrosis (OSF) has not been proven yet. Besides the direct cytotoxic and genotoxic effects of Areca nut (AN) on oral epithelium, indirect effects have also been identified, one of which is about the role of gingival fibroblasts influenced by AN. In this study, we mainly focused on the role of secretory molecules produced by the gingival fibroblasts upon AN extract (ANE) exposure.

We hypothesized that ANE could stimulate submucosal fibroblasts to secrete inflammatory cytokines continuously, which would cause a genotoxic effect to the OSF epithelium, and which may contribute to the malignant transformation of OSF.

Therefore as a start, cytokine antibody array was utilized to identify the cytokines secreted by ANE-stimulated fibroblasts. Water extract of AN was used in concentrations of 30  $\mu\text{g/ml}$  and 40  $\mu\text{g/ml}$  in *in vitro* studies. Normal human gingival fibroblasts (hNOF) and immortalized human gingival fibroblasts (hTERT-hNOF) were used in *in vitro* ANE stimulation. Cytokine antibody array data was

confirmed using ELISA, RT-PCR and immunofluorescence studies. The histologic sections of OSF patients were also used for immunohistochemical analysis of cytokine expressions.

hNOF and hTERT-hNOF were treated with ANE for short-term and hTERT-hNOF for long-term to study their cytokine secretion pattern and were analyzed by ELISA and immunofluorescence. As hNOF and hTERT-hNOF showed similar response pattern to ANE treatment, hTERT-hNOF were selected to expose for long term stimulation with ANE. Long-term ANE treated hTERT-hNOF were tested for senescence by  $\beta$ -galactosidase staining.

After identified the cytokines secreted from ANE-stimulated fibroblasts, to find their effect on oral epithelium, immortalized human oral keratinocytes (IHOK) were utilized. Namely GRO- $\alpha$ , IL-6, and IL-8 were used to stimulate IHOK. Cytokine effect on IHOK proliferation was measured by MTT assay. This study also investigated whether these cytokines could cause DNA damage in IHOK. Phospho-Histone H2A.X staining was used to detect DNA damage in a form of DNA double strand breaks (DSB) and FITC conjugated 8-oxo-guanine (8-oxoG) probing was used to detect the oxidative DNA damage. Tissue samples of OSF patients were also subjected to analyze for DNA DSB and oxidative DNA damage. In addition, H<sub>2</sub>DCFDA dye was used to detect reactive oxygen species (ROS) in IHOK by cytokine treatment. FACS analysis was used to test the cell cycle status and wound healing assay was used to test the cell motility in IHOK, after cytokine treatment. Finally to find out whether these cytokines could induce epithelial-mesenchymal transition (EMT) in IHOK, immunocytochemistry staining for EMT related molecules were carried out together with morphological examinations.

Cytokine antibody array showed that ANE treatment increased GRO- $\alpha$ , IL-6, and IL-8 expressions in both hNOF and hTERT-hNOF. Angiogenin expression was reduced in both hNOF and hTERT-hNOF after ANE treatment. These results were confirmed using ELISA and immunofluorescence. OSF patients' tissues were also showed increased GRO- $\alpha$ , IL-6, IL-8 and reduced angiogenin expressions which were compatible to the *in vitro* results. Long term stimulation of hTERT-hNOF with ANE also

showed increased GRO- $\alpha$ , IL-6, and IL-8 secretion. 8wks of ANE exposure made hTERT-hNOF to become senescence which was confirmed by  $\beta$ -galactosidase staining.

MTT assay showed the cytokines GRO- $\alpha$ , IL-6, IL-8 have no significant effect on the proliferation of IHOK. Phospho-Histone H2A.X staining clearly showed that GRO- $\alpha$ , IL-6, and IL-8 individually and in combination caused DNA damage; DNA double strand breaks (DSB) precisely. Patients' tissues of OSF were also positive for Phospho-Histone H2A.X staining showing positive foci in and around the basal layer. Furthermore, FITC conjugated 8-oxo-guanine (8-oxoG) probing detected these cytokines causing oxidative DNA damage in IHOK. Oxidative DNA damage was detected in the cells in and around the basal cell layer of the OSF patients' tissues as well. In addition, H<sub>2</sub>DCFDA dye detected GRO- $\alpha$ , IL-6, and IL-8 individually and in combination generates reactive oxygen species (ROS) in IHOK. FACS analysis revealed these cytokines causing increased cell aneuploidy in IHOK. Moreover these cytokines increased cell motility in IHOK and induced EMT changes as well.

To sum up, the present study attempted to identify the role of fibroblasts in carcinogenesis of OSF by investigating the cytokines produced by the gingival fibroblasts upon ANE stimulation. Results figured out that GRO- $\alpha$ , IL-6 and IL-8 were capable of causing DNA damage in IHOK and especially the oxidative DNA damage was evident. Increased ROS production by GRO- $\alpha$ , IL-6, and IL-8 could cause the DNA damage in IHOK. Studies involved using OSF patients' tissues supported our *in vitro* findings showing OSF tissues have elevated expressions of GRO- $\alpha$ , IL-6, and IL-8 and moreover, OSF tissues were positive for DNA damage and oxidative DNA damage markers as well. Furthermore long-term ANE stimulated hTERT-hNOF became senescent. This may be the senescence associated secretory phenotype (SASP) which has been extensively described in the literature, which contributes to the epithelial malignancies via producing secretory molecules such as cytokines and chemokines. GRO- $\alpha$ , IL-6 and IL-8 were capable of causing increased cell aneuploidy, increased cell motility and EMT changes in IHOK which are hallmarks of carcinogenesis.

This study clarified one aspect of the indirect effect of AN in the carcinogenic transformation of oral epithelium with special reference to the cytokines secreted from submucosal fibroblasts. Our approach of this study could be further elaborated to elucidate the role of inflammatory cytokines in the carcinogenesis of OSF.

---

**Key words:** Oral Submucous Fibrosis, Areca Nut extract, Carcinogenesis, Cytokines, DNA damage

## I. INTRODUCTION

Oral submucous fibrosis (OSF) is a premalignant, chronic insidious fibrous disease, mainly affecting oral cavity and sometimes oropharynx and the upper part of the esophagus as well (Haque et al., 1998). In 1950, Joshi described this disease first and even after fifty decades since, the pathogenesis of OSF is not fully understood. Premalignant nature of OSF was first identified by Paymaster (Paymaster, 1956) and this precancerous characteristics made this condition a candidate for continuous research.

Histologically, OSF is characterized by epithelial atrophy, juxta-epithelial hyalinization, collagen deposition in different density in submucosa, and infiltration of chronic inflammatory cells in juxta-epithelial region (Pindborg et al., 1980; Pindborg et al., 1970). According to the histological appearance, OSF indicates an excessive deposition of collagen in the lamina propria suggesting a loss of homeostatic mechanisms controlling collagen turn over, hence leading to fibrosis and functional impairment due to the irreversible alteration of the tissue architecture (Tilakaratne et al., 2006; Utsunomiya et al., 2005) .

The main etiology of OSF is consumption of Areca Nut (AN) alone or with betel quid (Tilakaratne et al., 2006). According to the literature, about 600 million people world wide practice this habit of AN chewing (Jeng et al., 2003) and mainly seen in south and south east Asian countries (Jeng et al., 2003). Due to heavy migration of people from these parts of Asia to the rest of the world, now both this habit and OSF are reported in other regions as well (McGurk and Craig, 1984). Epithelial dysplasia is evident in 7% - 25% of the OSF lesions and the malignant transformation into oral squamous cell carcinoma (OSCC) has been estimated as 7% -13 % (Tilakaratne et al., 2006).

AN categorized as one of the grade 1 carcinogen according to IACR grading ("Betel-quid and areca-nut chewing and some areca-nut derived nitrosamines," 2004), reported to have direct and indirect carcinogenic effect to the oral epithelium (Chang et al., 2002; Lu et al., 2008; Tsai et al., 2008). Epidemiological data also show a clear relationship with OSCC and habit of AN consumption (Gupta and Warnakulasuriya, 2002). Literature describes direct genotoxic and cytotoxic effect of AN extract (ANE) has a role to play in the carcinogenesis of OSF (Chang et al., 2002; Jeng et al., 2000; Jeng et al., 2003; Tsai et al., 2008). Arecoline, a major alkaloid of AN, inhibited p53 function of DNA repair, and triggered DNA damage response in human keratinocytes ( Tsai et al., 2008). The intracellular reactive oxygen species (ROS) are generated in keratinocytes by ANE exposure, resulting in genotoxic effects (Chang et al., 2002; Lai and Lee, 2006). Indirect AN effect is described as long term accumulation of AN carcinogens in the submucosal area supported by the unique fibrous architecture and less blood supply which facilitate carcinogens to accumulate and act for long time without absorption (Lu et al., 2008; Tilakaratne et al., 2006).

The unique nature of malignant transformation of OSF epithelium in the background of fibrosis gives a clue that, either fibrosis per se or factors promoting fibrosis might have a role to play in this malignant transformation process.

Some previous reports showed existence of various cytokines in OSF and their relation ship with the pathogenesis of OSF (Haque et al., 1998; Haque et al., 1997; Haque et al., 2000). Recently, the fact that senescent fibroblasts in OSF tissues secrete increased amount of cytokines have been reported (Pitiyage et al., 2011). OSF being a chronic disease, involves with inflammatory cytokines and especially, histologically also evident to have inflammatory cell infiltration at various stages of the disease.

The link between chronic inflammation and cancer has been discussed in related to several epithelial cancers such as skin cancer, prostate cancer, colon cancer, and endometrial cancer and has been a key

focus among cancer research during these days (Becker et al., 2005; Kogan-Sakin et al., 2009; Lederle et al., 2011; Li et al., 2001; Raman et al., 2007; Rojas et al., 2011; Scheller et al., 2006; Schneider et al., 2000). Up to 20% of all cancers arise in association with chronic inflammation and even those cancers that do not develop as a consequence of chronic inflammation, exhibit extensive inflammatory infiltrates with high levels of cytokine expression in the tumor microenvironment (Coussens and Werb, 2002; Grivennikov and Karin, 2011; Hussain and Harris, 2007). Involvement of various inflammatory cytokines such as TNF- $\alpha$ , IL-6, IL-8, and GRO- $\alpha$  has been extensively discussed in relation to cancer (Babbar and Casero, 2006; Becker et al., 2005; Ju et al., 2010; Jung et al., 2010; Kawanishi et al., 2008; Kogan-Sakin et al., 2009; Lederle et al., 2011; Li et al., 2001; Raman et al., 2007; Rojas et al., 2011; Scheller et al., 2006; Schneider et al., 2000; Yang et al., 2006). Literature evidenced TNF and IL-6 and other proinflammatory cytokines can influence all stages of tumor development such as tumor initiation, promotion, progression and metastasis (Aggarwal et al., 2009; Grivennikov et al., 2010; Grivennikov and Karin, 2010).

Based on this knowledge, we hypothesized that cytokines also may have a role to play in the carcinogenesis of OSF. To prove this hypothesis, we attempted to investigate the cytokines secreted from submucosal fibroblasts upon ANE exposure and to search whether these cytokines induce DNA damage in oral keratinocytes leading to the carcinogenic transformation in OSF epithelium.

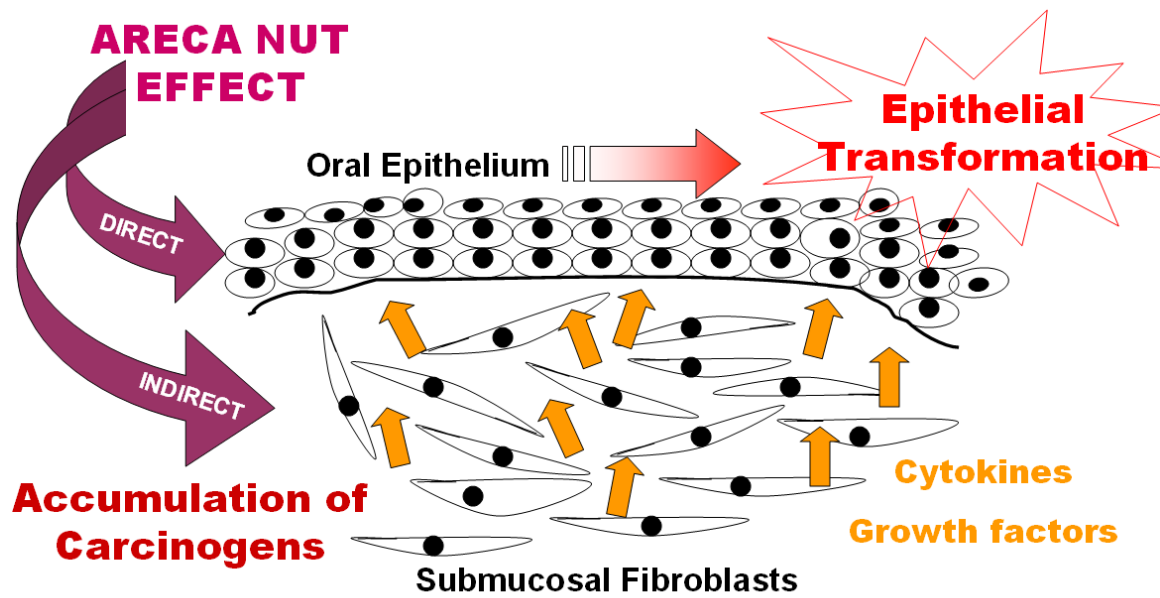


**Fig. 1.** Schematic diagram explaining main hypotheses postulated to explain carcinogenesis in OSF. Direct and indirect genotoxic effects and cytotoxic effects of Areca Nut have been studied extensively to explain carcinogenesis in OSF.

## **II. MATERIALS AND METHODS**

All studies involving human subjects were approved and ethical approval was granted by the Institutional Review Board of the Yonsei Dental Hospital, Yonsei University Health System, Seoul, Republic of Korea (IRB-2-2009-0002).

### **1. Cell culture**

Human gingival fibroblasts (hNOF) were obtained by explant method using tissue taken from a healthy individual with informed consent, who underwent third molar extraction at Yonsei Dental Hospital. hNOF below 10<sup>th</sup> passage were used for the study. Immortalized human gingival fibroblasts using hTERT transfection (hTERT-hNOF) which was previously established in our research institute (Illeperuma et al., 2011) was also used in this study. Immortalized human oral keratinocytes (IHOK) used in this study has been previously described (H. J. Lee et al., 2005) and is a gift from Prof. Eun-Cheol Kim, Kyunghee University College of Dentistry, Seoul, Korea. The cultured cells were maintained in F medium which was composed of Dulbecco's Modified Eagles Medium [DMEM] (Gibco, BRL, USA) and Ham's Nutrient Mixture F-12 (Gibco, BRL, USA) at a ratio of 3:1 supplemented with 10% fetal bovine serum [FBS] (Hyclone, Logan, UT, USA) and 1% penicillin / streptomycin (Invitrogen, NY, USA). All cell lines were maintained in a humidified incubator at 37 °C, in an atmosphere containing 5% CO<sub>2</sub> and culture medium was changed every 3 days in serial subculture.

## **2. Preparation of AN extract (ANE)**

ANE was prepared using dried ripe AN without husk as previously described (Jeng et al., 2003) with few modifications. The ANE was weighed and dissolved in sterilized ice cold distilled water vortexing at 4 °C overnight and centrifuged at 5000 rpm for 15 minutes. Then the supernatant was filtered using sterilized filter paper (Whatman® , Maidstone, UK) and then 0.45 µm pore size syringe filters (Minisart® , Sartorius Stedim Biotech, GmbH, Germany) and stored at -80 °C until use.

## **3. Cytotoxicity assessment of fibroblasts by ANE exposure**

In order to identify suitable ANE concentrations to stimulate fibroblasts *in vitro*, cytotoxic effect of hNOF and hTERT-hNOF exposed by ANE was measured by mitochondrial dehydrogenase activity assessed by MTT [3-(4,5-dimethylthiazol-2-yl)-2,5-diphenyltetrazolium bromide] assay as previously described (Illeperuma et al., 2011). In brief  $2 \times 10^4$  cells of either hNOF or hTERT-hNOF were seeded in to 96 well plates in F media. After overnight, the incubated cells were washed twice with phosphate buffered saline (PBS), incubated in P media (composed of DMEM and Ham's Nutrient Mixture F-12 at a ratio of 3:1) containing 0.5% FBS for 6 h and then treated with a concentration gradient of ANE (10 µg/ml,-160 µg/ml). Selection of ANE concentration gradient was supported by earlier published literature (Chang et al., 2009; Jeng et al., 1999; Wang et al., 2007). Mitochondrial dehydrogenase activity was assessed by MTT assay in every 24 h interval for 96 h. 100 µg of MTT solution (Sigma, St.Louis, MO, USA) was added to the wells at the desired time points. After 3 h incubation, 150 µl of di-methyl sulfoxide [DMSO] (Sigma, St.Louis, MO, USA) was added to dissolve the purple formazan formed by the reduction of MTT solution. The optical density was measured at a wavelength of 570 nm in a microplate reader (Bio-Rad, Model 680, Japan). Tests were repeated more than three times

and cell viability was expressed as the mean  $\pm$  SD relative to a control (media only) in the absence of ANE treatment.

#### **4. Cytokine antibody array**

Based on the cytotoxicity assay results, 30  $\mu\text{g/ml}$  and 40  $\mu\text{g/ml}$  of ANE were selected as suitable dose for *in vitro* stimulation of hNOF and hTERT-hNOF. These ANE concentrations were also in accord with previously published researches (Chang et al., 2009; Jeng et al., 1999; Wang et al., 2007).

RayBio® Human Cytokine Antibody Array 3 kit (Cat# AAH-CYT-3, Ray Biotech, Norcross, GA, USA) was used to screen the cytokine secretion in conditioned media of ANE stimulated hNOF and hTERT-hNOF according to the instructions given in the assay kit. Controls were maintained in the absence of ANE treatment (media only). In brief  $8 \times 10^5$  cells of either hNOF or hTERT-hNOF were seeded in to T-25 tissue culture flasks in F media and incubated overnight in a humidified incubator at 37 °C. Next day, after culture medium was removed, the cells were washed twice with PBS, and 5 ml of fresh P media containing either 30  $\mu\text{g/ml}$  or 40  $\mu\text{g/ml}$  of ANE was added. Cells were again incubated for 24 h and conditioned medium (CM) was collected, centrifuged at 1000 rpm for 5 minutes and used for cytokine antibody array. Conditioned media were normalized for cell number between samples by dilution with P media before exposing to array membranes. The relative expression level of the cytokines was determined by comparing signal intensities. Quantity one programme (Bio-Rad laboratories, USA) was used for densitometric analysis of the results.

## **5. Stimulation of hNOF and hTERT-hNOF with ANE**

To simulate ANE exposure of submucosal fibroblasts *in vitro* and to study the pattern of cytokine secretion by human gingival fibroblasts upon ANE stimulation, hNOF and hTERT-hNOF were stimulated with 30 µg/ml and 40 µg/ml of ANE in F media. Initially both hNOF and hTERT-hNOF were stimulated for 24 h and 72 h to compare cytokine secretion pattern between two cell lines and secondly only hTERT-hNOF was subjected to long term ANE exposure up to 8 weeks. hNOF being a normal human cell line, can not be used for a long term research due to the replicative senescence and the genomic instability occur in serial subculture with the advancement of passages. Hence hTERT-hNOF was used in long term ANE exposure study of gingival fibroblasts as hTERT-hNOF shows similar pattern of cytokine secretion compared to hNOF in cytokine antibody array and also as hTERT-hNOF found to harbor similar biological properties to hNOF in a previous study conducted by us (Illeperuma et al., 2011). Briefly,  $1 \times 10^6$  cells of hNOF or hTERT-hNOF were seeded in to 100 mm tissue culture dishes in F media and after overnight incubation the cells were treated with either 30 µg/ml or 40 µg/ml of ANE in F media. In long term ANE exposure studies, media was changed every 3 days with appropriate concentration of ANE and cells were split at a ratio of 1:3 at the confluence in serial subculture. Cell lines were maintained as above mentioned until desired time periods with ANE stimulation for further analysis. All the tests were repeated more than three times and controls were maintained in the absence of ANE treatment (media only) using similar volume of sterile distilled water (DW) for stimulation instead of ANE.

## **6. Senescence assay with $\beta$ -galactosidase staining**

The hTERT-hNOF cell line was continuously maintained with ANE exposure as above mentioned and after 8 wks they were stained to detect replicative senescence using  $\beta$ -galactosidase staining kit

(Cell Signaling, MA, USA), according to the manufacturer's instructions. In brief, the hTERT-hNOF cells maintained with ANE treatment for 8 wks were seeded in to 6-well plate. hTERT-hNOF which were simultaneously maintained up to 8 wks without ANE treatment, were used as control. Staining was performed and incubated overnight at 37 °C and visualized and photomicrographed in the following day. Senescent fibroblasts were identified as blue colour stained cells by inverted microscopy.

## **7. Collection of conditioned media and cytokine secretion assessment by ELISA**

Sandwich enzyme-linked immunosorbent assay (ELISA) was used to measure the cytokines levels in conditioned medium of ANE stimulated hNOF and hTERT- hNOF.

Conditioned media were collected at different time points as follows. hNOF were stimulated by ANE for 24 h and 72 h. hTERT- hNOF were stimulated by ANE for 24 h, 72 h, 2 weeks, 4 weeks and 8 weeks, respectively. Briefly, for collecting conditioned medium at 24 h and 72 h,  $1 \times 10^6$  cells of hNOF or hTERT-hNOF were cultured for 2 days in 100 mm culture plates with 5 ml of P media containing 1% FBS together with appropriate ANE concentrations or DW in controls. The supernatant was collected, centrifuged and filtered before storing at -80°C for using as conditioned media. In long term ANE exposure studies, at desired time points after ANE exposure, hTERT-hNOF cells were subcultured similarly as above mentioned for two days in 5 ml of P media containing 1% FBS but with appropriate ANE concentrations and the supernatant was collected and stored similarly after centrifugation and filtration. At the time of collecting supernatant, the number of cells in particular dish were counted for normalization between samples. When conditioned media were collected to treat IHOK, they were collected without containing ANE. That is after appropriate ANE stimulation, cells were washed with PBS and then were cultured for 2 days in P media containing 1% FBS before harvesting the supernatant. Each experiment was repeated three times independently.

Conditioned media collected as above mentioned, were tested for GRO- $\alpha$ , IL-6, IL-8 and angiogenin using sandwich ELISA, as these cytokines were identified differently expressed in the conditioned medium of ANE stimulated hNOF and hTERT-hNOF by cytokine antibody array. Furthermore, cytokine secretion patterns were compared among samples according to the period of ANE exposure. Sandwich ELISA was performed according to the manufacture's protocol (R&D Systems, Inc. Minneapolis, MN, USA) and all the relevant reagents including, capture antibodies (Mouse monoclonal anti-human GRO- $\alpha$ , IL-6, IL-8 and angiogenin), recombinant proteins (Recombinant human GRO- $\alpha$ , IL-6, IL-8 and angiogenin), detection antibodies (Biotinylated anti-human GRO- $\alpha$ , IL-6, IL-8 and angiogenin), and detection systems with colour reagent were purchased from R&D Systems (Minneapolis, MN, USA). Capture antibodies were diluted and applied as GRO- $\alpha$  (4  $\mu\text{g/ml}$ ), IL-6 (2  $\mu\text{g/ml}$ ), IL-8 (8  $\mu\text{g/ml}$ ) and angiogenin (2  $\mu\text{g/ml}$ ). Each experiment was repeated three times independently and cytokine secretions were normalized according to the number of cells at the time of conditioned media harvesting.

## **8. Reverse transcription PCR (RT-PCR)**

hNOF and hTERT-hNOF were stimulated with ANE as for taking conditioned medium above mentioned and total RNA was extracted using RNeasy kit (Qiagen, GmbH, Germany) according to the manufacturer's protocol. Template cDNA was prepared by reverse transcription of 1  $\mu\text{g}$  of total RNA using Transcriptor First Strand cDNA Synthesis Kit (Roche Diagnostics, GmbH, Germany) and semi quantitative RT-PCR was performed using primers mentioned in Table 1. GAPDH mRNA was co-amplified to serve as an internal control. The reaction mixture was placed at 95  $^{\circ}\text{C}$  for 5 min in the first cycle. The reaction was then run for 30 cycles of 94  $^{\circ}\text{C}$  for 1 min, 58  $^{\circ}\text{C}$  for 1 min and 72  $^{\circ}\text{C}$  for 2 min with a thermal cycler (Gene Amp<sup>®</sup> PCR System 9700, Applied Bio Systems, CA, USA). Finally

the reaction was terminated following an extension at 72 °C for 7 min. Amplified DNA products were then subjected to 1.5% agarose gel electrophoresis and stained with Ethidium bromide for reading. Each test was repeated at least three times.

**Table 1** Primer sequences used for RT-PCR

mRNA	Sense primer sequence	Antisense primer sequence	bp
GRO- $\alpha$	5'-ATGGCCCGCGCTGCTCTCCTCC-3'	5'-GTTGAATTTGTCAGTTCAG-3'	320
IL-6	5'-ATGAACTCCTTCTCCACAAGCGC-3'	5'-GAAAGCCCTCAGGCTGGACTG-3'	628
IL-8	5'-TGCTAAAGAACTTAGATGTCAGTGCAT-3'	5'-CGCAGTGTGGTCCACTCTCA-3'	101
Angiogenin	5'-CATCATGAGGACACGGGG-3'	5'-TCCAAGTGGACAGGTAAGCC-3'	269
GAPDH	5'-GAAGGTGAAGTCCGGAGT-3'	5'-GAAGATGGTATGGGATTC-3'	205

## 9. Immunocytochemistry

Fluorescence immunohistochemistry was performed as previously described (Montzka et al., 2010) using anti-human antibodies against GRO- $\alpha$ , IL-6, IL-8 and Angiogenin (R&D Systems, Minneapolis, MN, USA) with few modifications. In brief  $5 \times 10^4$  hNOF and hTERT- hNOF were grown in chamber slides (Nalge Nunc, Roskilde, Denmark) and were stimulated with ANE for desired time periods. Cells were washed with PBS and then were fixed with 4% para formaldehyde in PBS (Wako pure chemicals, Japan) for 30 minutes. Afterwards, cells were washed three times with PBS and blocked for 1 h at room temperature with PBS containing 3% normal goat serum (Vector, CA, USA), 1% bovine serum albumin [BSA] (Sigma, MO, USA), and 1% Triton X-100 (aMReSCO, Solon, Ohio, USA). The primary antibodies diluted in PBS having 1% BSA were applied at room temperature for overnight (GRO- $\alpha$ , IL-6, and Angiogenin 1:100 dilution and IL-8 1: 20 dilution). The secondary antibodies, goat anti-mouse Alex 594 and goat anti-mouse Alex 488 (Invitrogen, Oregon, USA) 1:500 diluted in 1% BSA in PBS were added for 2.5 h at room temperature. (Alex 488 for GRO- $\alpha$  and IL-8,

Alex 594 for IL-6 and Angiogenin). Then nuclei were stained with 10 µg/ml diamidinophenylindole [DAPI] (Sigma, MO, USA), cover-slipped with Dako fluorescent mounting medium (Dako, CA, USA), visualized and photographed using confocal microscopy (LSM 510 Meta, Carl Zeiss, Jena, Germany). Long term ANE exposed hTERT-hNOF were also stained as above mentioned at desired time points. Omission of primary antibody or mouse immunoglobulin fraction (Dakocytomation, Denmark) served as a negative control and resulted in no detectable staining. Three independent experiments were performed for each test.

To find out whether these cytokines could induce Epithelial-mesenchymal transition (EMT) in cultured IHOK, immunocytochemistry staining for EMT related molecules were carried out together with morphological examinations. In brief, IHOK cells were maintained *in vitro* for 2 wks, treated with cytokines (10 ng/ml and 50 ng/ml) and subjected to immunocytochemistry. Additionally, IHOK cells were treated with CM taken from ANE-stimulated hTERT-hNOF for 10 wks, and analyzed together. Media of cultured cells were changed every three days with fresh media containing cytokines or CM and at 90% confluency cells were split in to 1:3 ratio. Cells were closely monitored for morphological changes observed during this period and photographed using inverted microscope. Direct immunoflorescent staining was carried out for cytokeratin and vimentin (FITC conjugated anti-cytokeratin (1:200) and Cy3 conjugated anti-vimentin (1:200) (Sigma, MO, USA) according to the manufacturer's instructions and for sanil and E-cadherin (Mouse mAB, 1:100, Cell Signaling, MA, USA) indirect immunoflorescent staining was carried out as above mentioned. Goat anti-mouse Alex 488 (1:500 dilution Invitrogen, Oregon, USA) was used as the fluorescent conjugated secondary antibody. Finally slides were stained with 10 µg/ml DAPI, mounted, visualized and photomicrographed using confocal microscopy (LSM510 Meta, Carl Zeiss, Jena, Germany). Omission of primary antibody or mouse immunoglobulin fraction (Dakocytomation, Denmark) served as a negative control. Tests were preformed in triplicates.

## 10. Immunohistochemistry

Specimens from adult OSF patients from archives of the Department of Oral Pathology, Faculty of Dental Sciences, University of Peradeniya, Sri Lanka together with the specimens of normal oral mucosa (NOM) were selected for the study. These immunohistochemical investigations were carried out in order to detect the presence of cytokines identified in *in vitro* experiments (GRO- $\alpha$ , IL-6, IL-8 and Angiogenin), were whether present in an identical manner in the *in vivo* as well.

Formalin-fixed, paraffin-embedded serial tissue sections were cut to a thickness of 4  $\mu$ m and mounted on silane coated slides (Muto Pure Chemicals Co Ltd, Japan). Sections were de-waxed and re-hydrated using xylene and varying concentrations of ethanol. Antigen retrieval was achieved by autoclaving the sections for 20 min in 50 mM Tris EDTA buffer (pH 9) after which sections were allowed to cool and placed into PBS. Endogenous peroxidase was blocked in the sections by incubating them for 10 min with freshly prepared 3% hydrogen peroxide solution. Before applying primary antibodies, sections were blocked with normal horse serum (2.5% horse serum, ImmPRESS™ Reagent Kit, Vector Laboratories, CA, USA) for 30 min at room temperature. Immunostaining was achieved using four primary antibodies applied overnight at 4 C°, namely mouse monoclonal anti-human GRO- $\alpha$ , IL-6, IL-8 and Angiogenin (1:100 dilution in PBS). ImmPRESS™ Reagent Kit-anti mouse (Vector Laboratories, CA, USA) was used according to manufacture's protocol for the rest of the staining procedure. The sections were visualized with 3, 3-diaminobenzidine tetrachloride (DAB, Vector Laboratories, CA, USA), counterstained with Mayer's hematoxylin, mounted, and then examined with an Olympus BH-2 light microscope (Olympus Corp, Tokyo, Japan). In order to demonstrate the specificity of the staining, negative controls were included in which the primary antibody was replaced with PBS or mouse immunoglobulin fraction (Dakocytomation, Denmark).

## **11. Effect of cytokines on IHOK proliferation**

IHOK exposed to 10 ng/ml concentration of cytokines (GRO- $\alpha$ , IL-6, and IL-8) individually and in combination (GRO- $\alpha$  + IL-6, GRO- $\alpha$  +IL-8, and GRO- $\alpha$  + IL-6 +IL-8) together with control (media only) for 96 h in F media, and using MTT assay, the effect of cytokines on IHOK growth was measured in 24 h intervals. In brief,  $5 \times 10^3$  cells of IHOK were seeded in to 96 well plates in F media. After overnight incubation, the cells were washed twice with PBS, and incubated with recombinant cytokines in F media as described above. Mitochondrial dehydrogenase activity was assessed by MTT assay in every 24 h interval for 96 h as similarly mentioned in ANE cytotoxicity measurement. Results were expressed as the mean  $\pm$ SD of results from three independent tests.

## **12. Measurement of oxidative stress (ROS detection)**

Intracellular reactive oxygen species (ROS) were measured with the fluorescent probe 2',7'-dichlorofluorescein diacetate (H<sub>2</sub>DCFDA) dye (Molecular Probes Inc, OR, USA) according to the manufacture's instructions. In brief, IHOK cells grown to confluence overnight in 6 well plates were exposed to the 10 $\mu$ M H<sub>2</sub>DCFDA dye in PBS in dark at 37 °C for 20 min. Thereafter the cells were washed twice with PBS and followed by 30 min recovery period in P media. Cytokines (recombinant human GRO- $\alpha$ , IL-6, and IL-8 R&D Systems Minneapolis, MN, USA) dissolved in P media (10 ng/ml of each cytokine) were added in to wells and incubated for desired time periods in dark before they were scaped and collected to 5 ml polystyrene tubes (BD Biosciences, MA, USA) for FACS analysis. P media alone served as negative control and 10  $\mu$ M H<sub>2</sub>O<sub>2</sub> served as the positive control. All steps following incubation with dye were done protected from light. Ten thousand cells were then

analyzed by FACS (Becton Dickinson, CA, USA) at an excitation and emission wavelengths of 485 nm and 535 nm, respectively and Cell-Quest software (BD Biosciences) was utilized for data analysis.

ROS production caused by these cytokines in IHOK was also assessed by confocal microscopy (LSM510 Meta, Carl Zeiss, Jena, Germany). For this, IHOK grown in Lab-Tek chamber slides (Nalge Nunc In., NY, USA ) were stained with H<sub>2</sub>DCFDA as previously described by J.B Seidelin et al (Seidelin and Nielsen, 2005). IHOK, ten thousand cells grown per chamber were treated with cytokines 10 ng/ml (GRO- $\alpha$ , IL-6, and IL-8 alone or in combination), stained and visualized and photomicrographed using confocal microscopy. The nuclei were stained with 10  $\mu$ g/ml DAPI. Controls were same as for ROS detection by fluorescence intensity and each experiment was performed three times.

### **13. Detection of DNA Damage by Histone H2A.X**

To detect DNA damage caused by cytokines, Phospho-Histone H2A.X rabbit monoclonal antibody (Cell Signaling, MA, USA) was utilized to stain IHOK and paraffin sections of OSF and NOM.  $1 \times 10^4$  IHOK grown using F media in Lab-Tek chamber slides were treated with cytokines for 72 h, individually and in combination as for FACS analysis. Media alone served as the negative control and 10  $\mu$ M H<sub>2</sub>O<sub>2</sub> served as the positive control. After stimulation, cells were washed twice with PBS and stained using Phospho-Histone H2A.X primary antibody (1:400 dilution) followed by goat anti-rabbit Alex 488 (Invitrogen, Oregon, USA) as the fluorescence conjugated secondary antibody. Same procedure described under immunocytochemistry was adopted in staining and visualization. For quantitative analysis of DNA damage, slides for each test sample were photomicrographed randomly as ten fields per sample and green fluorescent stained cells (positive for Phospho-Histone H2A.X -DNA damage foci) were counted manually. Total cells were counted according to the blue colour DAPI stained nuclei. Percentage of DNA

damage foci was calculated by number of positive cells for Phospho-Histone H2A.X over total number of cells per test sample.

To find out whether oxidative stress induced by cytokines causes DNA damage in IHOK, above test was repeated with or without an antioxidant L- Glutathione reduced 5 mM (Sigma-Aldrich, St Louis, MO, USA). All tests were performed three times.

To detect Phospho-Histone H2A.X in paraffin sections, OSF, NOM and human colon cancer (Positive control) tissues were stained using a similar procedure as mentioned under immunohistochemistry. Primary antibody Phospho-Histone H2A.X was applied in 1:100 dilution at 4°C overnight and ImmPRESS™ Reagent Kit-anti rabbit (Vector Laboratories, CA, USA) was used according to manufacture's protocol. Immunoperoxidase stained cells in oral epithelium of OSF and NOM were visualized and photomicrographed (Olympus Corp, Tokyo, Japan). Rabbit IgG (DakoCytomation, Denmark) was used instead of primary antibody in the negative control.

#### **14. Detection of Oxidative DNA Damage**

To detect oxidative DNA damage caused by cytokines, OxyDNA assay kit (Caibiochem, CA, USA) consisted of FITC-conjugated probe specific for 8-oxoguanine (8-oxoG) was utilized. Oxidative DNA damage was also observed in paraffin sections of OSF and NOM. Oxidative DNA damage caused by cytokines in IHOK was assessed by both flow cytometry and fluorescence microscopy as previously reported (Maniscalco et al., 2005; Roper et al., 2004).

Briefly, IHOK treated with cytokines in combination for 72 h (as described in FACS analysis) were harvested as  $1 \times 10^6$  cells per sample and fixed with 2% paraformaldehyde and then permeabilized with ice-cold 70% ethanol. Then according to the manufacturer's protocol the cells were washed with

special wash solution and 100µl of 8-oxoG FITC conjugate (1:10 dilution) was added to each cell pellet and incubate in the dark for 1 hr. There after the cells were washed again in wash solution and DW and fluorescence intensity was read using flowcytometer at an excitation wavelength of 495 nm (Becton Dickinson, CA, USA). Media alone served as negative control and 10 µM H<sub>2</sub>O<sub>2</sub> served as the positive control. Three individual tests were performed.

For fluorescence microscopy, IHOK 1×10<sup>4</sup> grown using F media in Lab-Tek chamber slides, were treated with cytokines for 72 h, individually and in combination as for FACS analysis. After stimulation, cells were fixed and permeabilized as above mentioned and followed by two washes with PBS and wash solution. Thereafter, the cells were stained using 8-oxoG FITC conjugate (1:10 dilution) at 4 °C over night. Slides were also stained with 10 µg/ml DAPI and photomicrographed using confocal microscopy (LSM510 Meta, Carl Zeiss, Jena, Germany). Test was performed three times.

Staining of NOM and OSF tissues with 8-oxoG FITC conjugate was carried out as previously reported (Maniscalco et al., 2005; Roper et al., 2004). In brief, NOM and OSF tissue sections were deparaffinized and rehydrated as described under immunohistochemistry and autoclaved for 20 min in 50 mM Tris EDTA buffer (pH 9) after which sections were allowed to cool to room temperature. Then sections were blocked and incubated overnight with 8-oxoG FITC conjugate binding protein (1:10 dilution) at 4°C. Thereafter slides were stained with 10 µg/ml DAPI and photomicrographed using confocal microscopy (LSM510 Meta, Carl Zeiss, Jena, Germany).

## **15. Detection of cell ploidy change by flowcytometry (FACS)**

IHOK exposed to 10 ng/ml concentration of cytokines (GRO-α, IL-6, and IL-8) individually and in combination (GRO-α + IL-6, GRO-α +IL-8, and GRO-α + IL-6 +IL-8) together with control (media

only) for 72 h in F media, and subjected to fluorescence activated cell sorting (FACS) to analyze the cell ploidy status. In brief, IHOK cells grown in 100 mm culture dishes were treated with cytokines for 72 h and at the confluence of 80% - 90%, the cells were washed twice with PBS, trypsinized and collected in ice cold PBS. The cells were then re-suspended in 500 µl of ice cold ethanol in PBS (1:1 dilution) and maintained at 4 °C for 2 h. Prior to analysis, the cells were washed twice with ice cold PBS, re-suspended in 500 µl of ice cold PBS, treated with 1 mg/ml RNase A (Roche, GmbH, Germany) and kept at 37 °C for 30 min. Subsequently, propidium iodide [PI] (Sigma, Mo, USA) at a final concentration of 100 µg/ml was added to the cell suspensions, and then incubated on ice for 30 min and analyzed in a flow cytometer (Becton Dickinson, CA, USA). Cell ploidy in the test samples was analyzed using Modtif software (Becton Dickinson) and four independent testes were performed.

## **16. Wound healing assay**

To detect whether these cytokines (GRO- $\alpha$ , IL-6, and IL-8) promote cell migration, wound healing assay was carried out as previously reported (Che, et al., 2010; Jung et al., 2010). IHOK cells and HSC3 OSCC cells were utilized in the assay. In brief, IHOK and HSC3 cells were grown in 6 well culture plates overnight up to around 90 % confluence in growth media containing 1% FBS. The monolayer was wounded using sterile 200 µl pipette tip and then washed with PBS twice.

Subsequently fresh media containing various concentrations of cytokines (10 ng/ml) was added to the wounded monolayers with or without respective neutralizing antibodies (Mouse monoclonal anti-human antibodies, R&D Systems, MN, USA) and incubated for 24 h allowing cells to invade the wound. Photomicrographs were taken just after creating the wound and at desired time intervals and wound closure was evaluated. Experiment was performed three times independently.

## **17. Statistical Analysis**

Statistical analysis was done when ever applicable, by student's t test and one way ANOVA, using SPSS software version 17.0, to determine the statistical significance between measurements. p value of <0.05 was considered significant.

### **III. RESULTS**

#### **1. Cytotoxicity assessment of ANE**

hNOF and hTERT-hNOF were exposed to concentration gradient of ANE (10  $\mu\text{g/ml}$ , -160  $\mu\text{g/ml}$ ) for 96 h and then were assessed using MTT assay. During first 24 h both hNOF and hTERT-hNOF did not show any cytotoxic effects, but growth activity was stimulated in all concentrations (Figure 2A and Figure 2B). After 72 h both types of fibroblasts showed growth retardation to ANE concentration over 40  $\mu\text{g/ml}$ . We selected 30  $\mu\text{g/ml}$  and 40  $\mu\text{g/ml}$  of ANE concentration for our study to stimulate fibroblasts as these concentrations did not show any significant cytotoxic effects over fibroblasts for 96 h by MTT assay (Figure 2A).

2A.

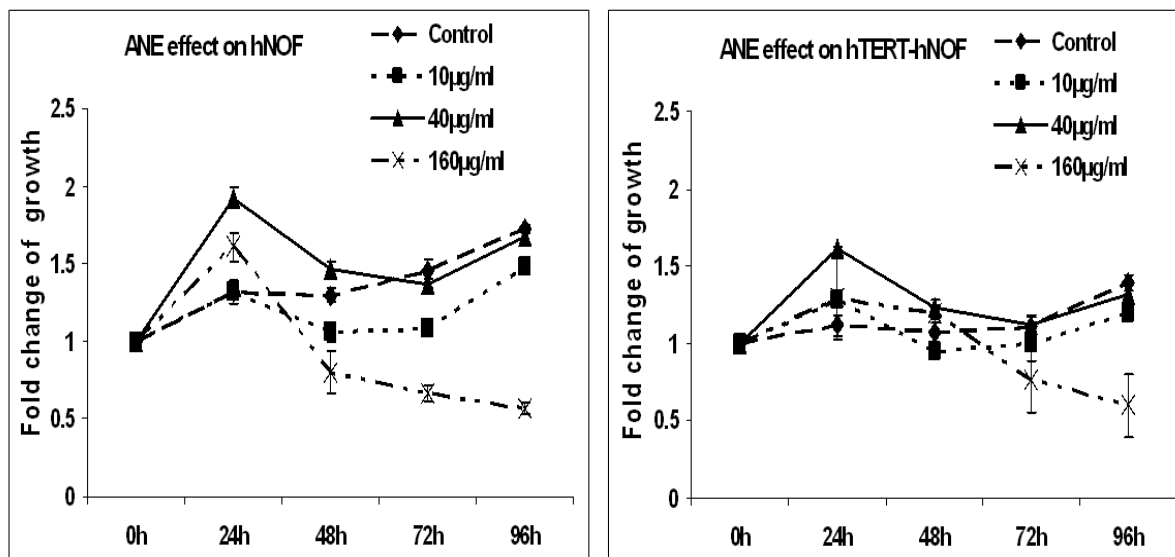


**Fig. 2.** Cytotoxicity assessment of ANE on fibroblasts

**Fig. 2A.** hNOF and hTERT-hNOF were treated with ANE and growth rate was measured using MTT assay. ANE 10 µg/ml, 40 µg/ml, and 160 µg/ml concentration gradient was used. Media only served as the negative control. In both hNOF and hTERT-hNOF, 10 µg/ml to 40 µg/ml of ANE showed no significant cytotoxicity. 160 µg/ml of ANE caused toxic effects after 24 h. Results were reported as the mean  $\pm$  SD relative to control of triplicate assays.

**2B.**

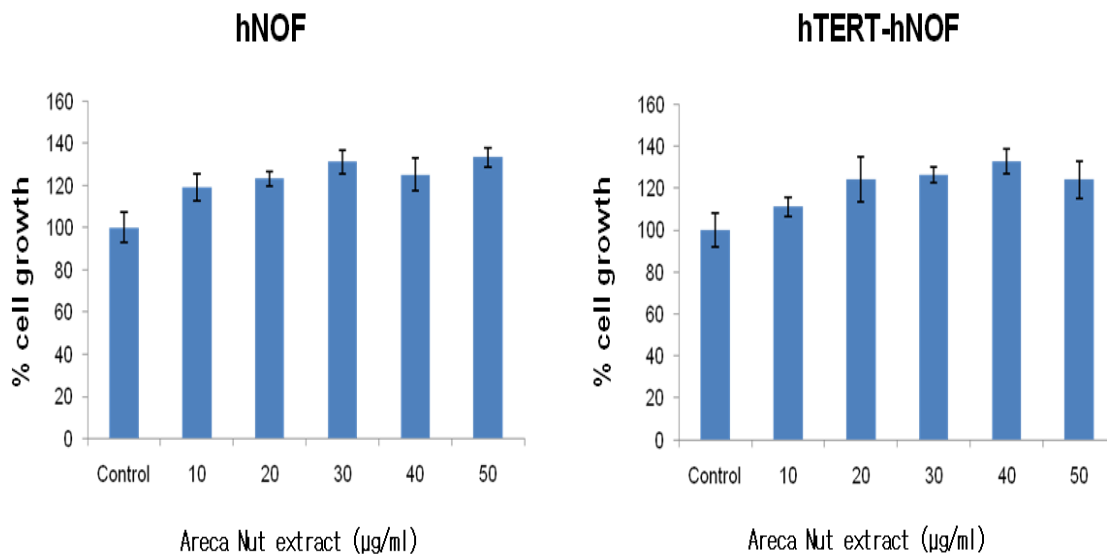
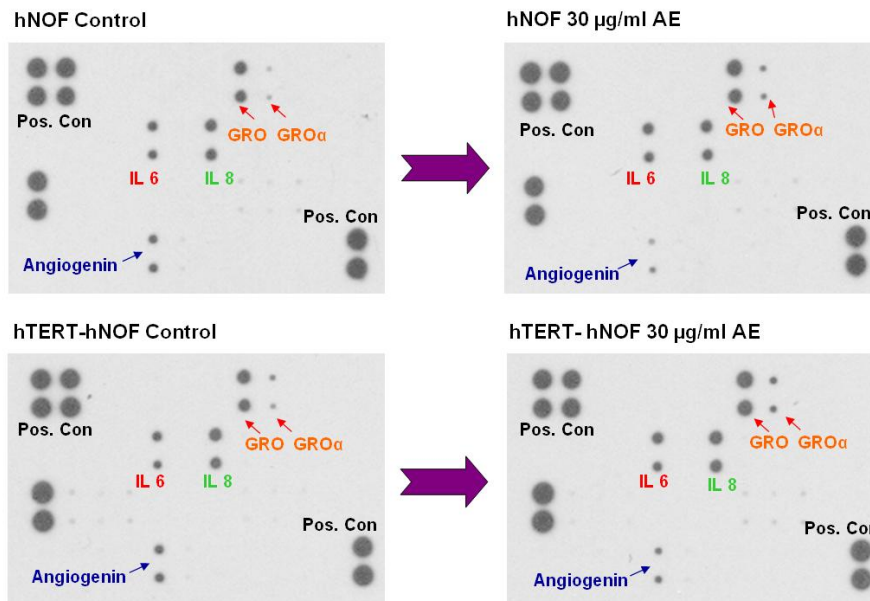


**Fig. 2B.** Cell viability of hNOF and hTERT-hNOF treated with ANE tested with MTT assay after 24 h. 10 µg/ml – 50 µg/ml of ANE concentration gradient was used. These ANE concentrations shown to be causing somewhat increased proliferation in hNOF and hTERT-hNOF, compared to the control. Percentage of cell growth is expressed relative to the control (media only).

## **2. Screening of cytokines secreted from ANE- stimulated fibroblasts**

Using RayBio® Human Cytokine Antibody Array 3 kit, CM taken from ANE-stimulated hNOF and hTERT-hNOF for 24 h were tested. Compared to control, both 30 µg/ml and 40 µg/ml ANE stimulated fibroblasts gave identical results. Moreover both hNOF and hTERT-hNOF showed same cytokine secretion pattern upon ANE stimulation. In detail, compared to control, both cytokine antibody arrays treated with CM from ANE- stimulated hNOF and hTERT-hNOF showed up-regulation of the expressions of GRO- $\alpha$ , IL-6 and IL-8 and down-regulation of angiogenin (Figure 3A). Schematic representation of the cytokines tested was shown in Figure 3B.

3A.



3B.

	a	b	c	d	e	f	g	h	i	j	k	l
1	Pos	Pos	Neg	Neg	ENA-78	GCSF	GM-CSF	GRO	GRO-α	I-309	IL-1α	IL-1β
2	Pos	Pos	Neg	Neg	ENA-78	GCSF	GM-CSF	GRO	GRO-α	I-309	IL-1α	IL-1β
3	IL-2	IL-3	IL-4	IL-5	IL-6	IL-7	IL-8	IL-10	IL-12	IL-13	IL-15	IFN-γ
4	IL-2	IL-3	IL-4	IL-5	IL-6	IL-7	IL-8	IL-10	IL-12	IL-13	IL-15	IFN-γ
5	MCP-1	MCP-2	MCP-3	MCSF	MDC	MIG	MP-1β	RANTES	SCF	SDF-1	TARC	TGF-β
6	MCP-1	MCP-2	MCP-3	MCSF	MDC	MIG	MP-1β	RANTES	SCF	SDF-1	TARC	TGF-β
7	TNF-α	TNF-β	EGF	IGF-1	Ang	OSM	Tpo	VEGF	PDGF β	Leptin	Neg	Pos
8	TNF-α	TNF-β	EGF	IGF-1	Ang	OSM	Tpo	VEGF	PDGF β	Leptin	Neg	Pos

**Fig. 3.** Cytokine antibody array to screen cytokine secretion by ANE-stimulated fibroblasts

**Fig. 3A.** Cytokine antibody array performed to screen cytokines secreted from ANE stimulated hNOF and hTERT-hNOF . Both hNOF and hTERT-hNOF showed increased secretion of GRO-α, IL-6 and IL-8 and down-regulation of angiogenin.

**Fig. 3B.** Schematic representation of the results of the human cytokine antibody array after treatment with CM of ANE stimulated fibroblasts.

### 3. Assessment of cytokine secretion by ELISA

Cytokines secreted from ANE-stimulated hNOF and hTERT-hNOF were measured at 24 h and 72 h intervals using sandwich ELISA method. GRO- $\alpha$  secretion of ANE-stimulated fibroblasts was more prominent in hNOF compared to hTERT-hNOF during early exposure (Figure 4A). IL-6 secretion also shown to be increased in ANE-treated hNOF and hTERT-hNOF during early exposure to ANE, except hTERT-hNOF showed somewhat reduction after 72 h stimulation (Figure 4B). ANE stimulation caused increase IL-8 secretion in both hNOF and hTERT-hNOF in early exposure. After 72 h exposure of hTERT-hNOF failed to show marked increase in IL-8 secretion (Figure 4C). Angiogenin secretion from hNOF and hTERT-hNOF in early exposure of ANE seems to be reduced but not very significant (Figure 4D). Results shown are representative of multiple repeats (means  $\pm$  SD of triplicates).

#### 4A.

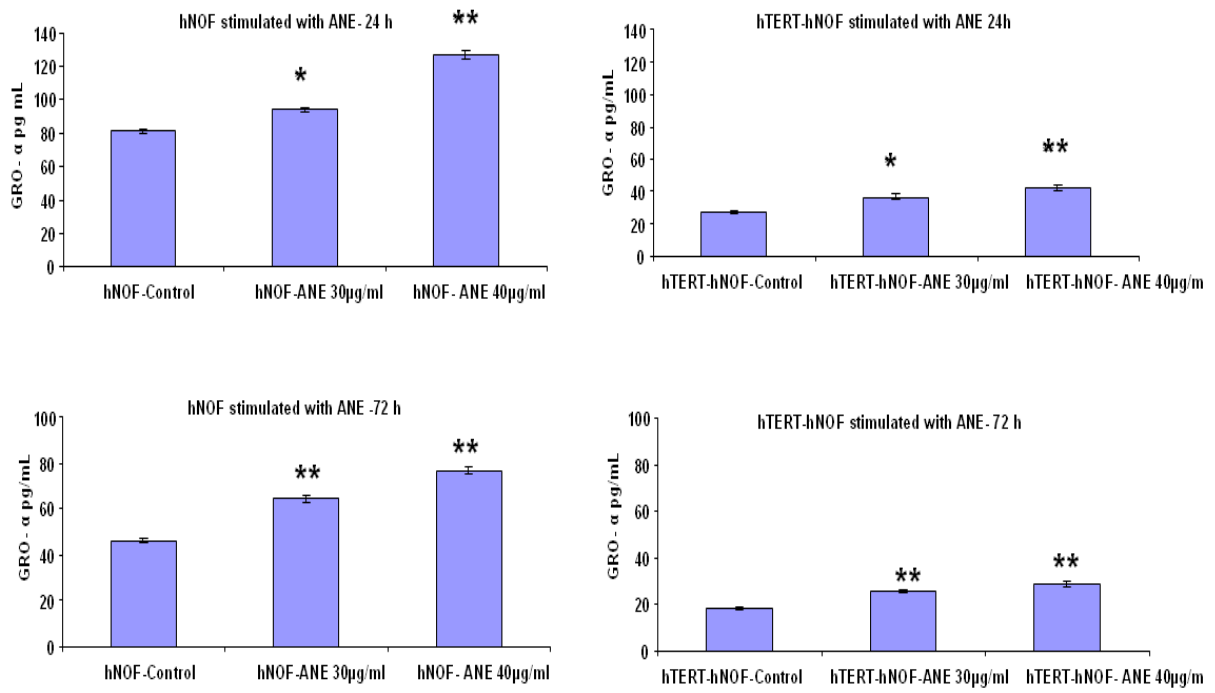


**Fig. 4.** Assessment of cytokine secretion by ANE-stimulated fibroblasts by ELISA

**Fig. 4A.** GRO- $\alpha$  secretion of ANE-stimulated fibroblasts was measured by ELISA. Both hNOF and hTERT-hNOF were stimulated for short term. GRO- $\alpha$  secretion was always found significantly increased compared to control. Results were reported as the mean  $\pm$  SD of triplicate assays. Cytokine levels were expressed in pg/ml per  $1 \times 10^6$  cells. (\* designates p value of  $< 0.05$  and \*\* designates p value  $< 0.01$ )

**4B.**

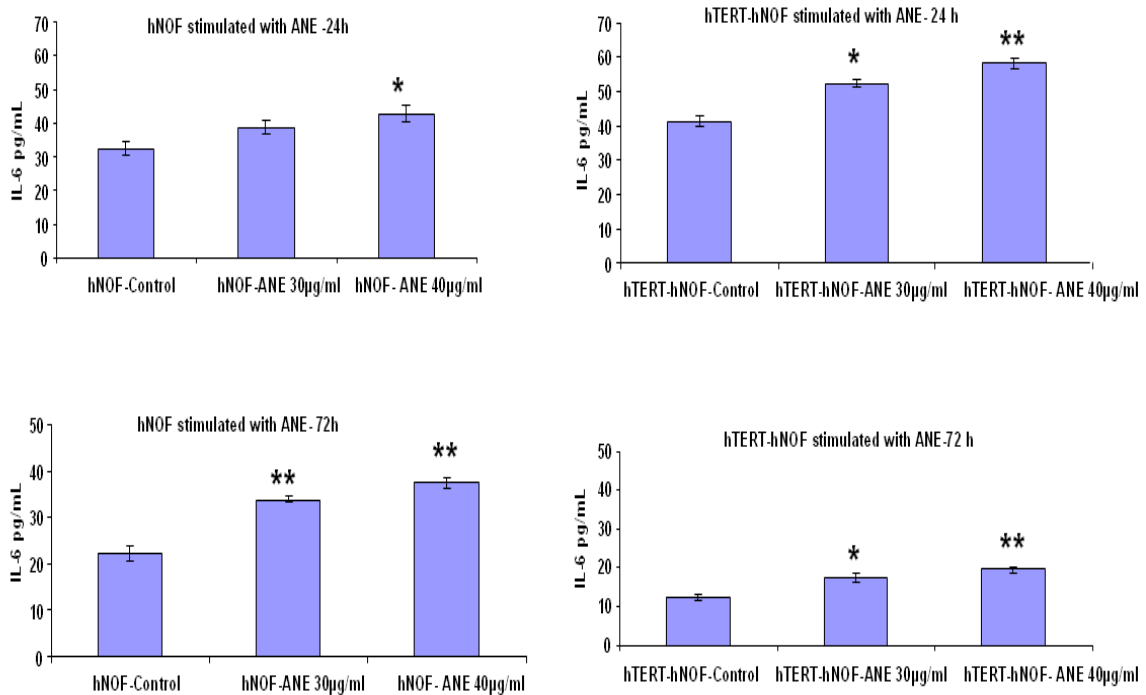


**Fig. 4B.** IL-6 secretion of ANE-stimulated fibroblasts was measured by ELISA. Both hNOF and hTERT-hNOF were stimulated for short term. IL-6 secretion was always found significantly increased compared to control. Results were reported as the mean  $\pm$  SD of triplicate assays. Cytokine levels were expressed in pg/ml per  $1 \times 10^6$  cells. (\* designates p value of  $< 0.05$  and \*\* designates p value  $< 0.01$ )

4C.

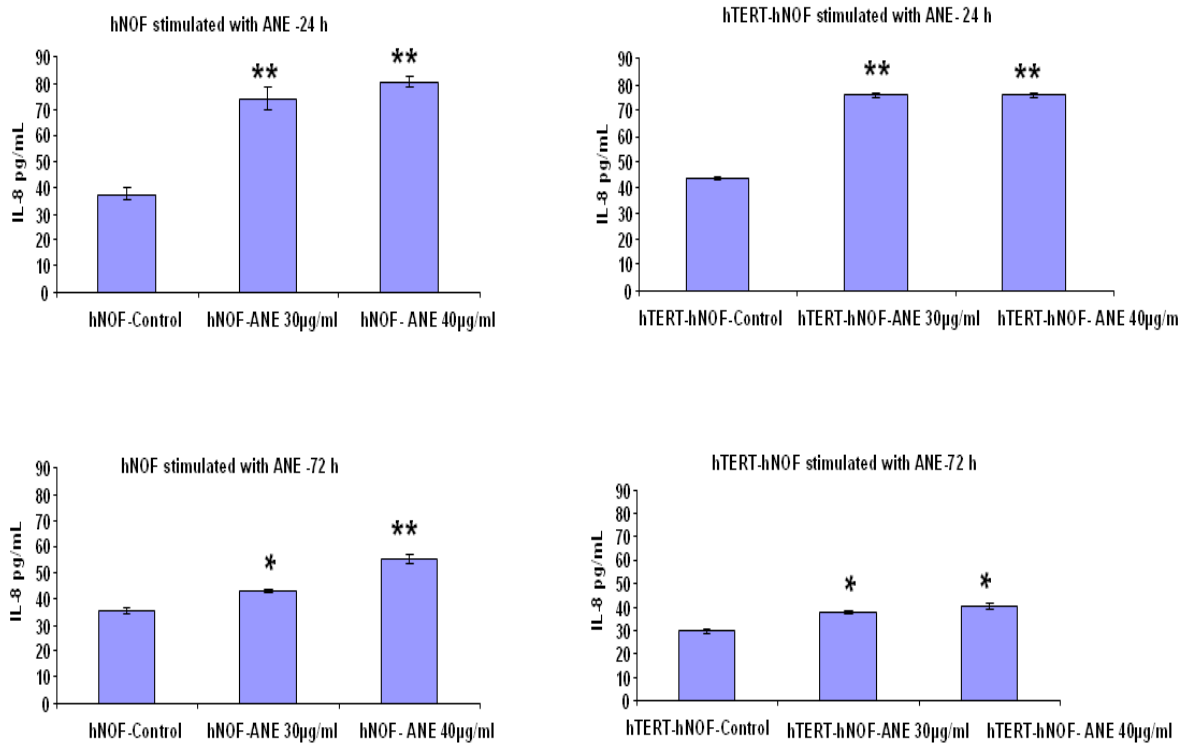


**Fig. 4C.** IL-8 secretion of ANE-stimulated fibroblasts was measured by ELISA. Both hNOF and hTERT-hNOF were stimulated for short term. IL-8 secretion was always found significantly increased compared to control. Results were reported as the mean  $\pm$  SD of triplicate assays. Cytokine levels were expressed in pg/ml per  $1 \times 10^6$  cells. (\* designates p value of < 0.05 and \*\* designates p value < of 0.01)

4D.

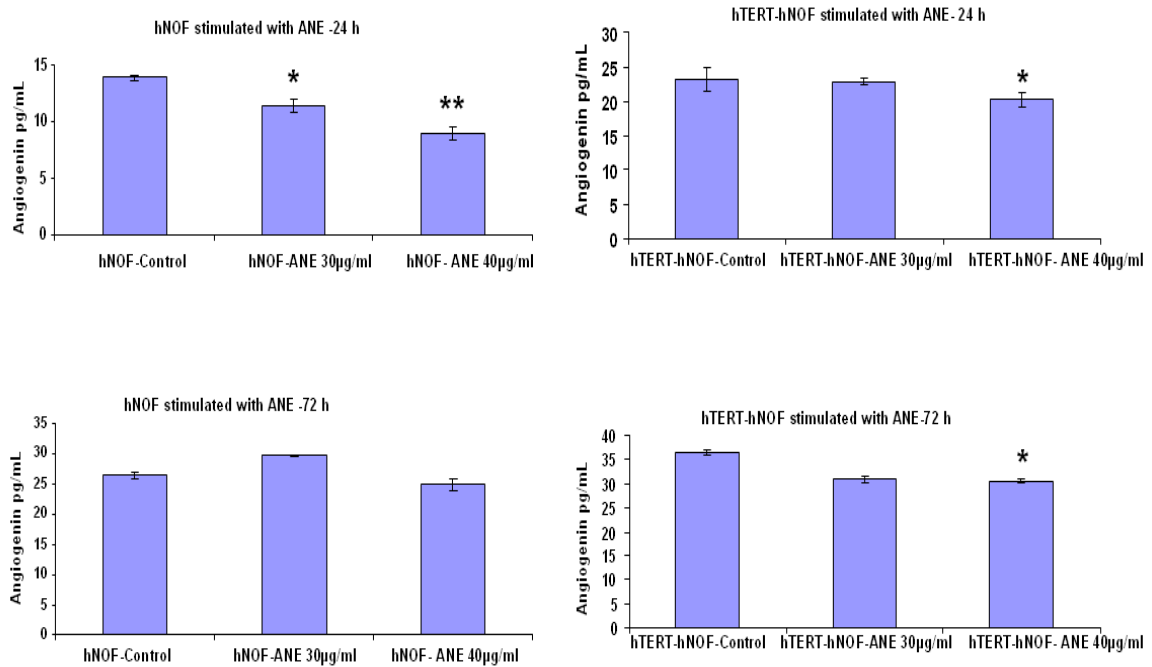


**Fig. 4D.** Angiogenin secretion of ANE-stimulated fibroblasts was measured by ELISA. Both hNOF and hTERT-hNOF were stimulated for short term. Angiogenin secretion was always found reduced compared to control in short term stimulation. Results were reported as the mean  $\pm$  SD of triplicate assays. Cytokine levels were expressed in pg/ml per  $1 \times 10^6$  cells. (\* designates p value of  $< 0.05$  and \*\* designates p value  $< 0.01$ )

#### **4. Detection of mRNA expression of cytokines in fibroblasts by RT-PCR**

mRNA levels of corresponding cytokines were assessed with RT-PCR . Representative results were shown. RT-PCR results were failed to show exact correspondence with cytokine secretion pattern observed in ELISA and immunofluorescence studies. mRNA expression of angiogenin showed slight reduction with ANE. Early exposure to ANE showed slight increase in GRO- $\alpha$ , IL-6 and IL-8 mRNA levels in hNOF (Figure 5).

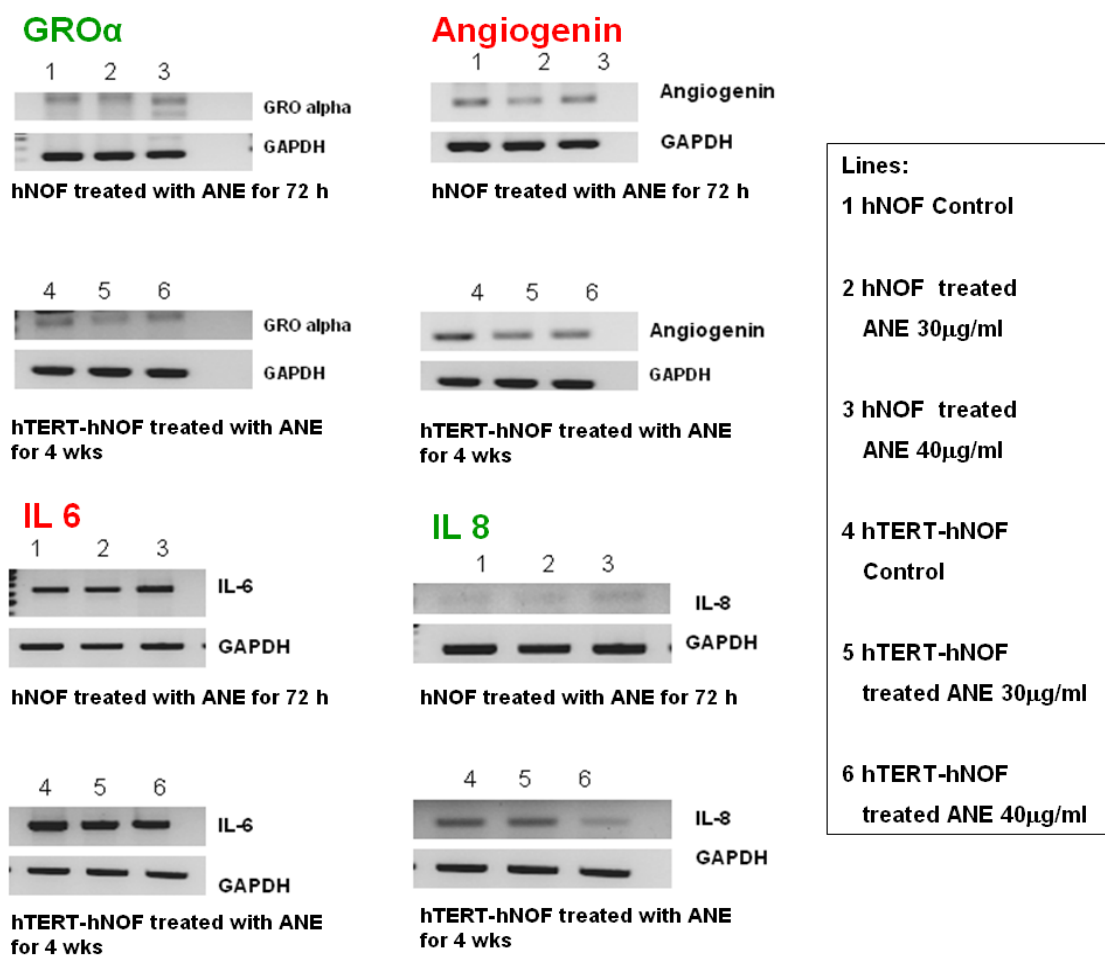
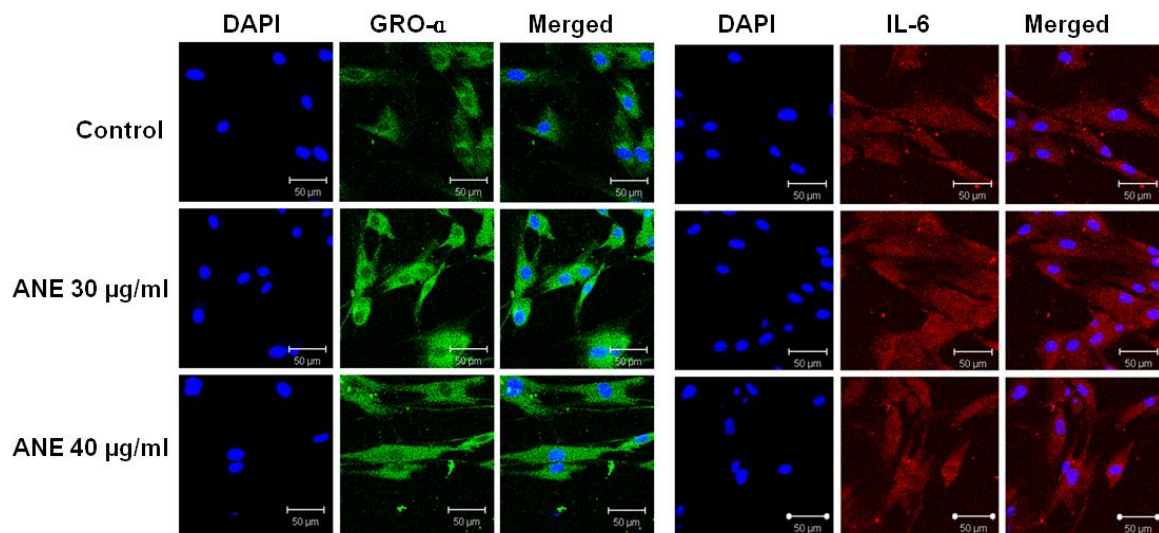


**Fig. 5.** Relative mRNA expressions of the cytokines in ANE-stimulated hNOF and hTERT hNOF. GAPDH served as the loading control. mRNA expression is not always compatible with the cytokine secretion pattern of ANE-stimulated fibroblasts.

## **5. Immunofluorescence staining to detect cytokine secretion**

Both hNOF and hTERT-hNOF stimulated with ANE were tested for expressions of GRO- $\alpha$ , IL-6, IL-8 and angiogenin using immunofluorescence. Compared to control, GRO- $\alpha$ , IL-6, and IL-8 expressions in ANE-treated hNOF and hTERT-hNOF showed relatively increased expressions in confocal microscopy (Figure 6). Only angiogenin expression in ANE-treated hNOF and hTERT-hNOF reduced compared to control. These patterns of expressions further validated the results of cytokine antibody array results (Figure 6).

6A.



6B

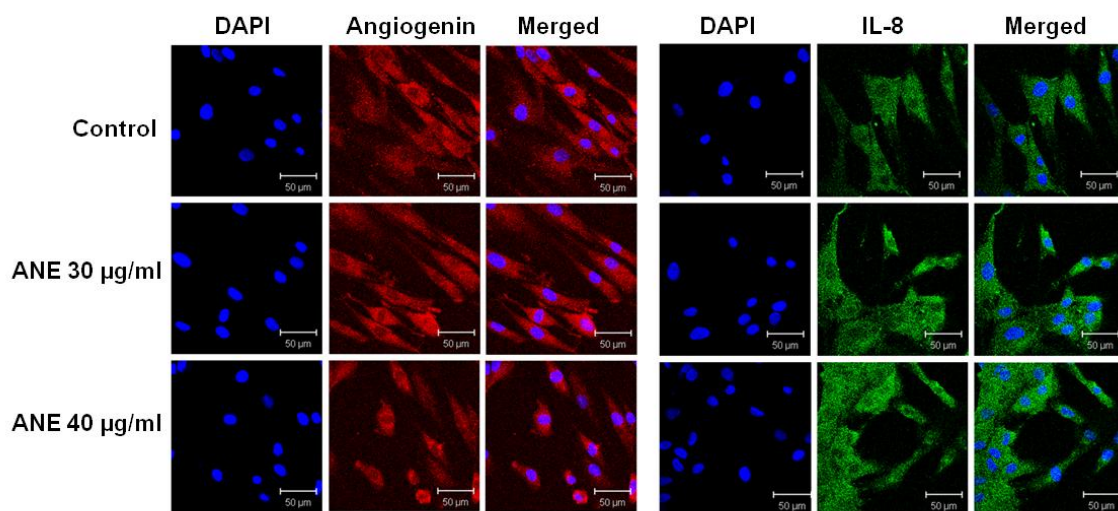


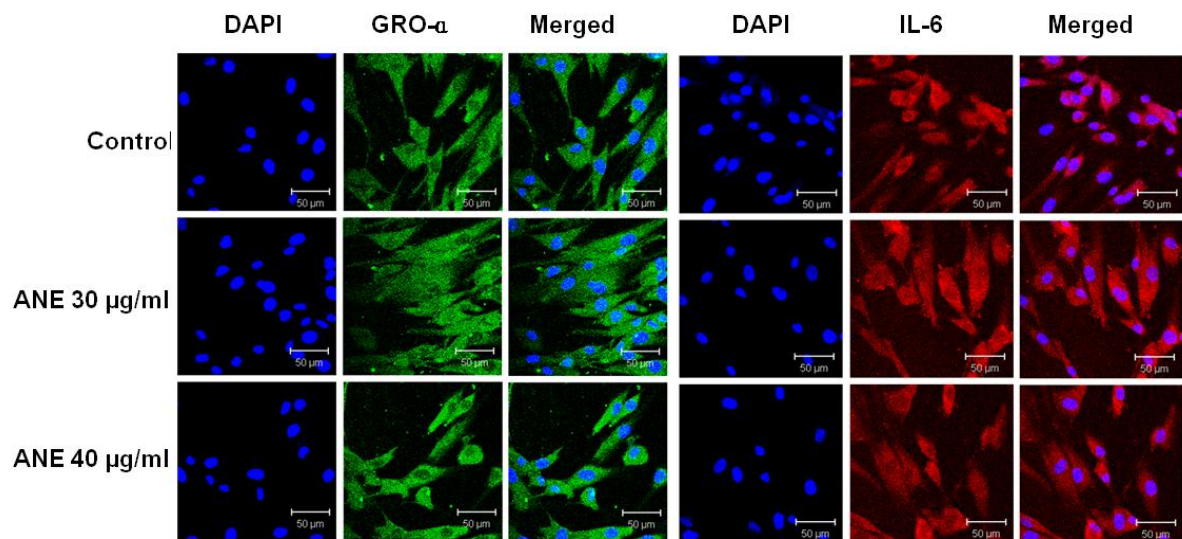
**Fig. 6.** Short-term ANE-stimulated hNOF and hTERT-hNOF stained for immunofluorescence

**Fig. 6A.** ANE caused increased GRO- $\alpha$  and IL-6 expressions in hNOF.

**Fig. 6B.** ANE caused reduced Angiogenin and increased IL-8 expressions in hNOF

(Representative photomicrographs, Scale bar 50 µm)

6C.



6D.

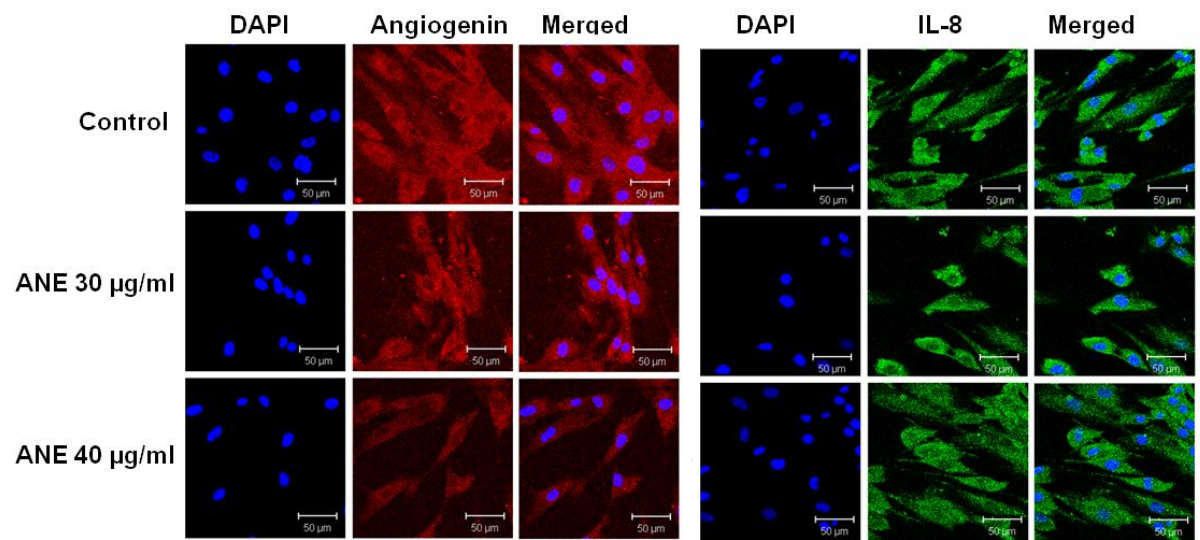


**Fig. 6C.** ANE caused increased GRO- $\alpha$  and IL-6 expressions in hTERT-hNOF.

**Fig. 6D.** ANE caused reduced Angiogenin and increased IL-8 expressions in hTERT-hNOF

(Representative photomicrographs, Scale bar 50  $\mu$ m)

## **6. Immunohistochemistry to detect cytokine expressions in human tissue**

H & E stained OSF and NOM studied to understand histology of OSF (Figure 7A).

Paraffin-embedded tissue taken from OSF patients and control subjects were subjected to immunoperoxidase staining against GRO- $\alpha$ , IL-6, IL-8 and angiogenin and visualized in light microscopy. Compared to NOM, OSF mucosal fibroblasts showed increased expressions of GRO- $\alpha$ , IL-6, and IL-8. Among them IL-6 and IL-8 showed more intense signaling. Angiogenin expression in OSF fibroblasts showed attenuated compared to NOM (Figure 7B). These findings supported *in vitro* results shown by ANE-stimulated fibroblasts.

7A.

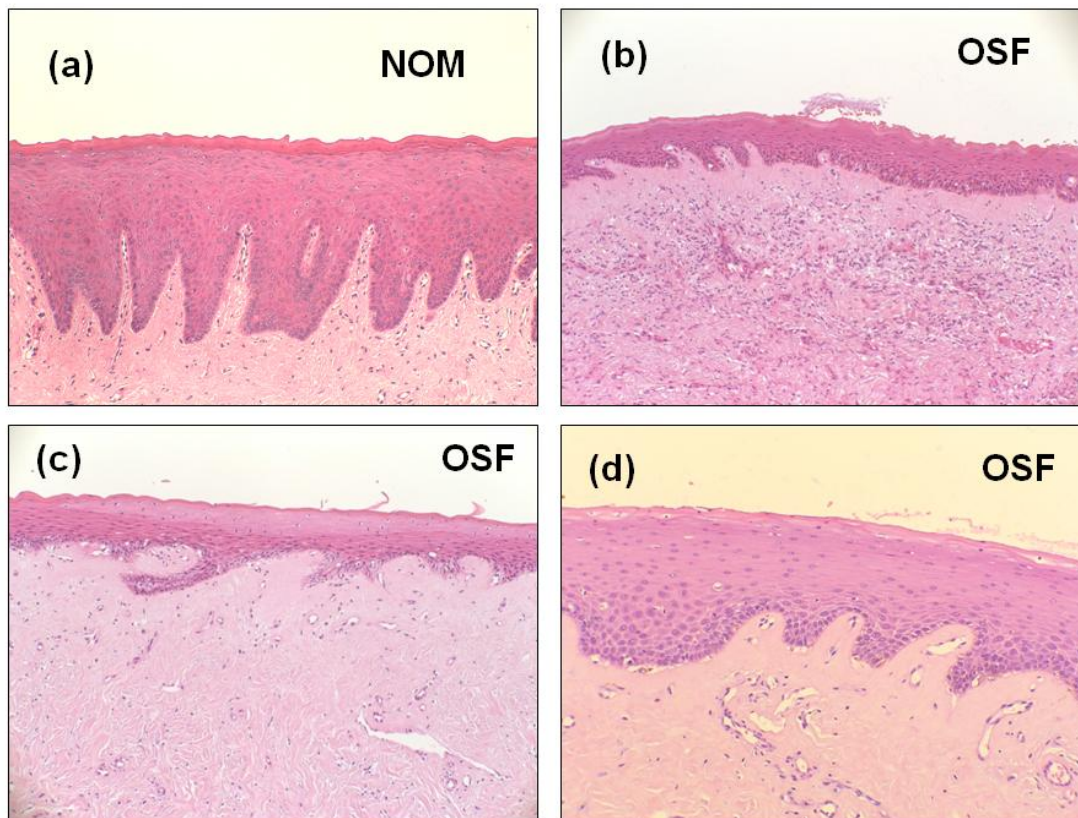


**Fig.7** H & E staining and immunoperoxidase staining of NOM and OSF tissues

**Fig. 7A.** . Histology of Normal Oral Mucosa (NOM) (a) and Oral Submucous Fibrosis (OSF) (b-d) by light microscopy. ( H&E Magnification X 100). Atrophic epithelium with loss of rete ridges (b and c), extensive fibrosis of submucosal tissues (b, c, and d), chronic inflammatory cell infiltration in early stages (b), and juxta-epithelial hyalinization (d) are hall marks of OSF histology.

7B.

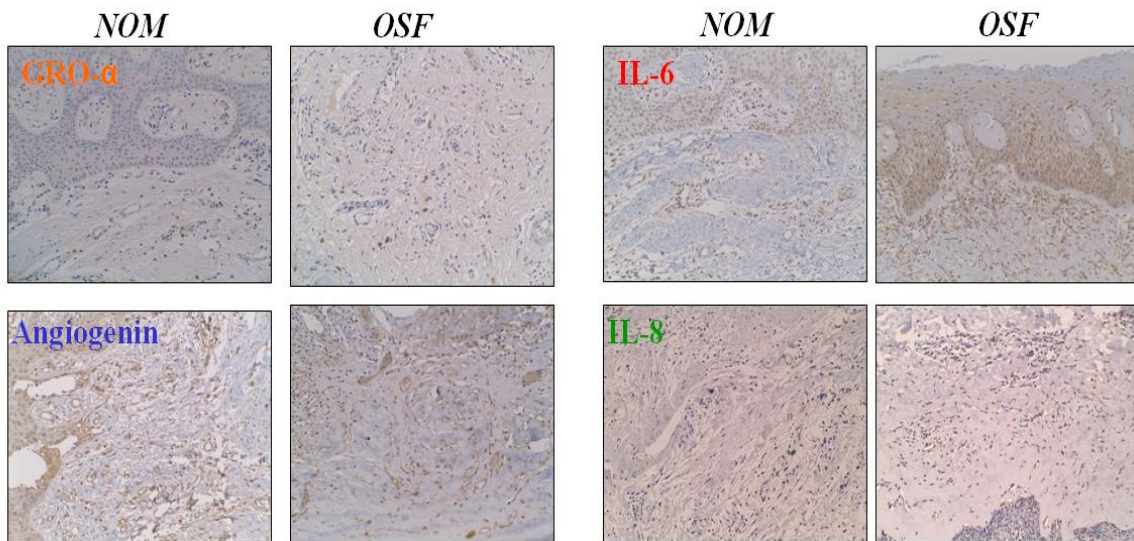


**Fig. 7B** Immunoperoxidase staining against GRO- $\alpha$ , IL-6, IL-8 and Angiogenin in OSF and NOM tissues. Compared to NOM, in OSF submucosal area showed increased expressions of GRO- $\alpha$ , IL-6, and IL-8. Angiogenin expression was reduced in OSF compared to NOM. (Representative photomicrographs, magnification X 200)

## **7. Senescence of long-term ANE-treated hTERT-hNOF**

hTERT-hNOF maintained over 8 wks continuously treating with ANE were subjected to Senescence-associated  $\beta$ -galactosidase staining. Compared to the control hTERT-hNOF cells which were simultaneously maintained with out ANE exposure, ANE-exposed hTERT-hNOF showed positive blue colour stained nuclei extensively in both 30  $\mu$ g/ml and 40  $\mu$ g/ml ANE-stimulated fibroblasts groups (Figure 8). Tests were preformed three times, i.e. three independent sets of cell lines were maintained over 8 wks with ANE exposure.

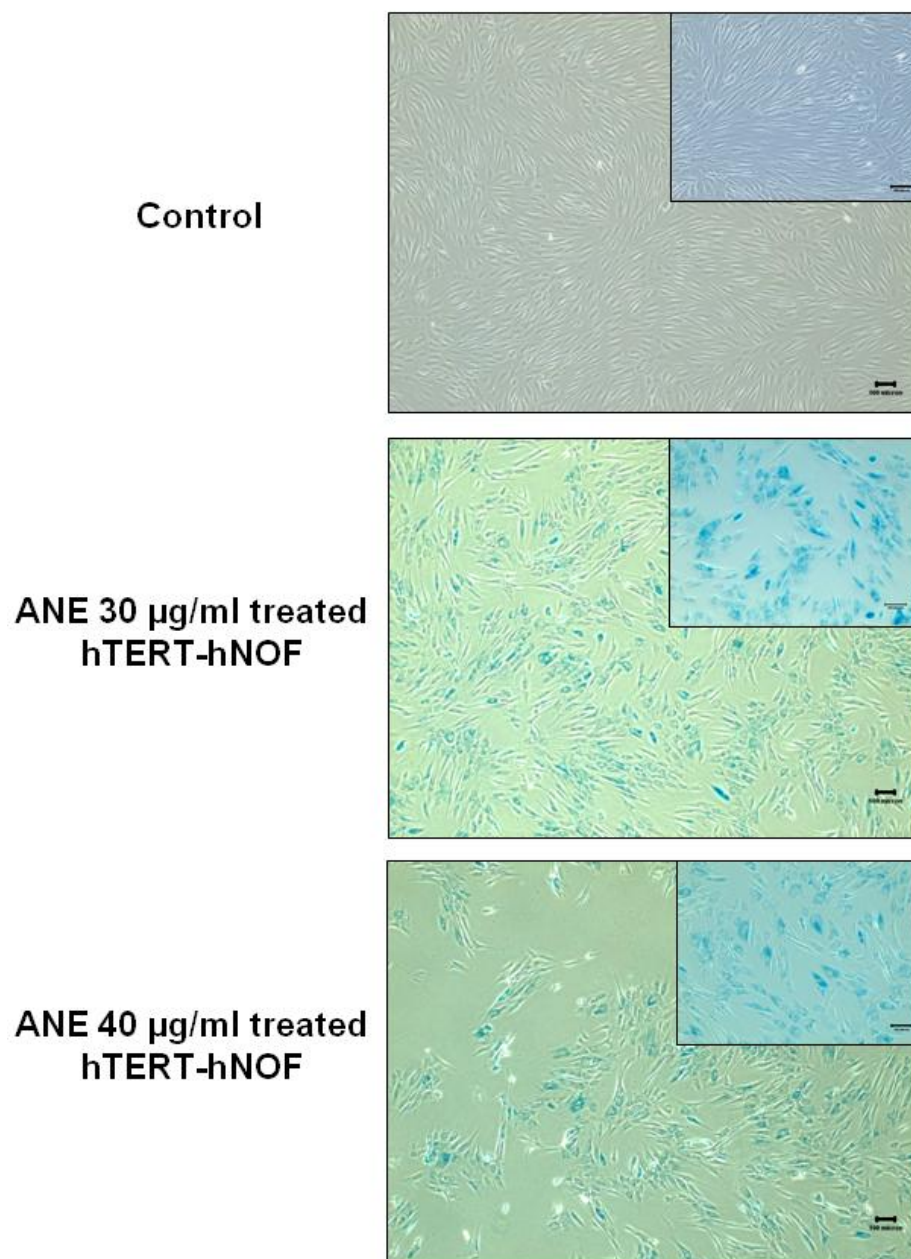


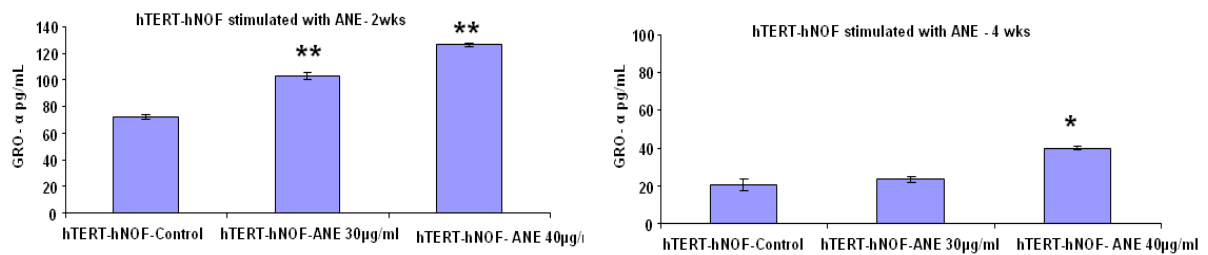
**Fig. 8.** Senescence-associated  $\beta$ -galactosidase staining of hTERT-hNOF maintained for 8 wks with ANE exposure. Compared to control, ANE treated fibroblasts revealed senescence by blue colour stained nuclei after 8 wks of ANE exposure. (Representative photomicrographs of three independent tests. Scale bar 50  $\mu\text{m}$ )

## **8. Cytokine secretion in long-term ANE-treated hTERT-hNOF**

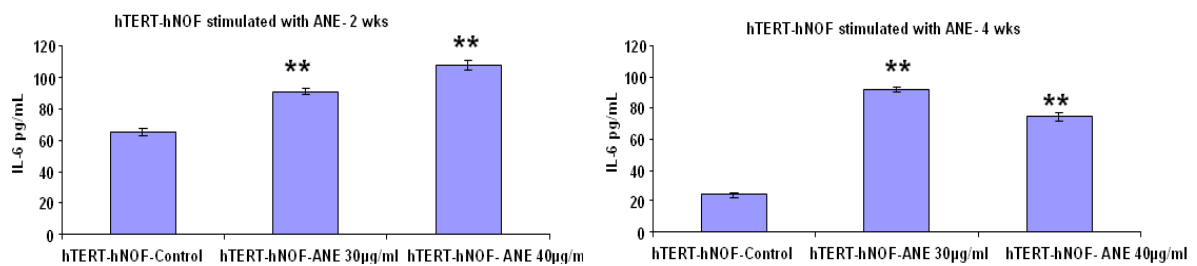
### **Assessed by ELISA**

Cytokines secreted from long term ANE-treated hTERT-hNOF were measured at 2wks and 4 wks intervals using sandwich ELISA method. GRO-  $\alpha$  secretion in 2 wks showed gradual increase compared to control. In 4 wks GRO-  $\alpha$  secretion showed gradual decrease but maintained at a higher level compared to controls (Figure 9A). IL-6 secretion also shown to be increased in ANE-treated hTERT-hNOF during both 2 wks and 4 wks stimulation compared to controls (Figure 9B). ANE stimulation caused increase IL-8 secretion in hTERT-hNOF in 2 wks and 4 wks (Figure 9C).

9A.



9B.



9C.

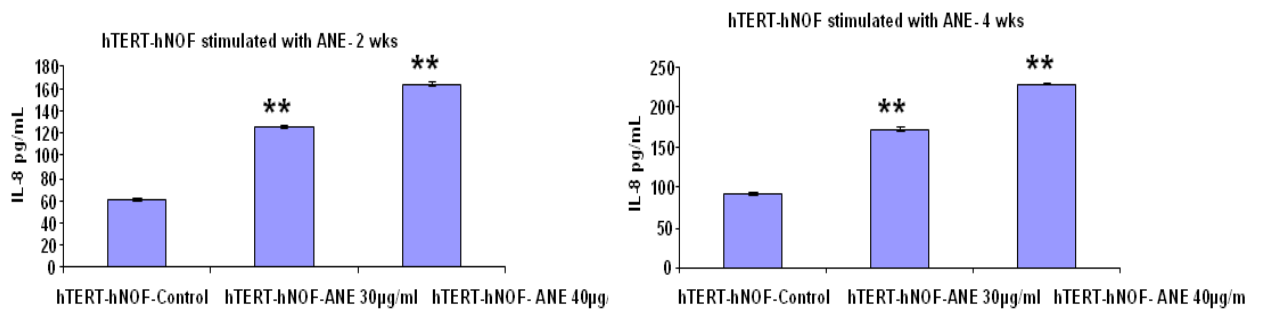


**Fig. 9** Cytokine secretion in long-term ANE-treated hTERT-hNOF

Long term ANE treatment caused increase GRO-α (9A), IL-6 (9B) and IL-8 (9C) production in hTERT-hNOF measured in 2wks and 4wks intervals. Results were reported as the mean ± SD of triplicate assays. Cytokine levels were expressed in pg/ml per  $1 \times 10^6$  cells.

(\* designates p value of < 0.05 and \*\* designates p value < of 0.01)

## **9. Cytokine secretion in long-term ANE-treated hTERT-hNOF**

### **Assessed by immunofluorescence**

hTERT-hNOF stimulated with ANE for 8wks were tested for expressions of GRO- $\alpha$ , IL-6, and IL-8 using immunofluorescence. Compared to control, GRO- $\alpha$ , IL-6, and IL-8 expressions in ANE-treated hTERT-hNOF showed relatively increased expressions in confocal microscopy (Figure 10). These patterns of expressions further validated the results of ELISA which was shown in long-term ANE exposure of hTERT-hNOF.

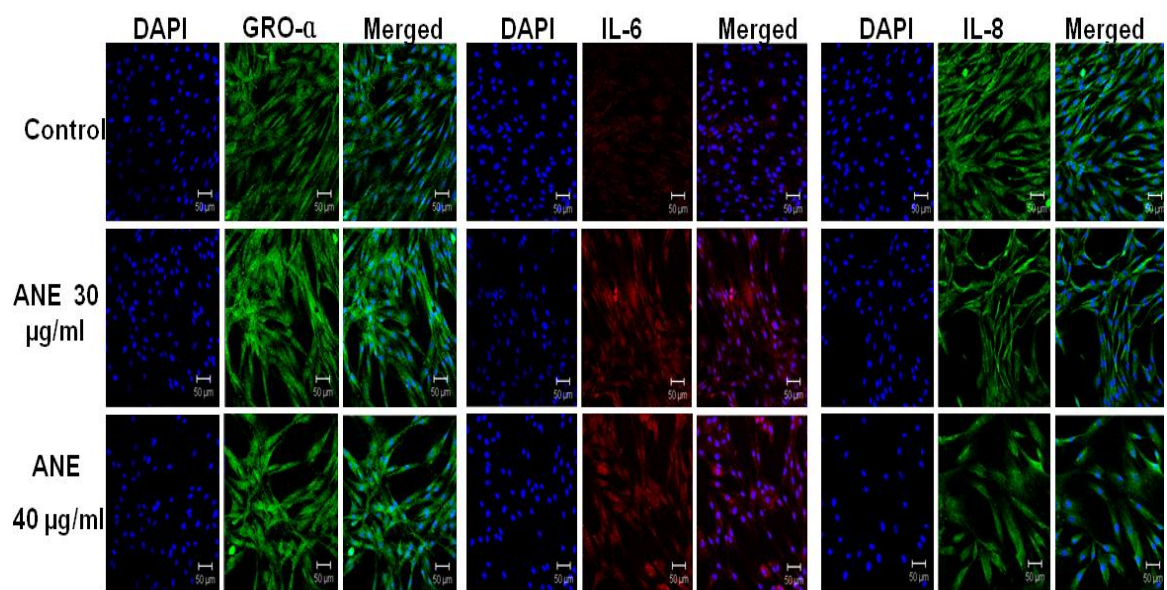


**Fig. 10.** Long-term ANE-stimulated hTERT-hNOF stained for immunofluorescence and visualized using confocal microscopy.

ANE caused increased GRO- $\alpha$ , IL-6, and IL-8 expressions in hTERT-hNOF

(Representative photomicrographs, Scale bar 50  $\mu$ m)

## 10. IHOK growth by cytokine treatment

IHOK exposed to cytokines in F media in 96 well plates were assessed by MTT assay for 96 h. 10 ng/ml concentration of cytokines (GRO- $\alpha$ , IL-6, and IL-8) individually and in combinations (GRO- $\alpha$  + IL-6, GRO- $\alpha$  +IL-8, and GRO- $\alpha$  + IL-6 +IL-8) did not show any significant toxic effect on growth of IHOK. Although IL-6 and IL-8 seems to have some stimulatory effect on IHOK growth compared to control, failed to show any significance.

(Figure 11). The results also showed 10 ng/ml concentration of recombinant cytokine was safe to be used in further study to stimulate IHOK *in vitro*.

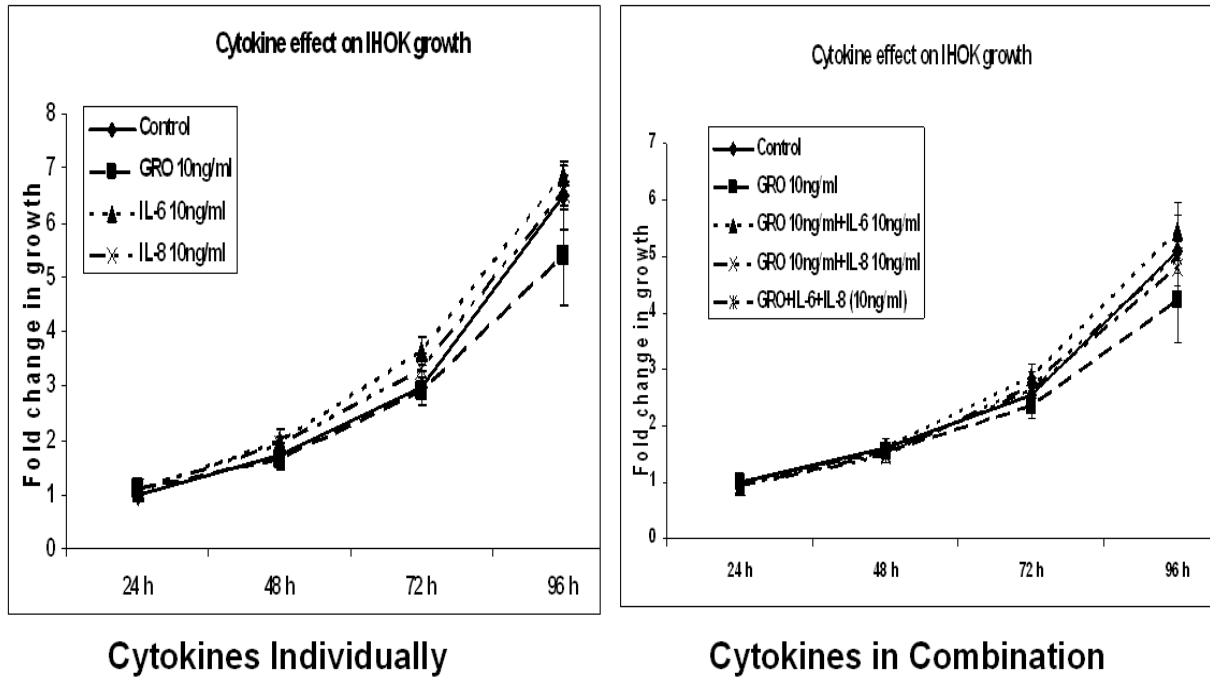


**Fig. 11.** Cytokine-treated IHOK were tested for proliferation by MTT assay. GRO- $\alpha$ , IL-6, and IL-8 individually or in combination did not cause any significant growth stimulation in IHOK at the treated concentrations. Results were reported as the mean  $\pm$  SD relative to control of triplicate assays.

## **11. ROS production in IHOK by cytokine treatment**

IHOK exposed to cytokines were tested for ROS generation using 2',7'-dichlorofluorescein diacetate (H<sub>2</sub>DCFDA) dye by FACS and confocal microscopy. When exposed to cytokines, IHOK produced ROS, which was confirmed by green fluorescent signals by confocal microscopy. Each cytokine individually (GRO- $\alpha$ , IL-6, and IL-8) and in combination induced ROS production in IHOK (Figure 12A). Further analyzed by FACS, also showed that cytokines were capable of causing ROS generation in IHOK compared to controls (Figure 12B).

12A.

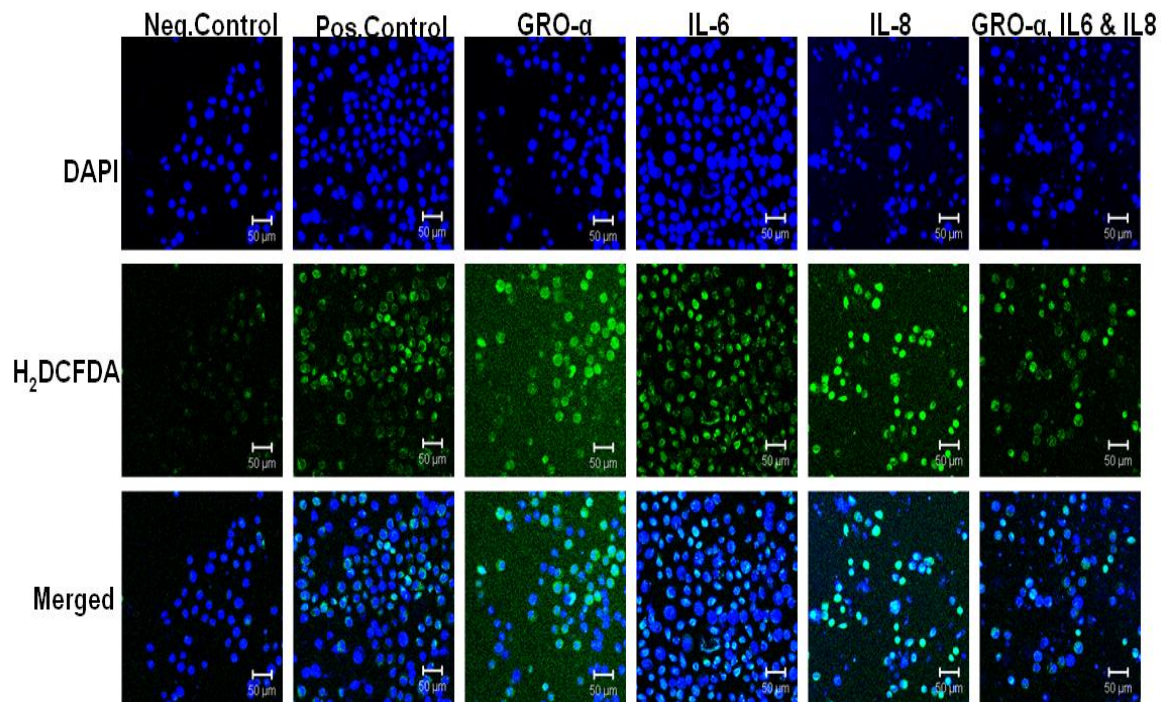


**Fig. 12.** Cytokines caused ROS generation in IHOK was detected using H<sub>2</sub>DCFDA dye

**Fig. 12A.** Cytokines caused ROS generation in IHOK was detected using H<sub>2</sub>DCFDA dye and visualized with confocal microscopy. Green fluorescent staining indicated cytokines individually (GRO- $\alpha$ , IL-6, and IL-8) and all together in combination showed inducing ROS production in IHOK. (Positive control- 10  $\mu$ M H<sub>2</sub>O<sub>2</sub>, Negative control- media only, Representative photomicrographs are shown of three tests. Scale bar 50  $\mu$ m)

12B.

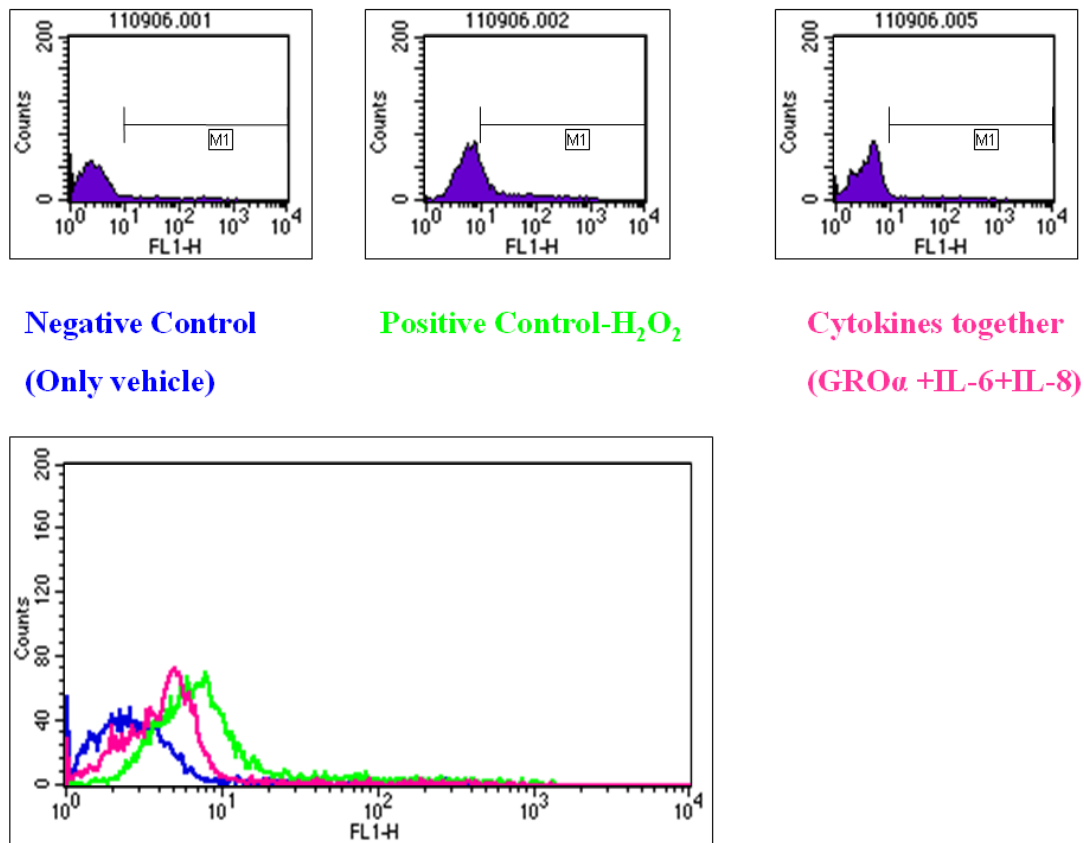


**Fig. 12 B.** ROS generation in cytokine-treated IHOK were measured using H<sub>2</sub>DCFDA dye by flowcytometry. Cytokines together caused increased intensity compared to negative control indicating generation of ROS.

## **12. Detection of DNA damage in IHOK treated by cytokines**

DNA damage in IHOK by cytokines was detected using DNA damage marker which specially recognizes DNA double strand breaks, Phospho-Histone H2A.X.

Using confocal microscopy, cytokine-exposed IHOK stained with Phospho-Histone H2A.X were visualized for fluorescent signals. It clearly showed the cytokines (GRO- $\alpha$ , IL-6, and IL-8) individually and all in combination causing DNA damage in IHOK cells (Figure 13A and 13B). Furthermore, it showed over 50% of DNA damage foci by manual cell counting, after IHOK were exposed to cytokines for 72 h (Figure 13B). This result was statistically significant ( $p < 0.05$ ).

13A.

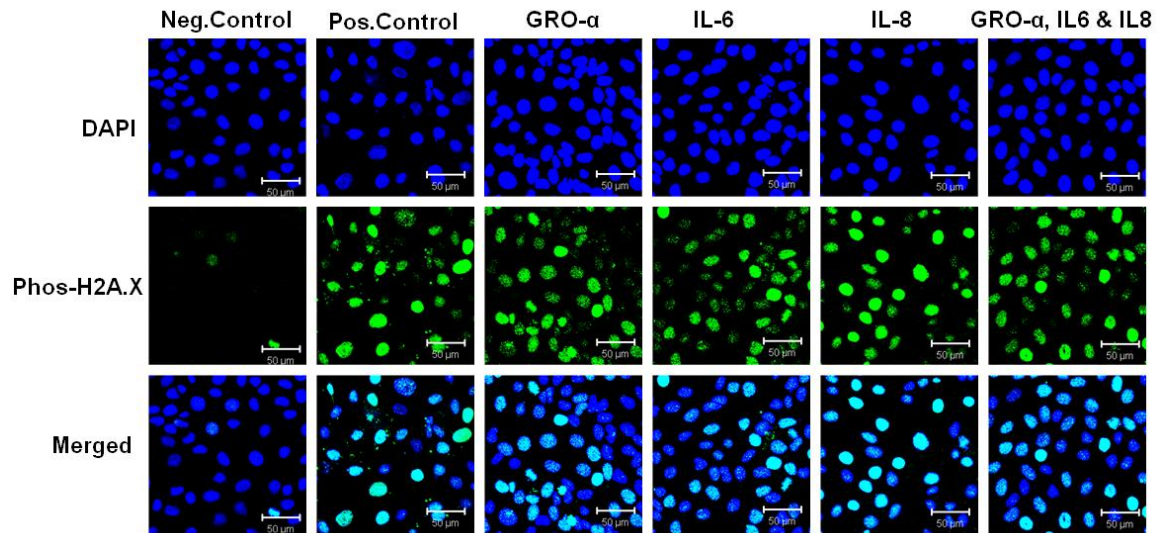


**Fig. 13.** Detection of DNA Damage by Phospho-Histone H2A.X in cytokine-treated IHOK.

**Fig .13A.** Immunofluorescent staining against Phospho-Histone H2A.X in IHOK visualized by confocal microscopy. Green fluorescent stained foci indicate DNA damage nuclei. Cytokines individually and in combination caused DNA damage in IHOK. (Positive control- 10  $\mu$ M H<sub>2</sub>O<sub>2</sub>, Negative control- media only. Representative data of three independent tests. Scale bar 50  $\mu$ m)

13B.

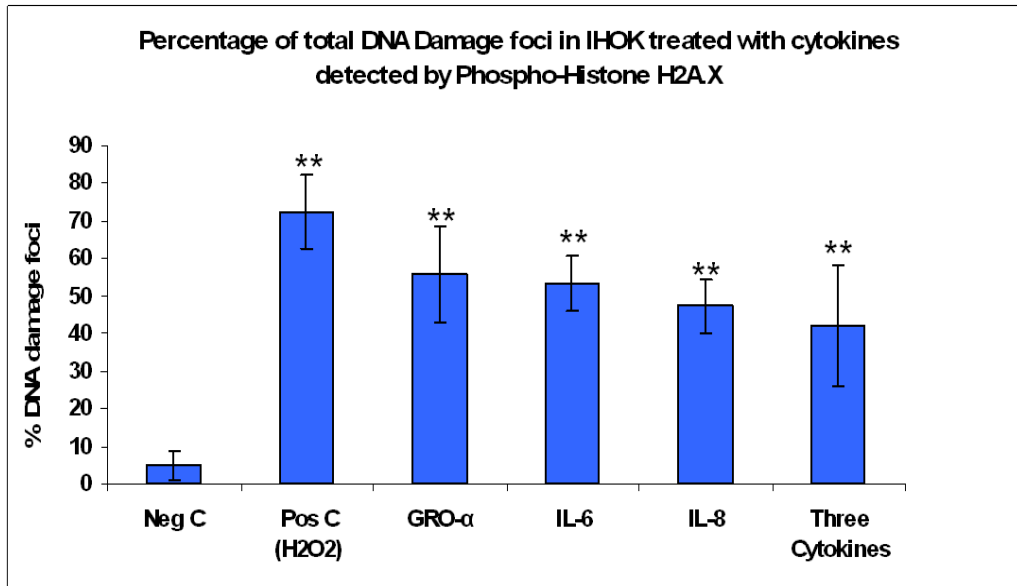


**Fig. 13B.** Detection of DNA Damage by Phospho-Histone H2A.X in cytokine-treated IHOK.

Quantitative analysis.

DNA damage foci in cytokine-treated IHOK found significantly increased compared to negative control. Results were reported as the mean percentage  $\pm$  SD relative to control of three assays.

(\*\* designates a p value of  $< 0.01$ )

### **13. ROS produced by cytokines causing DNA damage in IHOK**

To find out and confirm that, cytokine-induced DNA damage in IHOK is due to oxidative stress, cytokines-treated IHOK with or without an antioxidant (L-Glutathione reduced) were tested using DNA damage marker, Phospho-Histone H2A.X, using confocal microscopy. Green fluorescent signals were reduced in antioxidant-treated IHOK samples. It was clearly noticed that antioxidant treatment reduced cytokine-caused DNA damage in IHOK (Figure 14).

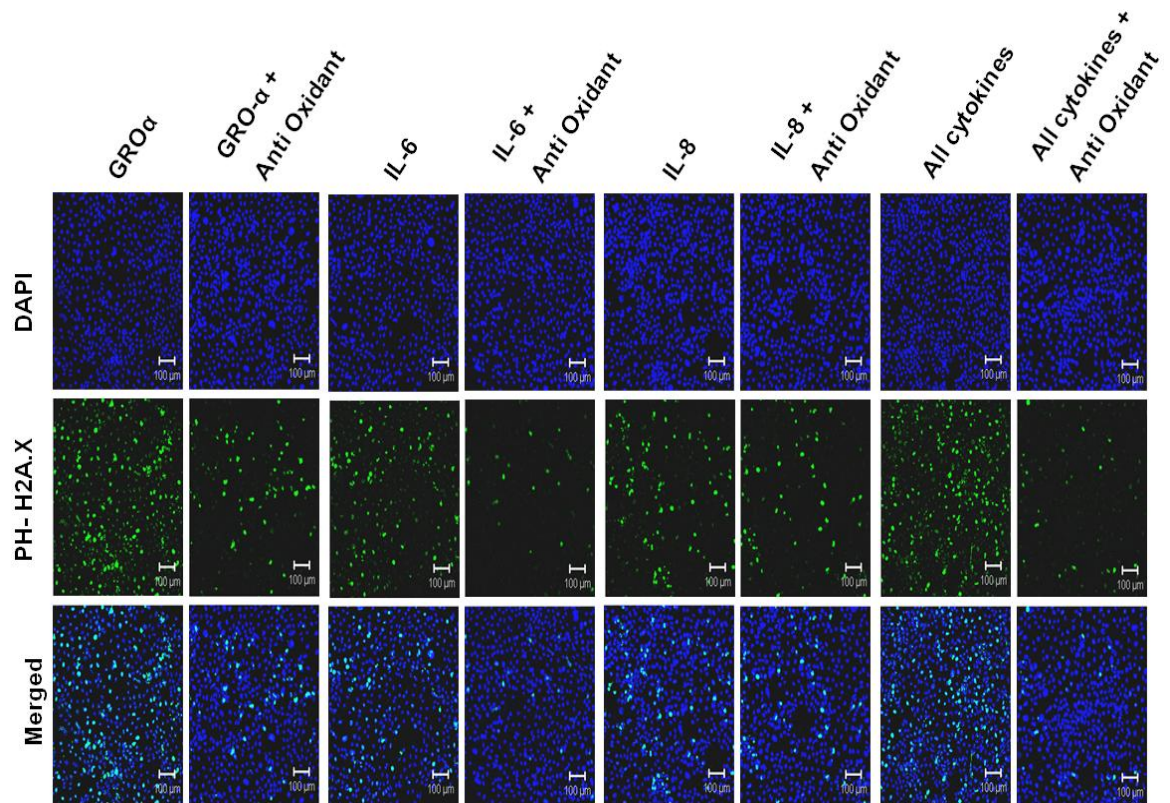


**Fig. 14.** Effect of Anti-Oxidant (Glutathione) in cytokine-induced DNA damage, measured with Phospho-Histone H2A.X visualized by confocal microscopy. Antioxidant treatment clearly reduced cytokines induced DNA damage in IHOK confirming that cytokines cause DNA damage through ROS production. Representative photomicrographs are shown of three tests. Scale bar 50  $\mu$ m)

#### **14. DNA damage in OSF tissue**

OSF and NOM tissues were stained using anti Phospho-Histone H2A.X antibody. Human colon cancer tissue served as positive control. Immunoperoxidase staining showed positively stained cells in OSF mucosa especially in basal cell layer of the epithelium. NOM was negative for Phospho-Histone H2A.X staining (Figure 15).

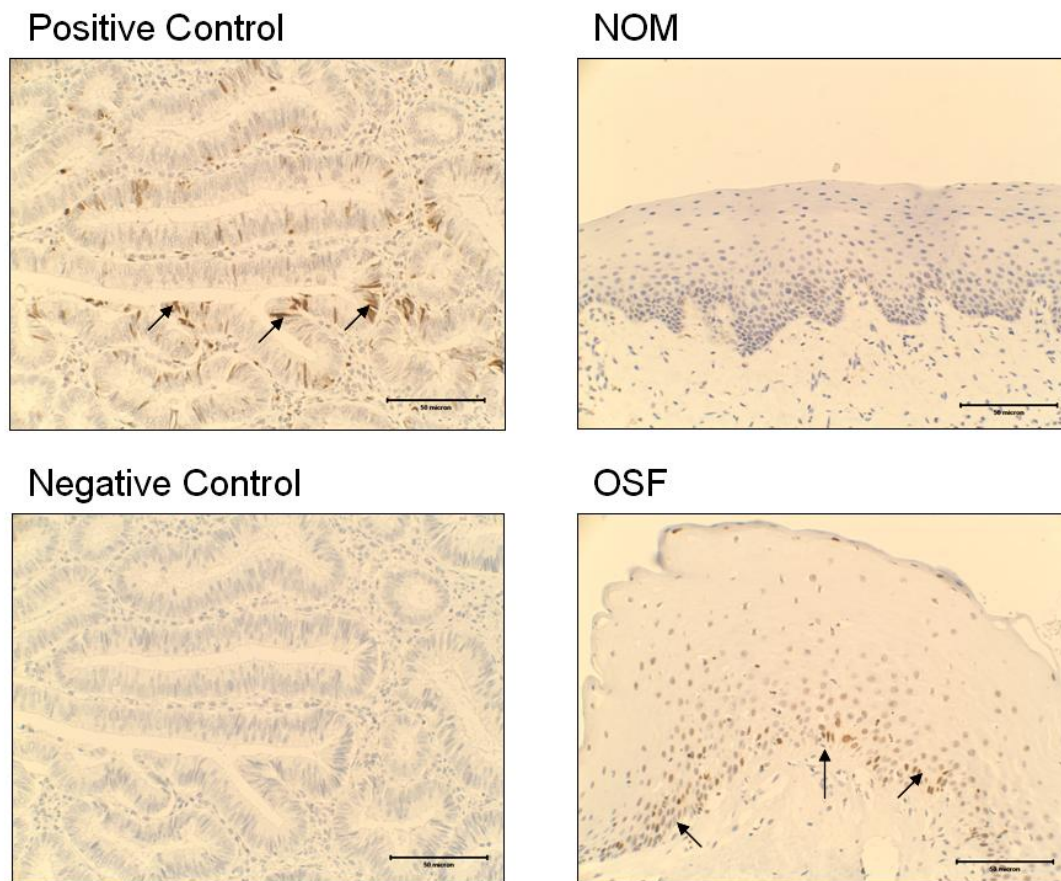


**Fig. 15.** Detection of DNA damage in OSF tissue by Phospho-Histone H2A.X staining. OSF epithelium contained positive DNA damage foci specially in relation to basal cell layer. NOM did not show any positive staining. Human colon cancer tissue served as positive control and rabbit IgG was used in negative control instead of Phospho-Histone H2A.X antibody (Representative photomicrographs are shown. Scale bar 50  $\mu$ m)

## **15. Oxidative DNA damage in IHOK by cytokine treatment**

To find out whether oxidative DNA damage occur in IHOK upon cytokine exposure, we used special staining which detects oxidative DNA damage in cells, namely 8-oxoG. Confocal microscopic data revealed all the cytokines tested (GRO- $\alpha$ , IL-6, and IL-8) individually and in combination had the potential of causing oxidative DNA damage in cultured IHOK pre-exposed to cytokines. The oxidative DNA damage foci was seen in nuclei as well as in peri-nuclear area suggesting that peri-nuclear area might be DNA damage caused to mitochondrial DNA (Figure 16A). FACS analysis also performed on cytokine-treated IHOK and it clearly showed cytokines (GRO- $\alpha$ , IL-6, and IL-8) in combination caused nearly two fold increase in oxidative DNA damage compared to negative control (Figure 16B).

16A.

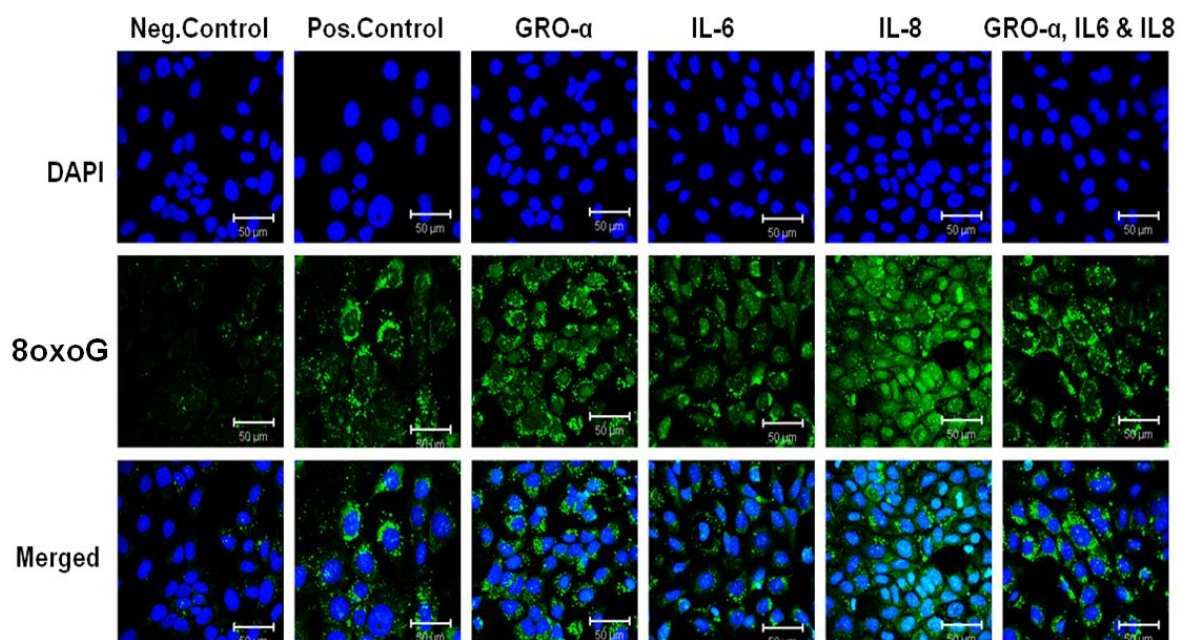


**Fig.16** . Detection of oxidative DNA damage in IHOK treated with cytokines using OxyDNA assay.

**Fig.16A** . Green fluorescent staining indicates oxidative DNA damage foci. Cytokines GRO-α, IL-6, and IL-8 individually and in combination caused oxidative DNA damage in IHOK. Perinuclear staining might indicate oxidative DNA damage foci in mitochondria like organelles. (Positive control- 10 μM H<sub>2</sub>O<sub>2</sub>, Negative control- media only, Representative photomicrographs are shown. Scale bar 50 μm)

16B.

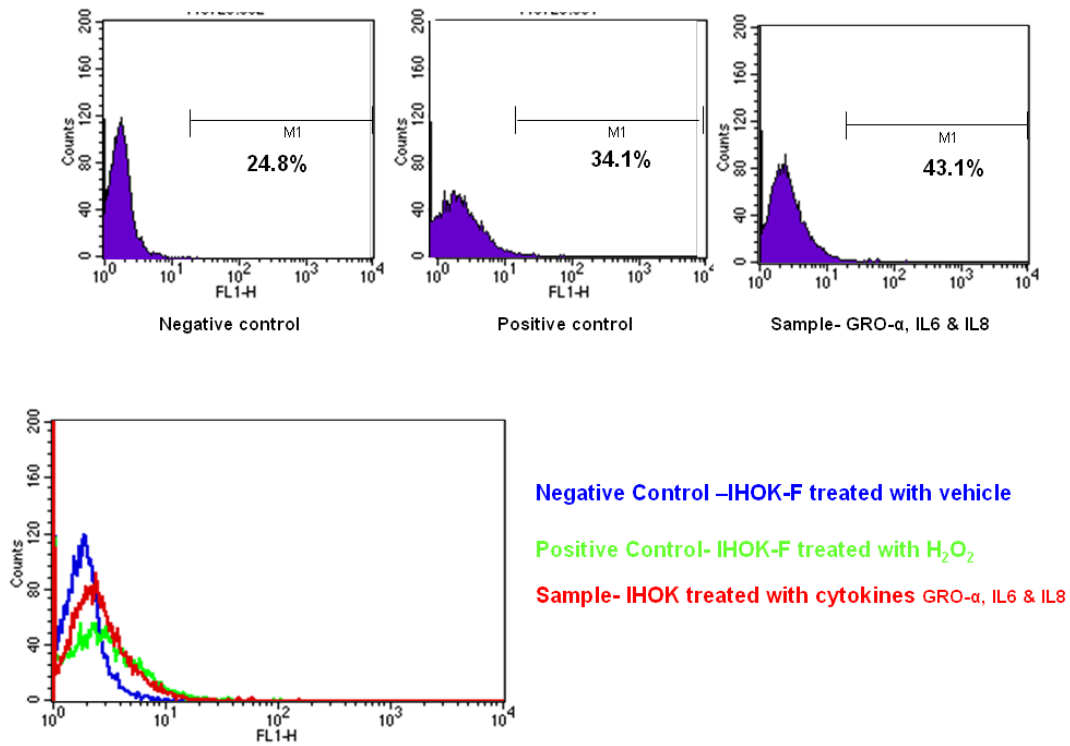


**Fig. 16B.** Detection of oxidative DNA damage in cytokine treated IHOK by flowcytometric analysis using FITC conjugated OxyDNA assay. All three cytokines caused nearly two fold increase intensity compared to negative control indicating increased oxidative DNA damage in cytokine-treated IHOK. (Test was performed three times and representative data is shown)

## **16. Oxidative DNA damage in OSF tissues**

OSF and NOM tissues were stained with 8-oxoG green fluorescent signaling was visualized by confocal microscopy. In OSF tissues, fluorescent signaling was evident as a band in basal epithelial region while NOM was negative for the staining (Figure 17). Higher magnification images revealed positive signaling generated in both nuclear and perinuclear areas of the basal cells in OSF tissues.

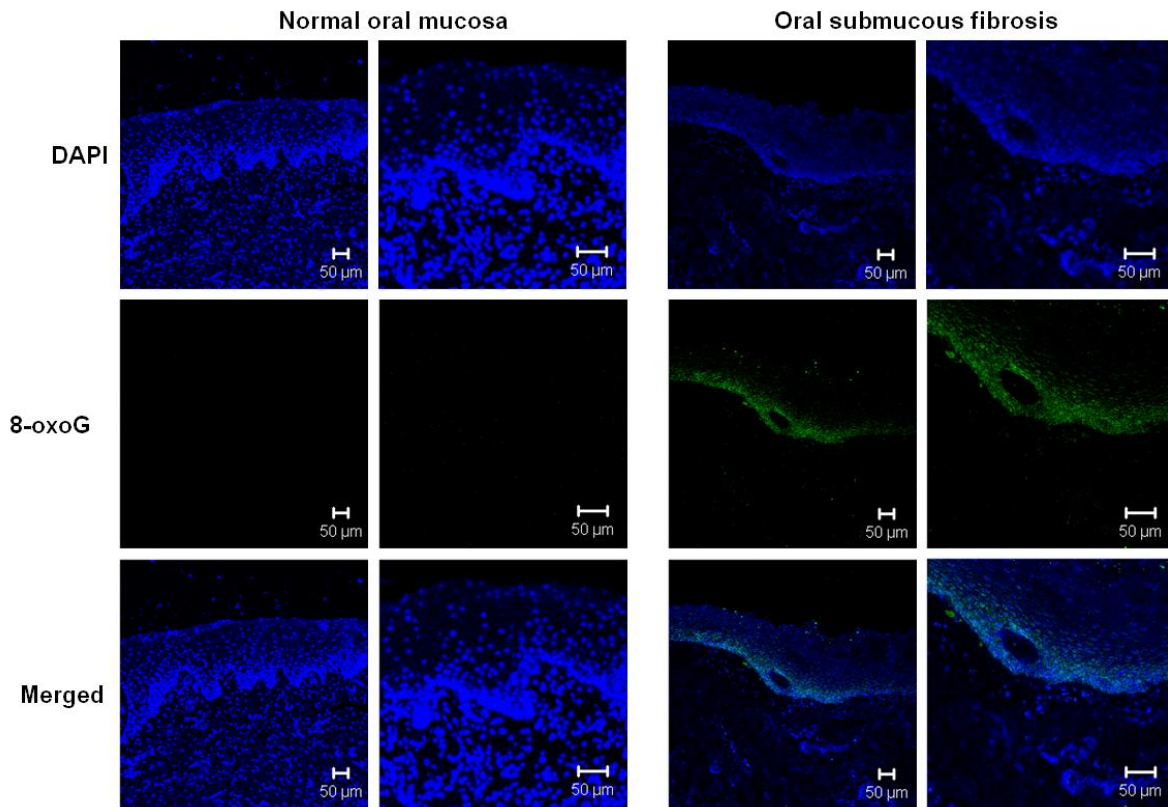


**Fig. 17.** Detection of oxidative DNA damage in OSF and NOM using FITC conjugated OxyDNA assay, visualized by confocal microscopy. OSF tissues showed green fluorescence as a band in basal cell layers of the epithelium while NOM was negative.

Representative photomicrographs are shown, Scale bar 50 µm)

## **17. Aneuploid cell population in IHOK by cytokine treatment**

IHOK treated with cytokines for 72 h analyzed with FACS for cell ploidy. Compared to the control, cytokine-treated IHOK had increase aneuploid cell populations (Figure 18A and 18B). GRO- $\alpha$  alone and in combination with other cytokines (IL-6 and IL-8) showed to cause nearly two fold increase in aneuploid cell population. When all three cytokines added together, IHOK showed nearly three fold increase in aneuploid cell population (Figure 18A and 18B).

18A.

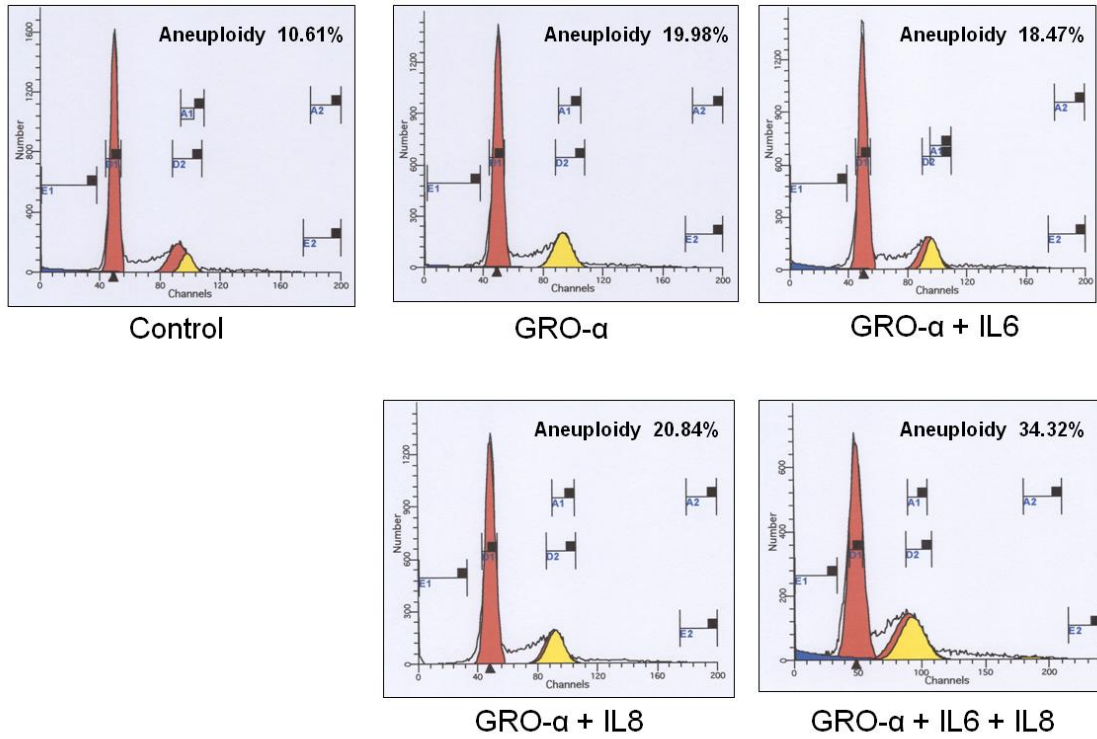


**Fig. 18.** FACS analysis of cytokine-treated IHOK for cell cycle status.

**Fig. 18A.** Cell cycle status of cytokine treated IHOK were analyzed using FACS. GRO- $\alpha$ , IL-6, and IL-8 individually and in combination caused increased cell aneuploidy in IHOK. (Representative data of four independent tests.)

18B.

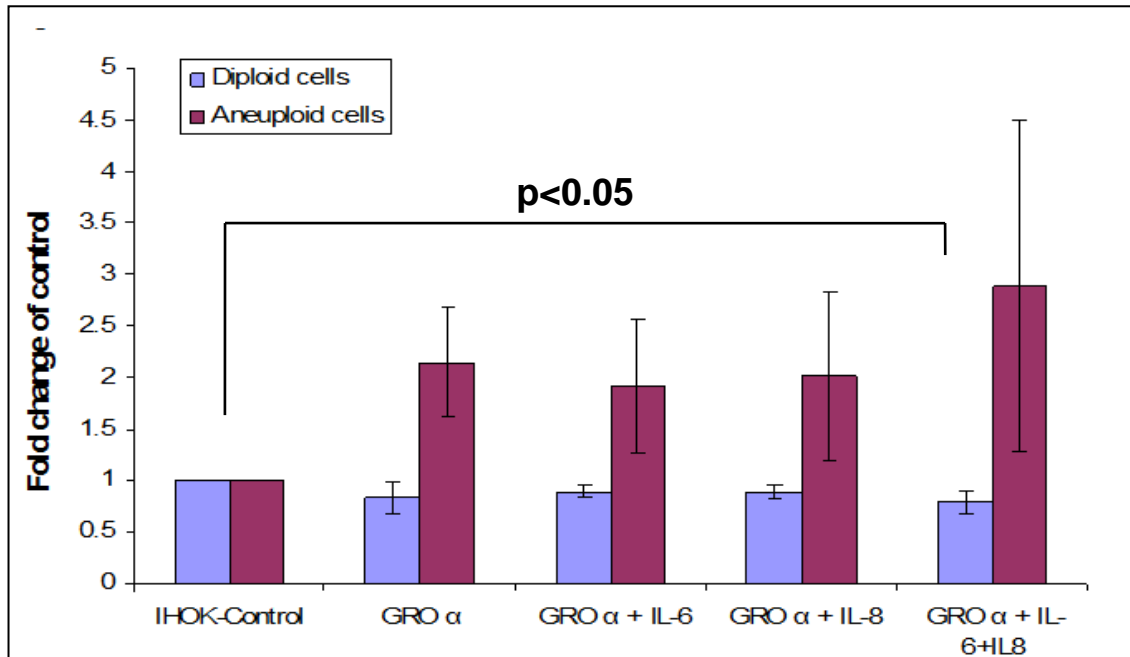


**Fig . 18 B.** Cell cycle status of cytokine-treated IHOK were analyzed using FACS.

Statistical analysis revealed significant increase in aneuploid cell population when IHOK treated with cytokines ( $p < 0.05$ ). Individual cytokines caused more than two fold increase in aneuploid cell population while all three cytokines in combination caused more than three fold increase. Results were reported as the mean  $\pm$  SD relative to control of four assays.

## **18. Cytokines effect on cell migration**

To evaluate how these cytokines induce cell migration, wound healing assay was incorporated. GRO- $\alpha$ , IL-6, and IL-8 similarly induced IHOK and HSC3 cell migration in 24 h and relevant anti-antibodies reduced the migration activity. Figure 19 shows the results obtained from the IHOK cells in wound healing assay. Cytokines induced cell migration dose dependently (Figure 19).

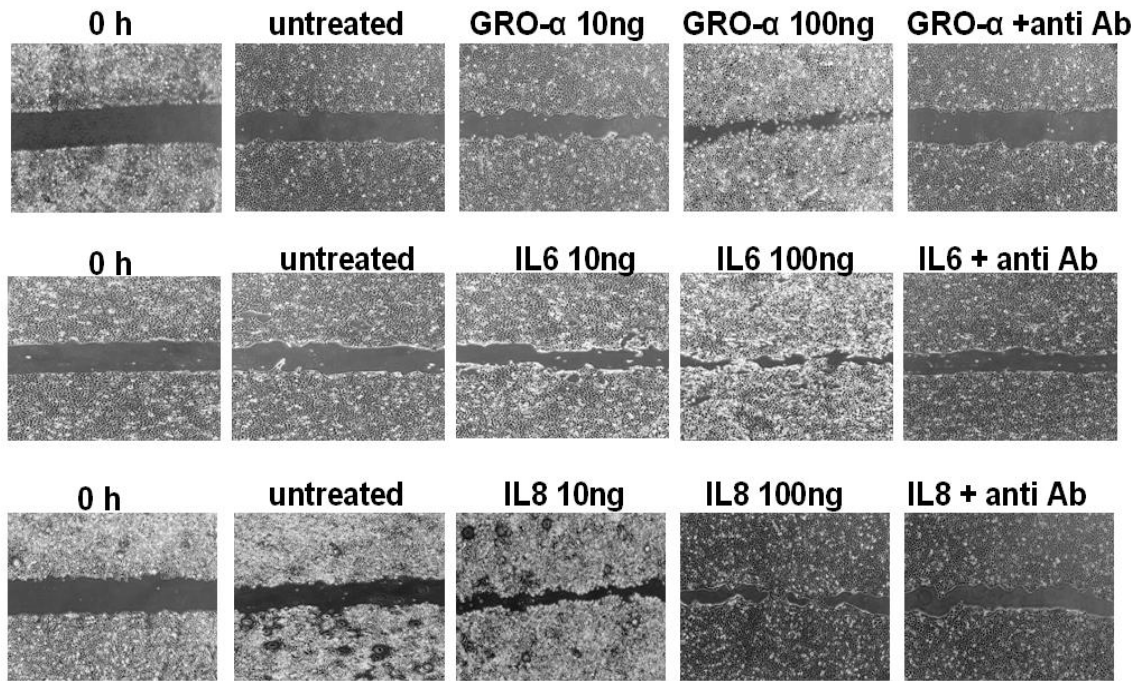
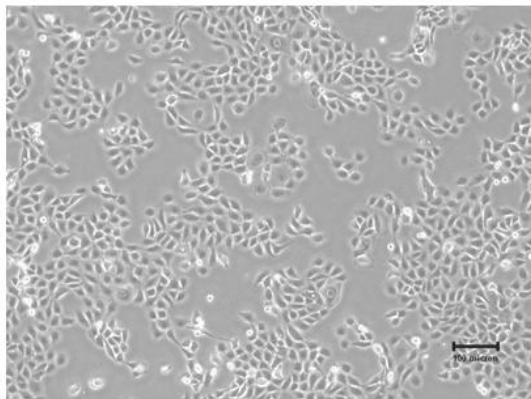


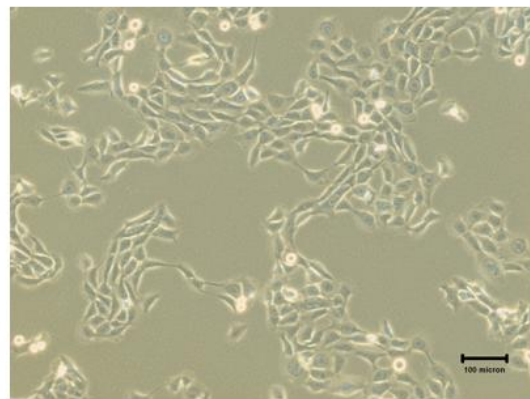
**Fig. 19.** Cytokines causing increased cell motility in IHOK detected by wound healing assay. Neutralizing antibody treatment successfully reduced cytokines-induced cell migration.

## **19. Effect of cytokines and conditioned medium on IHOK towards EMT**

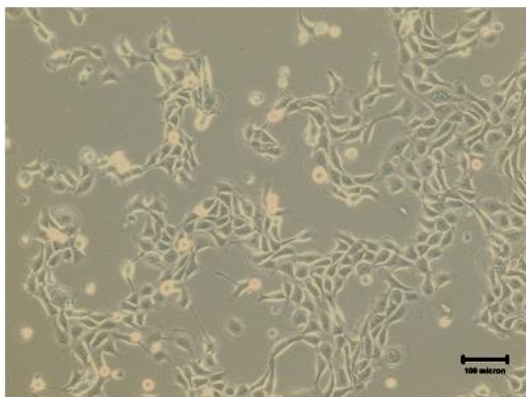
IHOK exposed to cytokines for 2 wks, showed some transient morphological changes of EMT. IHOK showed some what fibroblastic morphology with cytokine treatment (Figure 20). We evaluated expressions of Snail, Vimentin, and E-cadherin in cytokine treated IHOK using immunofluorescence staining and visualized in confocal microscopy. Simultaneously CM treated IHOK also tested for Snail, Vimentin, and E-cadherin. IHOK treated with CM taken from fibroblasts stimulated with ANE, clearly showed increased Snail (Figure 21A) and Vimentin (Figure 21B) expressions compared to control. E-cadherin expression reduced in CM-treated IHOK (Figure 21A). GRO- $\alpha$  treated IHOK also showed up regulated Snail and Vimentin expressions while E-cadherin was down regulated. It also showed these changes of expressions, up regulated or down regulated according to the dose of cytokine concentration (Figure 22A, and 22B).



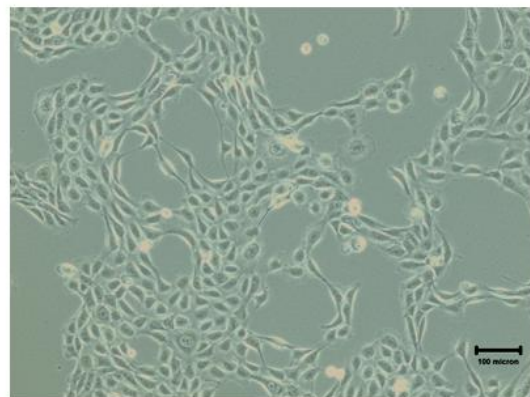
IHOK-Control



IHOK + GRO-α



IHOK + IL-6

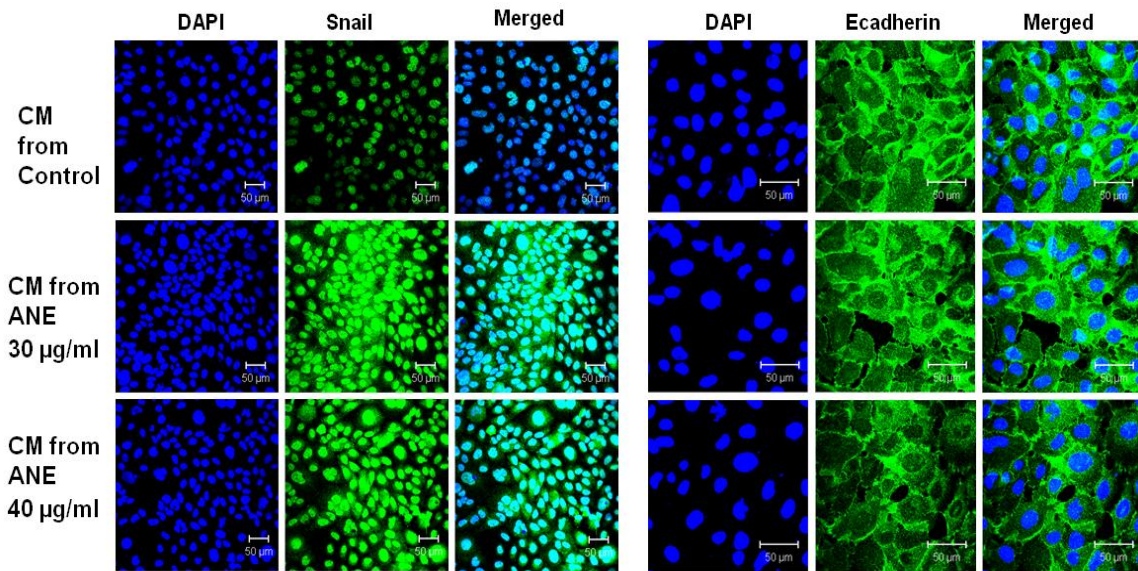


IHOK + IL-8

**Fig. 20.** IHOK exposed to cytokines for 2 wks, showed fibroblast-like change in the morphology, indicating potential of EMT changes caused by these individual cytokines.

(Representative photomicrographs are shown. Scale bar 100 μm)

21A.



21B.

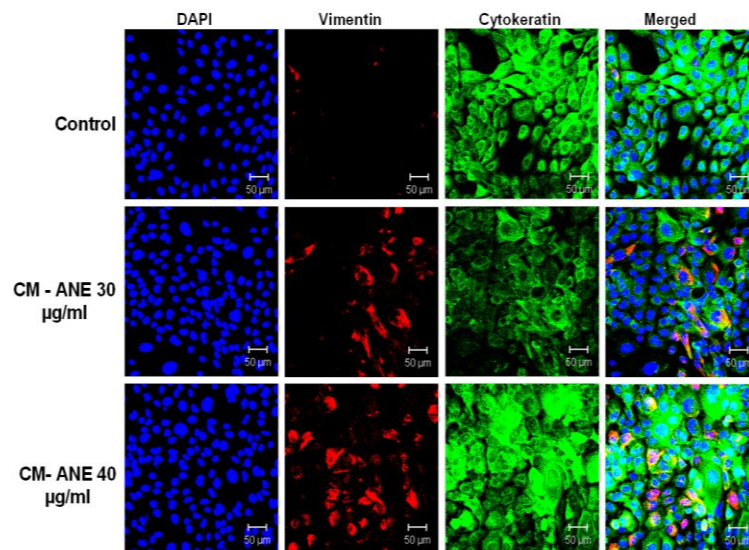


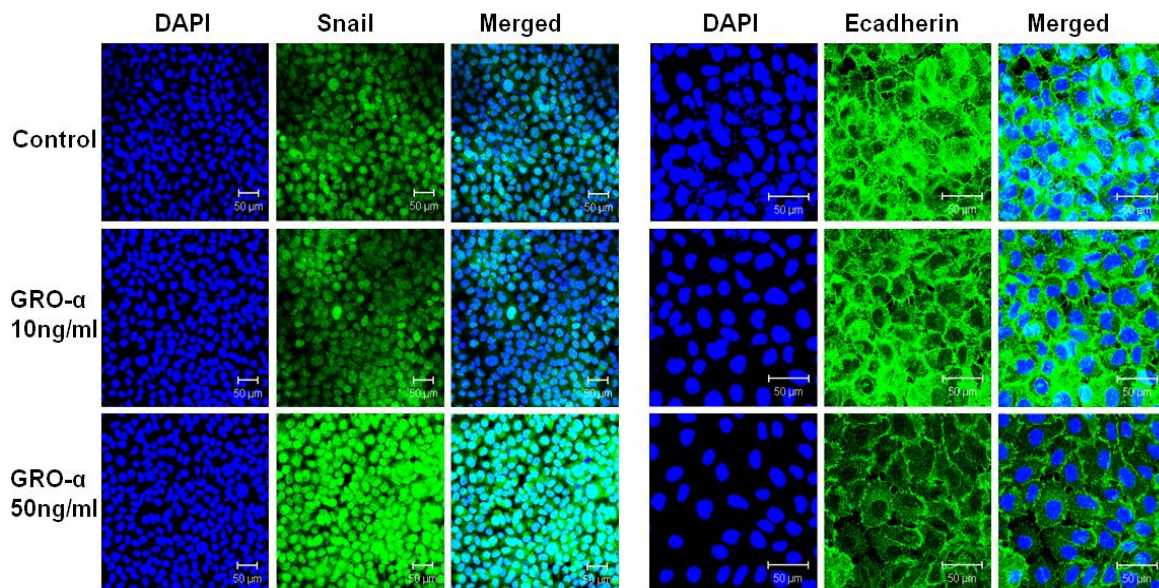
**Fig.21.** Immunofluorescence staining of CM-treated IHOK to detect EMT changes

.Snail and E-cadherin (20A), Vimentin and Cytokeratin (20B) in CM-treated IHOK for 10 wks.

Long-term CM treatment caused increased Snail and Vimentin and reduced E-cadherin and

Cytokeratin expressions in IHOK. (Representative photomicrographs are shown. Scale bar 50 µm)

22A.



22B.

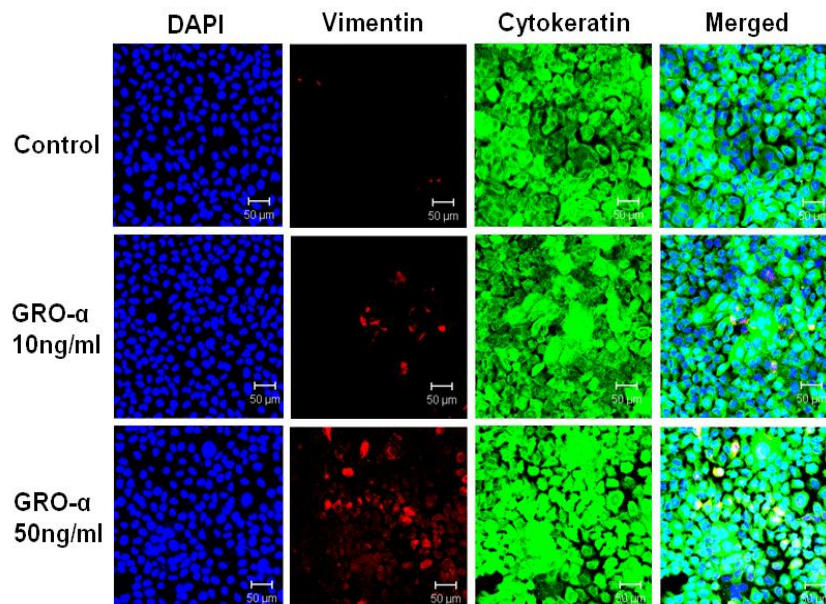


**Fig.22.** Immunofluorescence staining of GRO- $\alpha$ -treated IHOK to detect EMT changes. IHOK treated with GRO- $\alpha$  for two weeks, stained against Snail and E-cadherin (21A) and Vimentin and Cytokeratin (21B). GRO- $\alpha$  caused increased Snail and Vimentin expressions and reduced E-cadherin expressions dose dependently. (Representative photomicrographs are shown. Scale bar 50 )

## IV. DISCUSSION

Carcinogenesis in OSF is still a question among researchers which is not yet fully understood. The causative factor of carcinogenesis in OSF has also been understood as the long-term exposure to AN (Gupta and Warnakulasuriya, 2002; Jeng et al., 2001; Pillai et al., 1992; Trivedy et al., 2002). ANE as well as AN constituents like Arecoline and Arichadine cause direct cytotoxic and genotoxic effect to the oral epithelium (Jeng et al., 1999). As the unique feature of the OSF is fibrosis, scientists have suspected a relationship between carcinogenesis and fibrosis. For several decades researchers have postulated various hypotheses and attempted to discover many aspects of the carcinogenesis of OSF. Some have attributed to the direct effect of ANE that cause genotoxic effects in oral epithelium, and that induces the carcinogenic transformation in OSF (Jeng et al., 1999; Jeng et al., 2000; Jeng et al., 2003; Tsai et al., 2008). Tilakaratne et al suggested that, long term accumulation of AN carcinogens in the submucosal tissue have a contribution to the carcinogenic transformation, as fibrous nature and reduced vasculature of the OSF submucosa facilitate long term accumulation of carcinogens without being absorbed and taken away from the juxtra-epithelial region (Tilakaratne et al., 2006). Literature supports both of these hypotheses, i.e. direct effect and indirect effect of AN in the carcinogenesis of OSF (Chang et al., 1998; Jeng et al., 1999; Jeng et al., 2000; Jeng et al., 2003; Lu et al., 2008; Sundqvist et al., 1989; Tilakaratne et al., 2006; Tsai et al., 2008).

Fibrosis also might contribute to the carcinogenesis of OSF as the fibrotic process in OSF is regulated via complex signaling molecules in extracellular matrix. Many studies have shown the role of chemokines and cytokines in the fibrosis of OSF (Haque et al., 1998; Haque et al., 2000; Jeng et al., 2000). Moreover, the chronic inflammatory cell infiltration seen in OSF at various stages, further emphasizes the inflammatory nature of the disease. That is a one reason some have looked at OSF as a wound healing disorder (Tilakaratne et al., 2006; Utsunomiya et al., 2005).

More than a century ago, Virchow postulated a link between inflammation and cancer, based on the presence of leukocytes in neoplastic tissue (Balkwill and Mantovani, 2001). There after this concept has been confirmed by a number of studies. Infection and chronic inflammation contribute to about 25% of cancer (Hussain and Harris, 2007). Inflammatory conditions have been associated with cellular transformation and malignancy, as recently confirmed in experiments using animal models (Greten et al., 2004; Houghton and Wang, 2005; Pikarsky et al., 2004) . Although the molecular mechanisms of inflammation-associated cancer have been not fully understood, a possible mechanism could include the induction of DNA damage and chromosomal abnormalities by proinflammatory cytokines (Higashimoto et al., 2006). In fact, chronic inflammation has a direct link to carcinogenesis and many inflammatory cytokines have been identified as playing a major role in carcinogenesis including head and neck cancer as well (Chan et al., 1999; Hong et al., 2000; Nakano et al., 1999; Woods et al., 1998). Elevated serum levels of pro-inflammatory cytokines like IL-1, IL-6, IL-8 or TNF are often associated with tumor progression and poor prognosis (Balkwill, 2006; Lewis et al., 2006; Lin and Karin, 2007; Yuan et al., 2005).

Jeng et al identified that, ANE causing keratinocyte inflammation regulated by prostaglandin, IL-6 and TNF  $-\alpha$ , links to oral cancer (Jeng et al., 2003). It has also found that ANE-treated fibroblasts enhance tumorigenesis of oral epithelial cells via their secreted molecules and activation of AKT signaling pathway (Lu et al., 2008). Accumulating studies have demonstrated stromal fibroblasts get senescence due to DNA-damaging agents and this senescence stroma promotes tumor formation in the neighboring epithelium (Shan et al., 2009). Pitiyage et al in a recent study found that OSF tissue contains accumulation of senescent fibroblasts due to oxidative DNA damage (Pitiyage et al., 2011).

Based on this background, we hypothesized that AN-stimulated stromal fibroblasts in OSF would secrete some molecules which facilitate the tumorigenesis in OSF epithelium. This aspect might play a contributory role in OSF-carcinogenesis as an indirect effect.

Using *in vitro* studies and analyzing OSF patients' tissue, we attempted to elucidate the secretory molecules produced by ANE-stimulated gingival fibroblasts and their role in malignant transformation of OSF epithelium.

To stimulate fibroblasts *in vitro* for several weeks with ANE, we utilized hTERT-hNOF (Illeperuma et al., 2011), as hNOF derived from primary culture can not be subcultured for a long term due to replicative senescence and genomic instability at later passages. hTERT-hNOF showed to have similar biological properties to hNOF and maintained its replicative potential even beyond 70 passages in serial subculture (Illeperuma et al., 2011).

Selection of ANE concentration suitable to stimulate fibroblasts was done based on the results of the MTT assay and previous literature (Chang et al., 2009; Jeng et al., 1999; Wang et al., 2007). Up to 40  $\mu\text{g/ml}$  of ANE showed to be safe in using in *in vitro* studies as for no significant cytotoxic effect was observed.

As a start, to identify the cytokines secreted from ANE stimulated fibroblasts, both hNOF and hTERT-hNOF were stimulated with 30  $\mu\text{g/ml}$  and 40  $\mu\text{g/ml}$  ANE and condition media were subjected to cytokine antibody array. There we found up-regulated GRO- $\alpha$ , IL-6, and IL-8 and down-regulated angiogenin expressions in both hNOF and hTERT-hNOF. Immunofluorescence and ELISA results also helped to confirm the cytokine secretion pattern in ANE-stimulated fibroblasts.

Angiogenin is a potent angiogenic factor which is found to be expressed in variety of human cells (Fett et al., 1985; Moenner et al., 1994). It is a secreted polypeptide that induces neovascularization *in vivo* (Moenner et al., 1994). Angiogenin induces angiogenesis by activating vessel endothelial and smooth muscle cells and triggering a number of biological processes, like cell migration, invasion, proliferation, and formation of tubular structures (Gao and Xu, 2008). It was also reported that angiogenin was up-regulated in various types of human cancers and it takes part in cancer development by stimulating both angiogenesis and cancer cell proliferation (Yoshioka et al., 2006). In this study we noticed down-regulation of angiogenin expression in ANE-treated fibroblasts. *In vivo*

experiments also supported these *in vitro* findings, i.e. reduced Angiogenin expressions in OSF tissues. Histologically OSF is characterized by reduced vasculature in submucosa due to progressive fibrosis seen as disease progressed (Utsunomiya et al., 2005). Down-regulation of angiogenin secretion in fibroblasts after ANE exposure might contribute to this reduced vasculature seen in OSF tissue *in vivo*.

GRO- $\alpha$  is a CXC family chemokine which promotes chemotaxis of granulocytes and endothelia (Shintani et al., 2004). GRO- $\alpha$  is also associated with oral cancer and its gene was found to be up-regulated in four out of five pairs in a microarray analysis (Alevizos et al., 2001). GRO- $\alpha$  is originally isolated as an autocrine growth factor from a human melanoma cell line (Richmond and Thomas, 1988) but can be expressed by all nucleated cells induced by inflammatory stimuli (Miller and Krangel, 1992). GRO- $\alpha$  produced by OSCC tumor and /or tumor environment found to have an important role to play in promoting tumorigenesis other than proinflammatory, proangiogenic, and immunoregulatory activities of GRO- $\alpha$  (Shintani et al., 2004). Involvement of GRO- $\alpha$  is reported in relation to chronic inflammation and cancer in several studies. For instance, in ulcerative colitis and colorectal cancer (Egesten et al., 2007), in gastric cancer (Jung, Noh, et al., 2010), in ovarian carcinoma and endometriosis (Furuya et al., 2007) in adenocarcinoma of the colon (Wen et al., 2006), in bladder cancer (Kawanishi et al., 2008), in adrenal cancer (Schteingart et al., 2001) and in prostate cancer (Kogan-Sakin et al., 2009; Moore et al., 1999). GRO- $\alpha$  binds to its specific receptor CXCR2 and involved several down stream signaling path ways such as Ras-mitogen activated protein kinases pathway, phosphatidylinositol 3-kinase pathway (Xia and Hyman, 2002), nuclear factor kB pathway ( Wang and Richmond, 2001) and PAK signaling (D. Wang et al., 2002), showing its different cellular functions. It was reported that GRO- $\alpha$  induced by prostaglandin E<sub>2</sub> via EP4-EGFR-MAPK cascade promotes angiogenesis in colorectal cancer (D. Wang et al., 2006). Furthermore one report showed GRO- $\alpha$  production in gingival fibroblasts after LPS stimulation via NF-kB pathway as a mechanism involved in periodontal inflammation (Jonsson et al., 2009).

IL-8, a known inflammatory mediator, also a chemokine of CXC family and also been shown to promote chemotaxis of neutrophils and endothelial cells during angiogenesis (Wang et al., 1998). IL-8

also is capable of promoting growth and metastasis of SCC and other cancers through both autocrine and host dependant mechanisms. In head and neck cancer IL-8 expression was shown related to cell survival and proliferation (Wolf et al., 2001). Link between IL-8 and tumor has been extensively discussed in past studies. It is mitogenic for melanoma cells (Schadendorf et al., 1993) and promotes angiogenesis in lung cancer (Yao et al., 2005) and bronchogenic carcinoma (Smith et al., 1994). Involvement of IL-8 in prostate tumor growth ( Inoue et al., 2000; Lee et al., 2004), multiple myeloma (Pellegrino et al., 2004; Pellegrino et al., 2005), ovarian cancer (Moscova et al., 2006), and gastric cancer (Ju et al., 2010; Kitadai et al., 1998) has been also described.

IL-6 is a pleiotropic cytokine which is produced by inflammatory cells and other cells in tissue microenvironment, through activation of nuclear factor kB (Grivennikov and Karin, 2008). It plays an important role in many chronic inflammatory diseases such as inflammatory bowel disease, peritonitis, rheumatoid arthritis, asthma, and colon cancer (Scheller et al., 2006). IL-6 is secreted by different cell types including fibroblasts, macrophages, T and B lymphocytes, endothelial cells and activated keratinocytes (Conze et al., 2001). IL-6 signals through a specific IL-6 receptor and a promiscuous transmembrane signal transducer, gp130, to activate the JAK2/STAT3 pathway (Corcoran and Costello, 2003). Role of IL-6 in tumorigenesis is well identified in several studies. In prostate cancer, IL-6 autocrine loop induces the tumorigenic conversion of prostate epithelial cells to invasive phenotype through a process accompanied by EMT via STAT3 activation (Rojas et al., 2011). Likewise in ovarian carcinomas, IL-6 causes EMT through cross-activation of STAT 3 and the epidermal growth factor receptor (Colomiere et al., 2009). In colorectal cancer, IL-6 stimulates colony formation of primary and metastatic cancer cells through a paracrine mechanism (Schneider et al., 2000). Role of IL-6 in promotion of malignant growth of skin SCC by regulating a network of autokrine and paracrine cytokines such as IL-8 is discussed in a resent report and it also emphasized that IL-6 is a key factor for mediating tumor progression from benign to malignant (Lederle et al., 2011).

In our study, as hTERT-hNOF was subcultured for a period of 8 wks with expose to ANE, we noticed signs of replicative senescence beyond 7 wks of ANE exposure and at 8 wks, blue stained nuclei in senescent associated  $\beta$ -Gal staining confirmed it. SA-  $\beta$ -Gal staining is a known marker of replicative senescence and aging (Dimri et al., 1995). It was shown that senescent fibroblasts get accumulate in the OSF during disease progression (Pitiyage et al., 2011). Senescent human cells also secrete many biologically active proteins, a phenotype known as senescence associated secretory phenotype (SASP) (Coppe et al., 2010; Coppe et al., 2008). The SASP secretes inflammatory cytokines that drive aging and age related diseases (Finch and Crimmins, 2004) and when chronically present can promote malignant phenotypes in nearby premalignant cells (Bavik et al., 2006; Krtolica et al., 2001; Liu and Hornsby, 2007). Senescent prostrate fibroblasts have found to modulate neoplastic epithelial cell proliferation via paracrine mechanisms (Bavik et al., 2006). Similar to epithelial cells mitotically active stromal cells, mainly fibroblasts, also undergo irreversible cell cycle arrest in response to DNA-damaging agents (Shan et al., 2009). Coppe et al demonstrated that GRO- $\alpha$  is a conserved SASP factor in human and murine senescent fibroblasts which promotes premalignant epithelial cell growth (Coppe et al., 2010).

Inducers of senescence in stromal fibroblasts and mechanism how cytokines regulate senescence and tumorigenesis in neighbor epithelium has been extensively discussed by Shan et al. They describe chemokine downstream in the RAS pathway may participate in the senescence programme of neighboring fibroblasts in a paracrine fashion (Shan et al., 2009). Moreover, in an earlier study they reported that, RAS induced GRO- $\alpha$  was adequate to cause ovarian stromal fibroblasts to senescence hence inducing ovarian tumorigenesis (Yang et al., 2006). Acosta et al reported GRO- $\alpha$ ,  $\beta$ , and  $\gamma$  and IL-8 induce senescence in human fibroblasts via CXCR2 and also describe that senescent cells have elevated levels of both GRO- $\alpha$  and CXCR2, thus completing a positive feedback loop culminating in strengthened cellular senescence (Acosta et al., 2008). Other recently documented mediators of oncogene-induced fibroblasts senescence include the IL-6 and IL-8, which were shown to be induced by protein downstream of RAS (Kuilman et al., 2008). It was interesting to know that these senescence fibroblasts stimulate only premalignant cells and malignant cells in to tumor, but not the

normal epithelial cells, according *in vitro* and *in vivo* study done by Krtolica et al. They also described even 10% population of senescence fibroblast *in vitro*, is capable enough to exert their effect through soluble factors to stimulate premalignant cells. Importantly they also showed what ever the stress which induced fibroblasts to senescence, whether replicative exhaustion, oncogenic RAS, P14<sup>ARF</sup>, or hydrogen peroxide, the action and potency of senescence fibroblasts remain unchanged (Krtolica et al., 2001) . Taken together it shows tumor promoting nature of senescent fibroblasts has been recognized as an important factor in the development of epithelial cancer. Further studies have elucidated that diffusible paracrine signaling molecules secreted by senescent fibroblasts orchestrate the senescence associated enhancement of tumorigenesis.

As evidenced in our study, ANE-stimulated fibroblasts to over secrete the same cytokines mentioned in literature (GRO- $\alpha$ , IL-6 and IL-8) which has autocrine and paracrine functions to strengthen cellular senescence and hence tumorigenesis. This might be a mechanism where OSF epithelium is transformed to OSCC through the effects of pro-inflammatory cytokines GRO- $\alpha$ , IL-6 and IL-8. When oral mucosa is exposed to AN for long term, this may explain how indirect effect is influenced in carcinogenesis. Previous studies explain that ANE and its components cause keratinocyte inflammation and induce pro-inflammatory cytokines like IL-6 and IL-8 in OSF epithelium (Jeng et al., 2003). *In vitro* production of IL-6 by human gingival and OSF fibroblasts treated with AN alkaloids arecoline and arecaidine has been also described (Chen et al., 1995).

In order to elucidate whether these cytokines influence on carcinogenesis in the oral epithelium, IHOK were selected as they are transformed simulating oral epithelium of AN chewers. Lai and Lee suggested that, long term ANE enhances oxidative stress and genetic damage in human keratinocytes (Lai and Lee, 2006). Also accumulating evidence is there to confirm that ANE and its components causing DNA damage and mutagenic changes to oral Keratinocytes (Dave et al., 1992; Jeng et al., 1999; Shirname et al., 1983; Sundqvist and Grafstrom, 1992; Sundqvist et al., 1989). For *in vitro* stimulation of IHOK, 10 ng/ml of cytokine concentration for individual cytokine tested was selected

according to the similar studies in literature (Babbar and Casero, 2006; Jung et al., 2010; Okamoto et al., 1997).

First this study tested whether these cytokines could affect proliferative activity of IHOK. As found by MTT assay, GRO- $\alpha$ , IL-6 and IL-8 individually or in combination failed to cause any significant growth increase in IHOK, at a concentration of 10 ng/ml of each cytokine.

Next this study evaluated whether cytokines secreted from ANE-treated fibroblasts cause DNA damage on IHOK. We utilized Phospho- Histone H2A.X a DNA damage response (DDR) marker which identifies DNA double strand breaks (DSB) (Burma et al., 2001). By immunofluorescence, cytokine treated IHOK expressed increased signals for Phospho- Histone H2A.X staining. GRO- $\alpha$ , IL-6, and IL-8 individually as well as in combination caused DNA DSB in cultured IHOK. Compared to control it showed nearly 50% of DNA damage foci in cytokine treated IHOK. Interestingly, immunoperoxidase staining of OSF tissues with Phospho- Histone H2A.X, clearly showed that positive foci in OSF basal cell layer compared to the negatively stained NOM. OSF tissues with dysplastic changes showed more DNA damage foci in their epithelium.

DNA damage accumulates early in the development of OSCC as evident by the detection of DNA damage markers such as Phospho- Histone H2A.X at peak levels at early stages of oral carcinogenesis (Chou and Alawi, 2011). DDR is an evolutionary conserved genome-protective mechanism whose activation occurs after exposure to genotoxic or oncogenic stress (Halazonetis et al., 2008). DSB are the most deleterious form of DNA damage (Celeste et al., 2003). Histone H2A.X is rapidly phosphorylated on serine 139 and accumulates at the site of DNA DSB, hence recognized as a quantitative marker of DNA DSBs (Burma et al., 2001). Chou et al further stress that Histone H2A.X expression is seen significantly elevated in the precancer stage of OSSC than in established OSCC. In addition they explained the higher the grade of dysplasia, the higher the expression of Histone H2A.X in patients' tissues (Chou and Alawi, 2011).

Our *in vitro* results clearly showed that these cytokines secreted from ANE-stimulated fibroblasts cause kind of stress on IHOK causing DNA damage. Furthermore, as *in vivo* data also evident of DNA damage foci in OSF, may be this DNA damage at least partially due to the effect of cytokines released by AN stimulated fibroblasts or the so called indirect effect.

Chronic inflammation and cytokine induced DNA damage has been discussed extensively as described above and some literature attribute the underlying mechanism to the ROS production. Continuous cytokine exposure (TNF- $\alpha$  and IFN- $\gamma$ ) of colonic epithelial cells found to induce DNA damage through ROS production (Seidelin and Nielsen, 2005). Babbar and Casero discussed the involvement of TNF- $\alpha$  and IL-6 on human lung epithelial cells to generate ROS and hence oxidative DNA damage, by the mechanism which they suggested for the inflammation induced carcinogenesis (Babbar and Casero, 2006).

Assuming that cytokine-induced DNA damage on IHOK may be due to oxidative stress, we tested the cytokine-treated IHOK for oxidative DNA damage. Simultaneously OSF tissues also were subjected to the same test to elucidate oxidative DNA damage in OSF.

Detection of Oxidative DNA damage by FITC conjugated 8-oxoG in cytokine-treated IHOK by FACS and confocal microscopy, clearly showed that each of these cytokine was capable of causing oxidative DNA damage. Positive signaling was seen in relation to the nuclear as well as perinuclear area suggesting that oxidative stress has caused not only nuclear DNA damage but mitochondrial DNA damage as well. In OSF patients' tissues also, we detected band like staining for 8-oxoG in basal cell layers. There also higher magnification revealed positive signaling from both nuclear and perinuclear regions of the epithelial cells. In contrast NOM did not show any positive signaling for 8-oxoG staining confirming oxidative DNA damage in OSF epithelium.

Literature is evident for successful detection of oxidative DNA damage in tissue samples (Maniscalco et al., 2005; Roper et al., 2004).

The most well studied and most abundant oxidative DNA lesion produced is 8-hydroxyguanine, which is mutagenic in bacterial and mammalian cells (Cheng et al., 1992). Literature extensively discussed the elevation of oxidized guanine bases in various forms in various human cancers and

therefore put forward that oxidative DNA damage as an etiology of those cancers (Tanaka et al., 2008; Valavanidis et al., 2009). Also in some animal models of tumor, describe this phenomenon (Harvilchuck et al., 2009; Muguruma et al., 2007; Pu et al., 2009). Based on these facts measurement of oxidized guanine bases has been widely used as a biomarker of oxidative DNA damage (Klaunig et al., 2011).

Epidemiological studies indicated that chronic oxidative stresses are strongly associated with carcinogenesis (Hwang and Bowen, 2007). For example link of ulcerative colitis with the high incidence of colorectal cancer and chronic gastritis with gastric cancer can be shown (Konturek et al., 2006; Seril et al., 2003). Oxidative DNA damage is a main source of mutation load in living organisms and more than one hundred oxidative DNA adducts have been identified (Demple and Harrison, 1994; Dizdaroglu, 1992; Lu et al., 2001; von Sonntag, 1987). Oxidative damage and modifications to DNA bases lead to changes in the genome. This damage may include point mutations, deletions, insertions, or chromosomal translocations which may cause oncogene activation and tumor suppressor gene inactivation, and potentially lead to initiation of carcinogenesis (Toyokuni, 2006).

As shown in our *in vitro* results we detected cytokines causing oxidative DNA damage. Especially when antioxidant glutathione was used to treat IHOK together with cytokines, it considerably reduced DNA damage caused by cytokines, further confirming that cytokine-caused DNA damage is mainly due to oxidative stress. OSF tissues also showed evidence of having oxidative DNA damage. These results explain ROS production *in vitro* is due to cytokines, and *in vivo* also OSF is subjected to sort of oxidative stress.

Next we analyzed the cell cycle status. We clearly identified cytokines individually and in combination would cause increase in aneuploid cell population via FACS analysis. Compared to control, each cytokine-treated IHOK showed nearly two fold increase in aneuploid cell population within 72 h exposure, while cytokines in combination showed over three fold increase in aneuploid cell population. Abnormal chromosome copy number or aneuploidy is the most common abnormality

in solid tumors (Williams et al., 2009). The occurrence of aneuploidy may merely reflect the instability of the mitotic process in cancer cell and also represent a dynamic event where the resultant imbalance of key genes is the mechanism driving carcinogenesis (Duesberg and Li, 2003; Duesberg et al., 2005; Weaver and Cleveland, 2006). Aneuploidy is concerned as a key biomarker of cancer development, as the universal presence of aneuploidy in cancer with accumulating evidence that aneuploidy is an early event during neoplastic progression (Doak, 2008). Especially in oesophageal and gastric cancer, aneuploidy is apparent at early premalignant stages and linked with neoplastic progression (Doak et al., 2003; Williams et al., 2005).

Additionally we observed the migration enhancing activity of these cytokines in wound healing assay with IHOK and HSC3 cells. These may be an added support to the transformed oral epithelial cells in the process of multistep carcinogenesis. Migration promoting activity of these cytokines was discussed in literature as well (Ju et al., 2010; Lederle et al., 2011; Rojas et al., 2011; Tsai et al., 2007).

When IHOK were treated with cytokines *in vitro* for 2 wks, we noticed some transient morphological changes similar to EMT changes. IHOK became elongated and showed some fibroblast-like morphology. Cytokine effect in EMT changes has been already described previously (Colomiere et al., 2009; Rojas et al., 2011). Hence we treated IHOK with CM taken from ANE-treated fibroblasts and checked them for EMT markers. After 10 weeks of exposure to CM, we noticed increased Vimentin and Snail expressions together with reduced E-cadherin in CM-treated IHOK. Up regulation of Vimentin and Snail expressions and down regulation of E-cadherin expression are hallmarks of EMT (Bernier et al., 2009; Kang and Massague, 2004; Park et al., 2011). To further probe in to this observation, we treated IHOK with GRO- $\alpha$  for 2 wks and stained for Vimentin, Snail and E-cadherin. Similar results with CM treated IHOK were achieved i.e. up regulation of Vimentin and Snail expressions and down regulation of E-cadherin expression. It was reported in benign prostate epithelium that, IL-6 causing EMT leading to an invasive phenotype through activation of STAT3 (Rojas et al., 2011). These results further facilitate our hypothesis how cytokines could contribute to the tumorigenesis.

In summery, this study showed that ANE increased secretion of cytokines (GRO- $\alpha$ , IL-6, and IL-8) from gingival fibroblasts irrespective of time of exposure. And these cytokines caused oxidative DNA damage and DNA double strand breaks in IHOK through ROS production. Continuous ANE exposure induced fibroblasts to undergo senescence but continuously secret increased cytokines, suggesting of SASP. Moreover, these cytokines also found to contribute to the increase cell aneuploidy, increase cell motility and EMT changes which are key contributory factors in tumorigenesis. Therefore, continuous insult of DNA damage due to cytokines might contribute to the malignant transformation of OSF epithelium in an indirect manner (Figure 22).

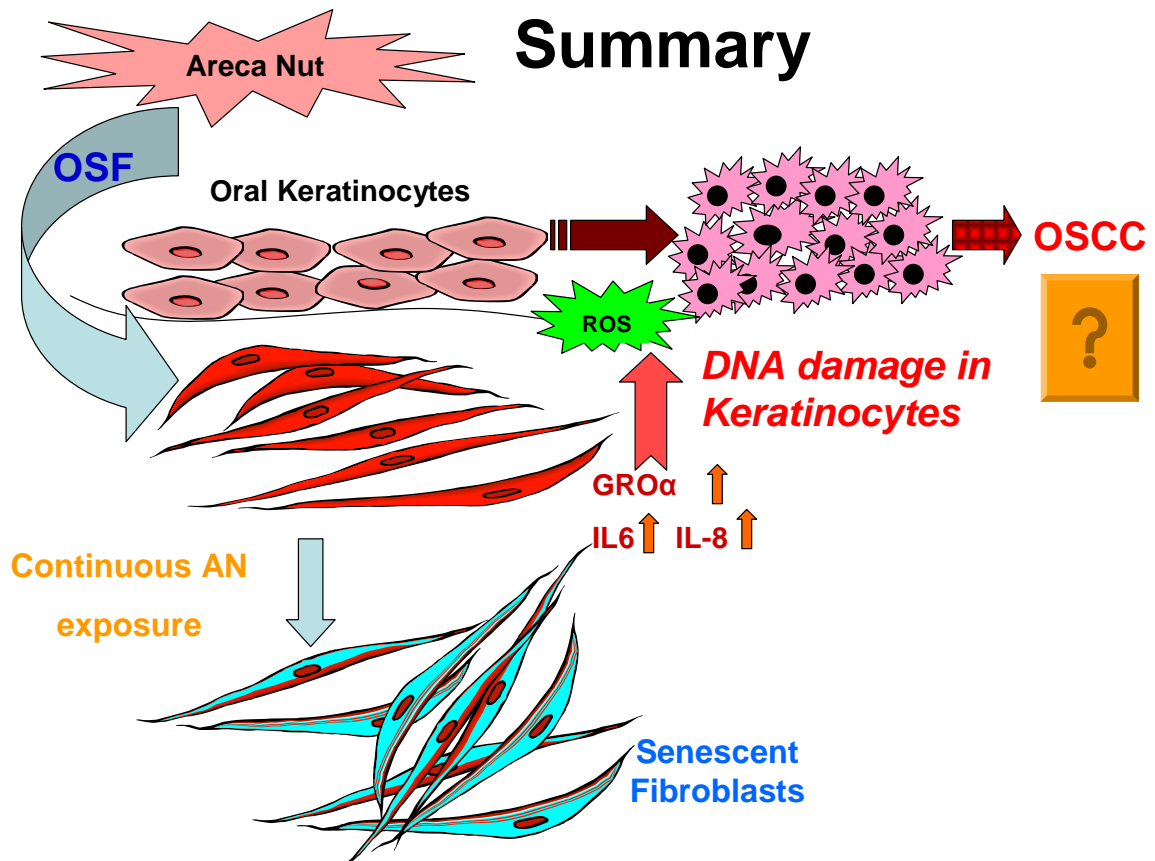


**Fig. 22.** Proposed mechanism that ANE-exposed gingival fibroblasts caused DNA damage in oral mucosal epithelium.

Cytokines produced by gingival fibroblasts cause DNA damage through production of reactive oxygen species (ROS). This persistent DNA damage might contribute to the malignant transformation of oral epithelium in an indirect manner. AN –Areca Nut, OSCC- Oral Squamous Cell Carcinoma.

## REFERENCE

- Acosta JC, O'Loughlen A, Banito A, Guijarro MV, Augert A, Raguz S, et al.: Chemokine signaling via the CXCR2 receptor reinforces senescence. *Cell* 133: 1006-1018, 2008.
- Aggarwal BB, Vijayalekshmi RV, Sung B: Targeting inflammatory pathways for prevention and therapy of cancer: short-term friend, long-term foe. *Clin Cancer Res* 15: 425-430, 2009.
- Alevizos I, Mahadevappa M, Zhang X, Ohyama H, Kohno Y, Posner M, et al.: Oral cancer in vivo gene expression profiling assisted by laser capture microdissection and microarray analysis. *Oncogene* 20: 6196-6204, 2001.
- Babbar N, Casero RA, Jr.: Tumor necrosis factor-alpha increases reactive oxygen species by inducing spermine oxidase in human lung epithelial cells: a potential mechanism for inflammation-induced carcinogenesis. *Cancer Res* 66: 11125-11130, 2006.
- Balkwill F: TNF-alpha in promotion and progression of cancer. *Cancer Metastasis Rev* 25: 409-416, 2006.
- Balkwill F, Mantovani A: Inflammation and cancer: back to Virchow? *Lancet* 357: 539-545, 2001.
- Bavik C, Coleman I, Dean JP, Knudsen B, Plymate S, Nelson PS: The gene expression program of prostate fibroblast senescence modulates neoplastic epithelial cell proliferation through paracrine mechanisms. *Cancer Res* 66: 794-802, 2006.
- Becker C, Fantini MC, Wirtz S, Nikolaev A, Lehr HA, Galle PR, et al.: IL-6 signaling promotes tumor growth in colorectal cancer. *Cell Cycle* 4: 217-220, 2005.
- Bernier J, Bentzen SM, Vermorken JB: Molecular therapy in head and neck oncology. *Nat Rev Clin Oncol* 6: 266-277, 2009.
- Betel-quid and areca-nut chewing and some areca-nut derived nitrosamines. *IARC Monogr Eval Carcinog Risks Hum* 85: 1-334, 2004.
- Burma S, Chen BP, Murphy M, Kurimasa A, Chen DJ: ATM phosphorylates histone H2AX in response to DNA double-strand breaks. *J Biol Chem* 276: 42462-42467, 2001.
- Celeste A, Fernandez-Capetillo O, Kruhlak MJ, Pilch DR, Staudt DW, Lee A, et al.: Histone H2AX phosphorylation is dispensable for the initial recognition of DNA breaks. *Nat Cell Biol* 5: 675-679, 2003.
- Chan G, Boyle JO, Yang EK, Zhang F, Sacks PG, Shah JP, et al.: Cyclooxygenase-2 expression is up-regulated in squamous cell carcinoma of the head and neck. *Cancer Res* 59: 991-994, 1999.
- Chang LY, Wan HC, Lai YL, Kuo YF, Liu TY, Chen YT, et al.: Areca nut extracts increased expression of inflammatory cytokines, tumor necrosis factor-alpha, interleukin-1beta, interleukin-6 and interleukin-8, in peripheral blood mononuclear cells. *J Periodontal Res* 44: 175-183, 2009.
- Chang MC, Ho YS, Lee JJ, Kok SH, Hahn LJ, Jeng JH: Prevention of the areca nut extract-induced unscheduled DNA synthesis of gingival keratinocytes by vitamin C and thiol compounds. *Oral Oncol* 38: 258-265, 2002.
- Chang YC, Tai KW, Cheng MH, Chou LS, Chou MY: Cytotoxic and non-genotoxic effects of arecoline on human buccal fibroblasts in vitro. *J Oral Pathol Med* 27: 68-71, 1998.
- Chen CC, Huang JF, Tsai CC: In vitro production of interleukin-6 by human gingival, normal buccal mucosa, and oral submucous fibrosis fibroblasts treated with betel-nut alkaloids. *Gaoxiong Yi Xue Ke Xue Za Zhi* 11: 604-614, 1995.
- Cheng KC, Cahill DS, Kasai H, Nishimura S, Loeb LA: 8-Hydroxyguanine, an abundant form of oxidative DNA damage, causes G----T and A----C substitutions. *J Biol Chem* 267: 166-172, 1992.

- Chou SJ, Alawi F: Expression of DNA damage response biomarkers during oral carcinogenesis. *Oral Surg Oral Med Oral Pathol Oral Radiol Endod* 111: 346-353, 2011.
- Colomiere M, Ward AC, Riley C, Trenerry MK, Cameron-Smith D, Findlay J, et al.: Cross talk of signals between EGFR and IL-6R through JAK2/STAT3 mediate epithelial-mesenchymal transition in ovarian carcinomas. *Br J Cancer* 100: 134-144, 2009.
- Conze D, Weiss L, Regen PS, Bhushan A, Weaver D, Johnson P, et al.: Autocrine production of interleukin 6 causes multidrug resistance in breast cancer cells. *Cancer Res* 61: 8851-8858, 2001.
- Coppe JP, Desprez PY, Krtolica A, Campisi J: The senescence-associated secretory phenotype: the dark side of tumor suppression. *Annu Rev Pathol* 5: 99-118, 2010.
- Coppe JP, Patil CK, Rodier F, Sun Y, Munoz DP, Goldstein J, et al.: Senescence-associated secretory phenotypes reveal cell-nonautonomous functions of oncogenic RAS and the p53 tumor suppressor. *PLoS Biol* 6: 2853-2868, 2008.
- Corcoran NM, Costello AJ: Interleukin-6: minor player or starring role in the development of hormone-refractory prostate cancer? *BJU Int* 91: 545-553, 2003.
- Coussens LM, Werb Z: Inflammation and cancer. *Nature* 420: 860-867, 2002.
- Dave BJ, Trivedi AH, Adhvaryu SG: In vitro genotoxic effects of areca nut extract and arecoline. *J Cancer Res Clin Oncol* 118: 283-288, 1992.
- Demple B, Harrison L: Repair of oxidative damage to DNA: enzymology and biology. *Annu Rev Biochem* 63: 915-948, 1994.
- Dimri GP, Lee X, Basile G, Acosta M, Scott G, Roskelley C, et al.: A biomarker that identifies senescent human cells in culture and in aging skin in vivo. *Proc Natl Acad Sci U S A* 92: 9363-9367, 1995.
- Dizdaroglu M: Oxidative damage to DNA in mammalian chromatin. *Mutat Res* 275: 331-342, 1992.
- Doak SH: Aneuploidy in upper gastro-intestinal tract cancers--a potential prognostic marker? *Mutat Res* 651: 93-104, 2008.
- Doak SH, Jenkins GJ, Parry EM, D'Souza FR, Griffiths AP, Toffazal N, et al.: Chromosome 4 hyperploidy represents an early genetic aberration in premalignant Barrett's oesophagus. *Gut* 52: 623-628, 2003.
- Duesberg P, Li R: Multistep carcinogenesis: a chain reaction of aneuploidizations. *Cell Cycle* 2: 202-210, 2003.
- Duesberg P, Li R, Fabarius A, Hehlmann R: The chromosomal basis of cancer. *Cell Oncol* 27: 293-318, 2005.
- Egesten A, Eliasson M, Olin AI, Erjefalt JS, Bjartell A, Sangfelt P, et al.: The proinflammatory CXC-chemokines GRO-alpha/CXCL1 and MIG/CXCL9 are concomitantly expressed in ulcerative colitis and decrease during treatment with topical corticosteroids. *Int J Colorectal Dis* 22: 1421-1427, 2007.
- Fett JW, Strydom DJ, Lobb RR, Alderman EM, Bethune JL, Riordan JF, et al.: Isolation and characterization of angiogenin, an angiogenic protein from human carcinoma cells. *Biochemistry* 24: 5480-5486, 1985.
- Finch CE, Crimmins EM: Inflammatory exposure and historical changes in human life-spans. *Science* 305: 1736-1739, 2004.
- Furuya M, Suyama T, Usui H, Kasuya Y, Nishiyama M, Tanaka N, et al.: Up-regulation of CXC chemokines and their receptors: implications for proinflammatory microenvironments of ovarian carcinomas and endometriosis. *Hum Pathol* 38: 1676-1687, 2007.
- Gao X, Xu Z: Mechanisms of action of angiogenin. *Acta Biochim Biophys Sin (Shanghai)* 40: 619-624, 2008.

- Greten FR, Eckmann L, Greten TF, Park JM, Li ZW, Egan LJ, et al.: IKKbeta links inflammation and tumorigenesis in a mouse model of colitis-associated cancer. *Cell* 118: 285-296, 2004.
- Grivennikov S, Karin M: Autocrine IL-6 signaling: a key event in tumorigenesis? *Cancer Cell* 13: 7-9, 2008.
- Grivennikov SI, Greten FR, Karin M: Immunity, inflammation, and cancer. *Cell* 140: 883-899, 2010.
- Grivennikov SI, Karin M: Dangerous liaisons: STAT3 and NF-kappaB collaboration and crosstalk in cancer. *Cytokine Growth Factor Rev* 21: 11-19, 2010.
- Grivennikov SI, Karin M: Inflammatory cytokines in cancer: tumour necrosis factor and interleukin 6 take the stage. *Ann Rheum Dis* 70 Suppl 1: i104-108, 2011.
- Gupta PC, Warnakulasuriya S: Global epidemiology of areca nut usage. *Addict Biol* 7: 77-83, 2002.
- Halazonetis TD, Gorgoulis VG, Bartek J: An oncogene-induced DNA damage model for cancer development. *Science* 319: 1352-1355, 2008.
- Haque MF, Harris M, Meghji S, Barrett AW: Immunolocalization of cytokines and growth factors in oral submucous fibrosis. *Cytokine* 10: 713-719, 1998.
- Haque MF, Harris M, Meghji S, Speight PM: An immunohistochemical study of oral submucous fibrosis. *J Oral Pathol Med* 26: 75-82, 1997.
- Haque MF, Meghji S, Khitab U, Harris M: Oral submucous fibrosis patients have altered levels of cytokine production. *J Oral Pathol Med* 29: 123-128, 2000.
- Harvilchuck JA, Pu X, Klaunig JE, Carlson GP: Indicators of oxidative stress and apoptosis in mouse whole lung and Clara cells following exposure to styrene and its metabolites. *Toxicology* 264: 171-178, 2009.
- Higashimoto T, Panopoulos A, Hsieh CL, Zandi E: TNFalpha induces chromosomal abnormalities independent of ROS through IKK, JNK, p38 and caspase pathways. *Cytokine* 34: 39-50, 2006.
- Hong SH, Ondrey FG, Avis IM, Chen Z, Loukinova E, Cavanaugh PF, Jr., et al.: Cyclooxygenase regulates human oropharyngeal carcinomas via the proinflammatory cytokine IL-6: a general role for inflammation? *FASEB J* 14: 1499-1507, 2000.
- Houghton J, Wang TC: Helicobacter pylori and gastric cancer: a new paradigm for inflammation-associated epithelial cancers. *Gastroenterology* 128: 1567-1578, 2005.
- Hussain SP, Harris CC: Inflammation and cancer: an ancient link with novel potentials. *Int J Cancer* 121: 2373-2380, 2007.
- Hwang ES, Bowen PE: DNA damage, a biomarker of carcinogenesis: its measurement and modulation by diet and environment. *Crit Rev Food Sci Nutr* 47: 27-50, 2007.
- Illeperuma RP, Park YJ, Kim JM, Bae JY, Che ZM, Son HK, et al.: Immortalized gingival fibroblasts as a cytotoxicity test model for dental materials. *J Mater Sci Mater Med*, 2011.
- Inoue K, Slaton JW, Eve BY, Kim SJ, Perrotte P, Balbay MD, et al.: Interleukin 8 expression regulates tumorigenicity and metastases in androgen-independent prostate cancer. *Clin Cancer Res* 6: 2104-2119, 2000.
- Jeng JH, Chang MC, Hahn LJ: Role of areca nut in betel quid-associated chemical carcinogenesis: current awareness and future perspectives. *Oral Oncol* 37: 477-492, 2001.
- Jeng JH, Hahn LJ, Lin BR, Hsieh CC, Chan CP, Chang MC: Effects of areca nut, inflorescence piper betle extracts and arecoline on cytotoxicity, total and unscheduled DNA synthesis in cultured gingival keratinocytes. *J Oral Pathol Med* 28: 64-71, 1999.

- Jeng JH, Ho YS, Chan CP, Wang YJ, Hahn LJ, Lei D, et al.: Areca nut extract up-regulates prostaglandin production, cyclooxygenase-2 mRNA and protein expression of human oral keratinocytes. *Carcinogenesis* 21: 1365-1370, 2000.
- Jeng JH, Wang YJ, Chiang BL, Lee PH, Chan CP, Ho YS, et al.: Roles of keratinocyte inflammation in oral cancer: regulating the prostaglandin E2, interleukin-6 and TNF-alpha production of oral epithelial cells by areca nut extract and arecoline. *Carcinogenesis* 24: 1301-1315, 2003.
- Jonsson D, Amisten S, Bratthall G, Holm A, Nilsson BO: LPS induces GROalpha chemokine production via NF-kappaB in oral fibroblasts. *Inflamm Res* 58: 791-796, 2009.
- Ju D, Sun D, Xiu L, Meng X, Zhang C, Wei P: Interleukin-8 is associated with adhesion, migration and invasion in human gastric cancer SCG-7901 cells. *Med Oncol*, 2010.
- Jung DW, Che ZM, Kim J, Kim K, Kim KY, Williams D: Tumor-stromal crosstalk in invasion of oral squamous cell carcinoma: a pivotal role of CCL7. *Int J Cancer* 127: 332-344, 2010.
- Jung JJ, Noh S, Jeung HC, Jung M, Kim TS, Noh SH, et al.: Chemokine growth-regulated oncogene 1 as a putative biomarker for gastric cancer progression. *Cancer Sci* 101: 2200-2206, 2010.
- Kang Y, Massague J: Epithelial-mesenchymal transitions: twist in development and metastasis. *Cell* 118: 277-279, 2004.
- Kawanishi H, Matsui Y, Ito M, Watanabe J, Takahashi T, Nishizawa K, et al.: Secreted CXCL1 is a potential mediator and marker of the tumor invasion of bladder cancer. *Clin Cancer Res* 14: 2579-2587, 2008.
- Kitadai Y, Haruma K, Sumii K, Yamamoto S, Ue T, Yokozaki H, et al.: Expression of interleukin-8 correlates with vascularity in human gastric carcinomas. *Am J Pathol* 152: 93-100, 1998.
- Klaunig JE, Wang Z, Pu X, Zhou S: Oxidative stress and oxidative damage in chemical carcinogenesis. *Toxicol Appl Pharmacol* 254: 86-99, 2011.
- Kogan-Sakin I, Cohen M, Paland N, Madar S, Solomon H, Molchadsky A, et al.: Prostate stromal cells produce CXCL-1, CXCL-2, CXCL-3 and IL-8 in response to epithelia-secreted IL-1. *Carcinogenesis* 30: 698-705, 2009.
- Konturek PC, Konturek SJ, Brzozowski T: Gastric cancer and Helicobacter pylori infection. *J Physiol Pharmacol* 57 Suppl 3: 51-65, 2006.
- Krtolica A, Parrinello S, Lockett S, Desprez PY, Campisi J: Senescent fibroblasts promote epithelial cell growth and tumorigenesis: a link between cancer and aging. *Proc Natl Acad Sci U S A* 98: 12072-12077, 2001.
- Kuilman T, Michaloglou C, Vredeveld LC, Douma S, van Doorn R, Desmet CJ, et al.: Oncogene-induced senescence relayed by an interleukin-dependent inflammatory network. *Cell* 133: 1019-1031, 2008.
- Lai KC, Lee TC: Genetic damage in cultured human keratinocytes stressed by long-term exposure to areca nut extracts. *Mutat Res* 599: 66-75, 2006.
- Lederle W, Depner S, Schnur S, Obermueller E, Catone N, Just A, et al.: IL-6 promotes malignant growth of skin SCCs by regulating a network of autocrine and paracrine cytokines. *Int J Cancer* 128: 2803-2814, 2011.
- Lee HJ, Guo HY, Lee SK, Jeon BH, Jun CD, Park MH, et al.: Effects of nicotine on proliferation, cell cycle, and differentiation in immortalized and malignant oral keratinocytes. *J Oral Pathol Med* 34: 436-443, 2005.
- Lee LF, Louie MC, Desai SJ, Yang J, Chen HW, Evans CP, et al.: Interleukin-8 confers androgen-independent growth and migration of LNCaP: differential effects of tyrosine kinases Src and FAK. *Oncogene* 23: 2197-2205, 2004.

- Lewis AM, Varghese S, Xu H, Alexander HR: Interleukin-1 and cancer progression: the emerging role of interleukin-1 receptor antagonist as a novel therapeutic agent in cancer treatment. *J Transl Med* 4: 48, 2006.
- Li A, Varney ML, Singh RK: Expression of interleukin 8 and its receptors in human colon carcinoma cells with different metastatic potentials. *Clin Cancer Res* 7: 3298-3304, 2001.
- Lin WW, Karin M: A cytokine-mediated link between innate immunity, inflammation, and cancer. *J Clin Invest* 117: 1175-1183, 2007.
- Liu D, Hornsby PJ: Senescent human fibroblasts increase the early growth of xenograft tumors via matrix metalloproteinase secretion. *Cancer Res* 67: 3117-3126, 2007.
- Lu AL, Li X, Gu Y, Wright PM, Chang DY: Repair of oxidative DNA damage: mechanisms and functions. *Cell Biochem Biophys* 35: 141-170, 2001.
- Lu HH, Liu CJ, Liu TY, Kao SY, Lin SC, Chang KW: Areca-treated fibroblasts enhance tumorigenesis of oral epithelial cells. *J Dent Res* 87: 1069-1074, 2008.
- Maniscalco WM, Watkins RH, Roper JM, Stavarsky R, O'Reilly MA: Hyperoxic ventilated premature baboons have increased p53, oxidant DNA damage and decreased VEGF expression. *Pediatr Res* 58: 549-556, 2005.
- McGurk M, Craig GT: Oral submucous fibrosis: two cases of malignant transformation in Asian immigrants to the United Kingdom. *Br J Oral Maxillofac Surg* 22: 56-64, 1984.
- Miller MD, Krangel MS: Biology and biochemistry of the chemokines: a family of chemotactic and inflammatory cytokines. *Crit Rev Immunol* 12: 17-46, 1992.
- Moenner M, Gusse M, Hatzi E, Badet J: The widespread expression of angiogenin in different human cells suggests a biological function not only related to angiogenesis. *Eur J Biochem* 226: 483-490, 1994.
- Montzka K, Fuhrmann T, Muller-Ehmsen J, Woltje M, Brook GA: Growth factor and cytokine expression of human mesenchymal stromal cells is not altered in an in vitro model of tissue damage. *Cytotherapy* 12: 870-880, 2010.
- Moore BB, Arenberg DA, Stoy K, Morgan T, Addison CL, Morris SB, et al.: Distinct CXC chemokines mediate tumorigenicity of prostate cancer cells. *Am J Pathol* 154: 1503-1512, 1999.
- Moscova M, Marsh DJ, Baxter RC: Protein chip discovery of secreted proteins regulated by the phosphatidylinositol 3-kinase pathway in ovarian cancer cell lines. *Cancer Res* 66: 1376-1383, 2006.
- Muguruma M, Unami A, Kanki M, Kuroiwa Y, Nishimura J, Dewa Y, et al.: Possible involvement of oxidative stress in piperonyl butoxide induced hepatocarcinogenesis in rats. *Toxicology* 236: 61-75, 2007.
- Nakano Y, Kobayashi W, Sugai S, Kimura H, Yagihashi S: Expression of tumor necrosis factor-alpha and interleukin-6 in oral squamous cell carcinoma. *Jpn J Cancer Res* 90: 858-866, 1999.
- Okamoto M, Lee C, Oyasu R: Interleukin-6 as a paracrine and autocrine growth factor in human prostatic carcinoma cells in vitro. *Cancer Res* 57: 141-146, 1997.
- Park I, Son HK, Che ZM, Kim J: A novel gain-of-function mutation of TGF-beta receptor II promotes cancer progression via delayed receptor internalization in oral squamous cell carcinoma. *Cancer Lett*, 2011.
- Paymaster JC: Cancer of the buccal mucosa; a clinical study of 650 cases in Indian patients. *Cancer* 9: 431-435, 1956.
- Pellegrino A, Antonaci F, Russo F, Merchionne F, Ribatti D, Vacca A, et al.: CXCR3-binding chemokines in multiple myeloma. *Cancer Lett* 207: 221-227, 2004.

- Pellegrino A, Ria R, Di Pietro G, Cirulli T, Surico G, Pennisi A, et al.: Bone marrow endothelial cells in multiple myeloma secrete CXC-chemokines that mediate interactions with plasma cells. *Br J Haematol* 129: 248-256, 2005.
- Pikarsky E, Porat RM, Stein I, Abramovitch R, Amit S, Kasem S, et al.: NF-kappaB functions as a tumour promoter in inflammation-associated cancer. *Nature* 431: 461-466, 2004.
- Pillai R, Balaram P, Reddiar KS: Pathogenesis of oral submucous fibrosis. Relationship to risk factors associated with oral cancer. *Cancer* 69: 2011-2020, 1992.
- Pindborg JJ, Bhonsle RB, Murti PR, Gupta PC, Daftary DK, Mehta FS: Incidence and early forms of oral submucous fibrosis. *Oral Surg Oral Med Oral Pathol* 50: 40-44, 1980.
- Pindborg JJ, Mehta FS, Daftary DK: Occurrence of epithelial atypia in 51 Indian villagers with oral submucous fibrosis. *Br J Cancer* 24: 253-257, 1970.
- Pitiyage GN, Slijepcevic P, Gabrani A, Chianea YG, Lim KP, Prime SS, et al.: Senescent mesenchymal cells accumulate in human fibrosis by a telomere-independent mechanism and ameliorate fibrosis through matrix metalloproteinases. *J Pathol* 223: 604-617, 2011.
- Pu X, Kamendulis LM, Klaunig JE: Acrylonitrile-induced oxidative stress and oxidative DNA damage in male Sprague-Dawley rats. *Toxicol Sci* 111: 64-71, 2009.
- Raman D, Baugher PJ, Thu YM, Richmond A: Role of chemokines in tumor growth. *Cancer Lett* 256: 137-165, 2007.
- Richmond A, Thomas HG: Melanoma growth stimulatory activity: isolation from human melanoma tumors and characterization of tissue distribution. *J Cell Biochem* 36: 185-198, 1988.
- Rojas A, Liu G, Coleman I, Nelson PS, Zhang M, Dash R, et al.: IL-6 promotes prostate tumorigenesis and progression through autocrine cross-activation of IGF-IR. *Oncogene* 30: 2345-2355, 2011.
- Roper JM, Mazzatti DJ, Watkins RH, Maniscalco WM, Keng PC, O'Reilly MA: In vivo exposure to hyperoxia induces DNA damage in a population of alveolar type II epithelial cells. *Am J Physiol Lung Cell Mol Physiol* 286: L1045-1054, 2004.
- Schadendorf D, Moller A, Algermissen B, Worm M, Sticherling M, Czarnetzki BM: IL-8 produced by human malignant melanoma cells in vitro is an essential autocrine growth factor. *J Immunol* 151: 2667-2675, 1993.
- Scheller J, Ohnesorge N, Rose-John S: Interleukin-6 trans-signalling in chronic inflammation and cancer. *Scand J Immunol* 63: 321-329, 2006.
- Schneider MR, Hoeflich A, Fischer JR, Wolf E, Sordat B, Lahm H: Interleukin-6 stimulates clonogenic growth of primary and metastatic human colon carcinoma cells. *Cancer Lett* 151: 31-38, 2000.
- Schteingart DE, Giordano TJ, Benitez RS, Burdick MD, Starkman MN, Arenberg DA, et al.: Overexpression of CXC chemokines by an adrenocortical carcinoma: a novel clinical syndrome. *J Clin Endocrinol Metab* 86: 3968-3974, 2001.
- Seidelin JB, Nielsen OH: Continuous cytokine exposure of colonic epithelial cells induces DNA damage. *Eur J Gastroenterol Hepatol* 17: 363-369, 2005.
- Seril DN, Liao J, Yang GY, Yang CS: Oxidative stress and ulcerative colitis-associated carcinogenesis: studies in humans and animal models. *Carcinogenesis* 24: 353-362, 2003.
- Shan W, Yang G, Liu J: The inflammatory network: bridging senescent stroma and epithelial tumorigenesis. *Front Biosci* 14: 4044-4057, 2009.
- Shintani S, Ishikawa T, Nonaka T, Li C, Nakashiro K, Wong DT, et al.: Growth-regulated oncogene-1 expression is associated with angiogenesis and lymph node metastasis in human oral cancer. *Oncology* 66: 316-322, 2004.

- Shirname LP, Menon MM, Nair J, Bhide SV: Correlation of mutagenicity and tumorigenicity of betel quid and its ingredients. *Nutr Cancer* 5: 87-91, 1983.
- Smith DR, Polverini PJ, Kunkel SL, Orringer MB, Whyte RI, Burdick MD, et al.: Inhibition of interleukin 8 attenuates angiogenesis in bronchogenic carcinoma. *J Exp Med* 179: 1409-1415, 1994.
- Sundqvist K, Grafstrom RC: Effects of areca nut on growth, differentiation and formation of DNA damage in cultured human buccal epithelial cells. *Int J Cancer* 52: 305-310, 1992.
- Sundqvist K, Liu Y, Nair J, Bartsch H, Arvidson K, Grafstrom RC: Cytotoxic and genotoxic effects of areca nut-related compounds in cultured human buccal epithelial cells. *Cancer Res* 49: 5294-5298, 1989.
- Tanaka H, Fujita N, Sugimoto R, Urawa N, Horiike S, Kobayashi Y, et al.: Hepatic oxidative DNA damage is associated with increased risk for hepatocellular carcinoma in chronic hepatitis C. *Br J Cancer* 98: 580-586, 2008.
- Tilakaratne WM, Klinikowski MF, Saku T, Peters TJ, Warnakulasuriya S: Oral submucous fibrosis: review on aetiology and pathogenesis. *Oral Oncol* 42: 561-568, 2006.
- Toyokuni S: Novel aspects of oxidative stress-associated carcinogenesis. *Antioxid Redox Signal* 8: 1373-1377, 2006.
- Trivedy CR, Craig G, Warnakulasuriya S: The oral health consequences of chewing areca nut. *Addict Biol* 7: 115-125, 2002.
- Tsai WH, Hsu HC, Lin CC, Ho CK, Kou YR: Role of interleukin-8 and growth-regulated oncogene-alpha in the chemotactic migration of all-trans retinoic acid-treated promyelocytic leukemic cells toward alveolar epithelial cells. *Crit Care Med* 35: 879-885, 2007.
- Tsai YS, Lee KW, Huang JL, Liu YS, Juo SH, Kuo WR, et al.: Arecoline, a major alkaloid of areca nut, inhibits p53, represses DNA repair, and triggers DNA damage response in human epithelial cells. *Toxicology* 249: 230-237, 2008.
- Utsunomiya H, Tilakaratne WM, Oshiro K, Maruyama S, Suzuki M, Ida-Yonemochi H, et al.: Extracellular matrix remodeling in oral submucous fibrosis: its stage-specific modes revealed by immunohistochemistry and in situ hybridization. *J Oral Pathol Med* 34: 498-507, 2005.
- Valavanidis A, Vlachogianni T, Fiotakis C: 8-hydroxy-2'-deoxyguanosine (8-OHdG): A critical biomarker of oxidative stress and carcinogenesis. *J Environ Sci Health C Environ Carcinog Ecotoxicol Rev* 27: 120-139, 2009.
- von Sonntag C: New aspects in the free-radical chemistry of pyrimidine nucleobases. *Free Radic Res Commun* 2: 217-224, 1987.
- Wang CC, Liu TY, Wey SP, Wang FI, Jan TR: Areca nut extract suppresses T-cell activation and interferon-gamma production via the induction of oxidative stress. *Food Chem Toxicol* 45: 1410-1418, 2007.
- Wang D, Richmond A: Nuclear factor-kappa B activation by the CXC chemokine melanoma growth-stimulatory activity/growth-regulated protein involves the MEKK1/p38 mitogen-activated protein kinase pathway. *J Biol Chem* 276: 3650-3659, 2001.
- Wang D, Sai J, Carter G, Sachpatzidis A, Lolis E, Richmond A: PAK1 kinase is required for CXCL1-induced chemotaxis. *Biochemistry* 41: 7100-7107, 2002.
- Wang D, Wang H, Brown J, Daikoku T, Ning W, Shi Q, et al.: CXCL1 induced by prostaglandin E2 promotes angiogenesis in colorectal cancer. *J Exp Med* 203: 941-951, 2006.
- Wang JM, Deng X, Gong W, Su S: Chemokines and their role in tumor growth and metastasis. *J Immunol Methods* 220: 1-17, 1998.

- Weaver BA, Cleveland DW: Does aneuploidy cause cancer? *Curr Opin Cell Biol* 18: 658-667, 2006.
- Wen Y, Giardina SF, Hamming D, Greenman J, Zachariah E, Bacolod MD, et al.: GROalpha is highly expressed in adenocarcinoma of the colon and down-regulates fibulin-1. *Clin Cancer Res* 12: 5951-5959, 2006.
- Williams L, Jenkins GJ, Doak SH, Fowler P, Parry EM, Brown TH, et al.: Fluorescence in situ hybridisation analysis of chromosomal aberrations in gastric tissue: the potential involvement of *Helicobacter pylori*. *Br J Cancer* 92: 1759-1766, 2005.
- Williams L, Somasekar A, Davies DJ, Cronin J, Doak SH, Alcolado R, et al.: Aneuploidy involving chromosome 1 may be an early predictive marker of intestinal type gastric cancer. *Mutat Res* 669: 104-111, 2009.
- Wolf JS, Chen Z, Dong G, Sunwoo JB, Bancroft CC, Capo DE, et al.: IL (interleukin)-1alpha promotes nuclear factor-kappaB and AP-1-induced IL-8 expression, cell survival, and proliferation in head and neck squamous cell carcinomas. *Clin Cancer Res* 7: 1812-1820, 2001.
- Woods KV, El-Naggar A, Clayman GL, Grimm EA: Variable expression of cytokines in human head and neck squamous cell carcinoma cell lines and consistent expression in surgical specimens. *Cancer Res* 58: 3132-3141, 1998.
- Xia M, Hyman BT: GROalpha/KC, a chemokine receptor CXCR2 ligand, can be a potent trigger for neuronal ERK1/2 and PI-3 kinase pathways and for tau hyperphosphorylation-a role in Alzheimer's disease? *J Neuroimmunol* 122: 55-64, 2002.
- Yang G, Rosen DG, Zhang Z, Bast RC, Jr., Mills GB, Colacino JA, et al.: The chemokine growth-regulated oncogene 1 (Gro-1) links RAS signaling to the senescence of stromal fibroblasts and ovarian tumorigenesis. *Proc Natl Acad Sci U S A* 103: 16472-16477, 2006.
- Yao PL, Lin YC, Wang CH, Huang YC, Liao WY, Wang SS, et al.: Autocrine and paracrine regulation of interleukin-8 expression in lung cancer cells. *Am J Respir Cell Mol Biol* 32: 540-547, 2005.
- Yoshioka N, Wang L, Kishimoto K, Tsuji T, Hu GF: A therapeutic target for prostate cancer based on angiogenin-stimulated angiogenesis and cancer cell proliferation. *Proc Natl Acad Sci U S A* 103: 14519-14524, 2006.
- Yuan A, Chen JJ, Yao PL, Yang PC: The role of interleukin-8 in cancer cells and microenvironment interaction. *Front Biosci* 10: 853-865, 2005.

## ABSTRACT IN KOREAN

### 아리카넛 (Areca Nut) 추출물에 의해 섬유모세포에서 분비된 싸이토카인이 발암과정에 미치는 영향

연세대학교 대학원 치의학과

라시카 일레페루마

구강 점막하 섬유증 (oral submucous fibrosis; OSF)의 암화 과정은 아직 잘 알려져 있지 않다. OSF와 구강 암의 발생기전에 있어서 아리카넛 (Areca nut; AN)의 효과에 대해 많은 연구가 진행되었으며 구강 상피층에 AN의 직접적인 독성과 유전자 독성 효과에 대한 연구들이 보고되고 있다. 본 연구는 섬유화가 OSF의 특징이란 점에 근거하여 AN 추출물에 의해 섬유모세포에서 분비된 인자들의 발암과정에 있어서 역할을 분석함을 목적으로 연구하였다. AN 추출물이 점막하 섬유모세포를 자극하여 염증성 싸이토카인을 분비하고, 분비된 싸이토카인에 의해 상피층에 유전자 독성효과를 주어 OSF의 암화 과정에 영향을 줄 것이라 가설을 세웠다. 이를 증명하기 위해 싸이토카인 어레이 (cytokine array)를 통해 AN 추출물을 처리한 후 섬유모세포에서 분비된 싸이토카인 GRO- $\alpha$ , IL-6 그리고 IL-8을 선별하였다. 이 결과는 ELISA와 RT-PCR 그리고 면역형광염색법을 통하여 입증하였다. OSF 환자 조직에서도 GRO- $\alpha$ , IL-6 그리고 IL-8의 발현을 면역형광염색법을 통하여 확인하였다.

AN 추출물을 섬유모세포에 8주간 처리하자 세포의 노화 현상이 일어난 것을  $\beta$ -갈락토시다아제 염색으로 확인하였다. 이러한 노화 현상에 따른 노화 관련 분비물에 의해서 상피의 악성으로의 이행에 영향을 준다는 보고가 있었기 때문에, 이러한 싸이토카인이 구강 상피층에 미치는 영향을 알아보기 위해서 불멸화 사람 구강 각화세포 (immortalized human oral keratinocytes; IHOK)를 이용하였다. IHOK를 GRO- $\alpha$ , IL-6 그리고 IL-8를 처리하였을 때 IHOK의 성장률은 변화하지 않았다. 하지만 IHOK의 이수성 (aneuploidy)이 증가한 것을 관찰하였고 이는 선별된 싸이토카인이 유전자 독성 효과를 줄 수 있을 것을 암시하고 있다.

다음으로, 선별된 싸이토카인 GRO- $\alpha$ , IL-6 그리고 IL-8이 IHOK의 DNA 손상을 야기하고 있음을 히스톤 H2AX의 인산화 염색과 FITC가 결합된 구아닌산화부산물 (8-oxo-

guanine) 염색을 통하여 확인하였다. OSF 환자 조직에서도 기저층 주위로 히스톤 H2AX의 s인산화에 대해 양성 반응을 보였다. 또한, H<sub>2</sub>DCFDA 염색을 통하여 GRO- $\alpha$ , IL-6 그리고 IL-8는 IHOK에서 활성산소 (reactive oxygen species; ROS)를 유도하고 있음을 확인했다.

본 연구는 GRO- $\alpha$ , IL-6 그리고 IL-8는 IHOK에 이수성과 세포손상 그리고 산화적 DNA 손상을 주고 있음을 밝혔다. GRO- $\alpha$ , IL-6 그리고 IL-8에 의한 DNA 손상은 ROS에 의해 유도된 것임을 확인했다. OSF 환자 조직에서 GRO- $\alpha$ , IL-6 그리고 IL-8의 증가를 관찰하였으며 DNA 손상 역시 확인할 수 있었다.

본 연구는 AN 추출물에 의해 유도된 구강점막하 섬유증의 암화과정에 있어서 섬유모세포의 역할, 특히 섬유모세포에서 분비된 사이토카인의 역할을 밝혔다. 본 연구를 통하여 구강점막하 섬유증의 발암과정에 있어 염증성 사이토카인의 역할을 이해하고 설명하는데 기초적인 연구가 될 것을 기대한다.